# Bioactive sugar surfaces for hepatocyte cell culture

A Thesis submitted to the University of Manchester for the degree of Doctor of Philosophy in the Faculty of Engineering and Physical Sciences

**MANCHESTER 1824**

**2010**

**RACHAEL FIONA AMBURY**

**SCHOOL OF MATERIALS**

**Table of Contents**

**Final Word Count: 40,641**

## List of Figures

# List of Tables

## Abbreviations

| | |
|---|---|
| **α-FP** | Alfa-Feta Protein |
| **α-LA** | α-lactoalbumin |
| **µg** | Microgram |
| **µl** | Microlitre |
| **AFM** | Atomic Force Microscopy |
| **AMV transcriptase** | Avian Myeloblastosis Virus Transcriptase |
| **ASGP** | Asialoglycoprotein |
| **ASGP-R** | Asialoglycoprotein Receptor |
| **BE** | Binding energy |
| **BSA** | Bovine serum albumin |
| **cDNA** | Complementary DNA |
| **CK18** | Cytokeratin 18 |
| **cm$^{-1}$** | Wavenumber |
| **CYP1A** | Cytochrome P450 1A |
| **DAPI** | 4, 6 diamidino-2-phenyladole |
| **DIPEA** | N' N- diisopropylethylamine |
| **dL** | Decilitre |
| **DLVO** | Derjaguin-Landau-Verwey-Overbeek Theory |
| **DMF** | Dimethylformamide |
| **DMSO** | Dimethyl Sulfoxide |
| **DNA** | Deoxyribonucleic Acid |
| **dNTP** | Deoxynucleotide Triphosphates |
| **ECM** | Extracellular Matrix |
| **EDC** | 1-ethyl-3-(3-dimethylaminopropyl) carbodiimide hydrochloride |
| **EDTA** | Ethylenediaminotetraacetic Acid |

| | |
|---|---|
| **EG** | Ethylene glycol |
| **EGF** | Epidermal growth factor |
| **eV** | Electron Volt |
| **F12-K** | Kaighn's modification of Ham's F12 medium with L-glutamine |
| **FACS** | Fluorescent activated cell sorter |
| **FAK** | Focal adhesion kinase |
| **FAT** | Fixed analyser transmission |
| **FBS** | Foetal bovine serum |
| **$Fe_2O_3$** | Haematite |
| **FEP-Teflon** | Fluorinated Ethylene-Propylene - Teflon |
| **FITC** | Fluorescein isothiocyanate |
| **FL83B** | Mouse Hepatocyte Cell Line |
| **Fmoc** | Fluorenyl-9-methoxycarbonyl |
| **Fmoc-Phe** | Fluorenyl-9-methoxycarbonyl - Phenylalanine |
| **FTIR** | Fourier Transform Infrared Spectroscopy |
| **GA** | D-Glucuronic Acid |
| **GAGs** | Glycoaminoglycans |
| **GAPDH** | Glucose-6-phosphate dehydrogenase |
| **GC** | Galactosylated chitosan |
| **GOPTS** | (3-glycidyloxypropyl) trimethoxysilane |
| **GRGDS** | glycine-arginine-glycine-aspartic acid-serine |
| **HBTu** | (2-(1H-Benzotriazole-1-yl)-1,1,3,3-tetramethyuronium hexafluorophosphate) |
| **Hep3B** | Hepatoma cell line |
| **HepG2** | Hepatoma cell line |
| **IGF-1** | Insulin like Growth Factor -1 |

| | |
|---|---|
| **IgG** | Immunoglobulin G |
| **IKVAV** | Isoleucine-Lysine-Valine-Alanine-Valine |
| **kB** | Kilobyte |
| **kDa** | Kilodalton |
| **KE** | Kinetic Energy |
| **KeV** | Kilo electron Volt |
| **kg** | Kilogram |
| **kPa** | Kilopascal |
| **kV** | Kilovolt |
| **LA** | Lactobionic Acid |
| **LSZ** | Lysosyme |
| **m/z** | Mass to charge ratio |
| **mA** | Milliamp |
| **mg** | Milligram |
| **MGB** | Myoglobin |
| **ml** | Millilitre |
| **mm** | Millimetres |
| **mmol** | Millimole |
| **MMP-12** | Matrix Metalloproteinase-12 |
| **Mw** | Molecular Weight |
| **ng** | Nanograms |
| **NHS** | N-hydroxysuccinimide ester |
| **nm** | Nanometres |
| **OD** | Optical Density |
| **P450** | Cytochrome P450 |
| **pA** | Pico Amps |

| | |
|---|---|
| **PBS** | Phosphate Buffered Saline |
| **PCR** | Polymerase Chain Reaction |
| **PEG** | Polyethylene Glycol |
| **PEGA** | Polyethlene glycol acrylamide |
| **PET** | Polyethylene terephthalate |
| **PFA** | Paraformaldehyde |
| **pFAK** | phosphorylated FAK |
| **pg** | Picogram |
| **PHBV** | Poly(3 hydroxybutyrate-co-3-hydroxyvalerate) |
| **pHEMA** | Poly(hydroxyethyl methacrylate) |
| **PLA** | Polylactic Acid |
| **PLGA** | Polylactic co-glycolic Acid |
| **PMMA** | Poly(methylmethacrylate), |
| **POM** | Polyoxometalate |
| **PS** | Polystyrene |
| **PVA** | Poly(vinyl alcohol) |
| **PVLA** | Poly (N-p-vinylbenzyl-4-o-β-D-galactopyranosyl-D-gluconamide) |
| **REDV** | Arginine-Glutamic acid-Aspartic acid-Valine |
| **RGD** | Arginine-Glycine-Aspartic acid |
| **RNA** | Ribonucleic Acid |
| **RNase** | Ribonuclease |
| **RPM** | Revolutions Per Minute |
| **RT** | Room temperature |
| **RT-buffer** | Reverse transcription buffer |
| **RT-PCR** | Reverse Transcription PCR |
| **SAMs** | Self Assembled Monolayers |

| | |
|---|---|
| **TAE** | Tris-Acetate-EDTA |
| **TCP** | Tissue culture plastic |
| **TNE** | Tris-NaCl-EDTA |
| **ToF-SIMS** | Time of Flight Secondary Ion Mass Spectrometry |
| **Tyr-397** | Tyrosine-397 |
| **UV** | Ultraviolet |
| **V** | Volts |
| **W** | Work function |
| **XPS** | X-ray Photo-electron Spectroscopy |

**Abstract**

The primary objective of this study was to identify, develop and characterise a novel bioactive surface capable of binding hepatocytes and enabling the retention of hepatocyte-specific cell function during *in-vitro* culture. The materials were designed to exploit a unique characteristic of hepatocyte biology, with β-galactose moieties displayed to allow cellular adhesion via the specific asialoglycoprotein receptors (ASGP-R) found on hepatocytes.

Hydrogels were created by modifying a commercially available block co-polymer of polyethylene glycol (PEG) and acrylamide, (PEGA) with galactose moieties contained within lactobionic acid (LA), producing a unique bioactive sugar-based gel. A control sugar, D-glucuronic acid (GA), was used as a non-ASGP-R binding control. Monomers used were mono- and bis-acryloamido PEG ($M_w$=1900 gmol$^{-1}$), and dimethylacrylamide. The pendant PEGA amine groups were used as ligands to bind to the sugars. The resultant gels were characterised using Fourier Transform Infrared Spectroscopy (FT-IR), protein adsorption, Fmoc-Phe and dansyl chloride labelling. The biocompatibility of the gel surfaces was evaluated using a hepatocyte cell line and the degree of attachment, proliferation, and morphology was characterised using light microscopy, live/dead assays, DNA assays, immunochemical staining, flow cytometry and reverse-transcription polymerase chain reaction (RT-PCR).

FT-IR analysis of LA revealed a distinctive band at approximately 1740cm$^{-1}$ corresponding to carbonyl stretching (C=O) of carboxylic acid. This unique peak disappeared as the galactose moieties within the LA were incorporated into the PEGA gel. A similar trend was also observed with the control GA sugar within the PEGA gel, confirming that the sugars had been integrated into the material. Protein adsorption assays confirmed the non-fouling nature of PEGA. Cell culture experiments showed that hepatocytes attached preferentially to the sugar surfaces, with few cells seen on the PEGA surfaces. It was observed that cells on the PEGA with LA surface were more metabolically active, than the controls and proliferated to a monolayer by day 7 in culture. Immunocytochemical staining of the cells for actin, vinculin and phosphorylated focal adhesion kinase illustrated differences in cell morphology between cells grown on different surfaces. It was determined that the sugar PEGA surfaces maintained some characteristics of hepatocyte functionality e.g. urea synthesis over the course of 7 days.

To improve the reproducibility of the surfaces generated, a preliminary investigation of two-dimensional PEG monolayer surfaces as a well defined platform for surface reactions was conducted. These were chemically functionalised in a stepwise manner with the sugars. The number of coupling steps and the choice of solvent were shown to affect the efficiency of the reaction. Further more, the need for careful sample preparation was highlighted as contamination could potentially inhibit the interpretation of the surface chemistry.

The overall conclusion of this work is that saccharides within non-fouling surfaces composed of thin layers of PEG-acrylamide hydrogels are able to support hepatocyte attachment and the retention of cell type specific functions in culture. However, this preliminary work has shown that much further research is necessary to elucidate the role that the surface chemistry plays in the attachment of hepatocytes.

**Declaration**

No portion of the work referred to in this thesis has been submitted in support of an application for another degree or qualification of this type or any other university of other institution of learning.

**Copyright Statement**

**(i)** The author of this thesis (including any appendices and/or schedules to this) owns any copyright in it (the "Copyright") and she has given The University of Manchester the right to use such Copyright for any administrative, promotional, educational and/or teaching purposes.

**(ii)** Copies of this thesis, either in full or in extracts, may be made **only** in accordance with the regulations of the John Rylands University Library of Manchester. Details of these regulations may be obtained from the Librarian. This page must form part of any such copies made.

**(iii)** The ownership of any patents, designs, trade marks and any and all other intellectual property rights except for the Copyright (the "Intellectual Property Rights") and any reproductions of copyright works, for example graphs and tables ("Reproductions"), which may be described in this thesis, may not be owned by the author and may be owned by third parties. Such Intellectual Property Rights and Reproductions cannot and must not be made available for use without the prior written permission of the owner(s) of the relevant Intellectual Property Rights and/or Reproductions.

**(iv)** Further information on the conditions under which disclosure, publication and exploitation of this thesis, the copyright and any Intellectual Property Rights and/or Reproductions described in it may take place is available from the Head of School of Materials

# Acknowledgements

The author would like to thank Prof. Rein Ulijn and Dr. Catherine Merry for their supervision, patience and encouragement shown during of this project. Thanks to Dr. Darren Wilson for his mentoring during the past 3 years, and providing guidance and positive criticism to improve ongoing work.

Thanks to Dr. David Scurr and the EPSRC Open Access Scheme for providing the author with an opportunity to use the ToF-SIMS facilities at Nottingham University, and providing valuable advice from time to time. The author would also like to thank Dr. John Walton for his assistance and guidance with regards to XPS analysis. Thanks to Dr. Claire Johnson and Dr. Rebecca Holley for assisting with the molecular biology and associated work.

Special thanks to Prof. Helen Grant at the University of Strathclyde for encouragement shown at crucial stages of the project by being involved in active discussions on various aspects of the project.

Thanks also to friends and colleagues within the Material Science Centre, particularly all members past and present of the Ulijn Lab and the members of the E20 coffee club; Riaz Akhtar, Rachel Saunders, Rob Thornton, Brian Cousins and Kate Thornton whose support over the past years has been an incentive to keep going even when nothing worked. Thanks to Olwen Richert and Sue Brandreth for their help and kindness in promptly dealing with administrative and academic matters.

Last but not least, the author would like to show her gratitude to all her family and friends, who were always there to provide help and support whenever the author needed it especially; Dan, Andrew, and Martin for always being there, Jen and Hayley for nights out and making me smile, and Klaudia for taking me horse riding regularly; all of whom made the process a little more enjoyable.

## The Author

**Education**

**2006-present**: PhD in Biomaterials. University of Manchester.

**2002-2006:** MEng with industrial experience in Biomedical Materials Science (1$^{st}$ Class). University of Manchester.

**Publications**

R.F. Ambury, C.L. Merry, R.V. Ulijn. Galactose functionalised PEGA supports metabolically active hepatocytes. Journal of Materials Chemistry (2010). In preparation.

**Conference Presentations**

- Tissue and Cell Engineering Society (TCES) 8-10$^{th}$ July 2009. University of Glasgow and University of Strathclyde. Oral Presentation. European Cells and Materials. Vol 18, Suppl 2, page 28.

- Tissue and Cell Engineering Society (TCES) 2-4$^{th}$ July 2008. University of Nottingham. Poster Presentation. European Cells and Materials. Vol 16, Suppl 3, page 33.

- The UK Society for Biomaterials (UKSB) conference. 26-27$^{th}$ June 2008. University of Liverpool. Poster Presentation.

- 2$^{nd}$ International Conference on Mechanics of Biomaterials and Tissues (ICMOBT). 9-13$^{th}$ December 2007. Lihue, Hawaii, USA. Poster Presentation.

**Chapter 1.0: Introduction**

There are strong reasons to recreate liver systems using tissue engineering for both clinical and commercial applications. At a clinical level, there is a critical shortfall in the number of donors to patients awaiting liver transplants. Liver disease is a major cause of morbidity and mortality worldwide and accounts for over 25000 deaths per year in the USA alone (Hammond *et al.*, 2006). The application of tissue engineering could radically alter this mismatch; by acting as a bridging device, tissue engineered scaffolds could provide lost functions whilst the liver regenerates or until a suitable donor liver is found (Allen and Bhatia, 2002). On a commercial level there is need for an *in vitro* liver model upon which metabolic and toxicological data can be generated on new chemicals and drugs.

The important role of the extracellular matrix (ECM) in liver development and maintenance has been reviewed extensively (Wells, 2007). Consequently in the development of new natural and synthetic biomaterials surface engineering techniques have become widely used to elicit an appropriate cellular response and mimic the ECM (Castner and Ratner, 2002). The chemical composition of biomaterials may influence the cellular response seen particularly by enhancing cellular adhesion and the maintenance of liver specific functions. The work presented in this study focuses on engineering surfaces to contain well defined carbohydrate ligands to direct liver cell behaviour. A particular carbohydrate recognition receptor on the hepatocyte cell surface; asialoglycoprotein receptor (ASGP-R) was targeted due to its specificity for galactose. The normal function of the ASGP-R is to bind to glycoproteins displaying exposed terminal galactose residues and remove them from circulation by endocytosis, Figure 1.1 (Hirose *et al.*, 2001, Cho *et al.*, 2007).

In this thesis the experimental chapters are presented separately, each with its own introduction, results and initial discussion, and conclusions sections. An overall discussion chapter pulls the main themes of this study together at the end.

Chapter 2 begins with a brief overview of the structure and function of the liver, followed by the biology of the native cells and the important role of the ECM in liver homeostasis. Then methods and strategies currently used to control and influence cellular behaviour on biomaterials are discussed in relation to natural and

synthetic materials, highlighted by numerous examples. Finally, the use of tissue engineered scaffolds for liver applications are discussed; this section is divided into non-galactosylated and galactosylated scaffolds in order to highlight the utility of the galactose-ASGP-R interaction.

Experimental Chapters 3 and 4 investigate the feasibility of incorporating saccharides into a non fouling hydrogel system to direct hepatocyte response. The system was specifically made to exploit the presence of specific carbohydrate recognition receptors; ASGP-R on the cell surface, Figure 1.2. This report shows the characterisation (Chapter 3) and favourable cellular response of hepatocytes (Chapter 4) to immobilised saccharides within a hydrogel system.

Chapter 5 develops the system further using bioinert polymer monolayers to directly immobilise saccharides onto a surface and consequently characterise them using ultra high vacuum techniques including Time of Flight Secondary Ion Mass Spectrometry (ToF-SIMS) and X-ray Photo-electron Spectroscopy (XPS). Additionally traditional materials characterisation techniques in the form of protein adsorption assays and water contact angle measurements were utilised.
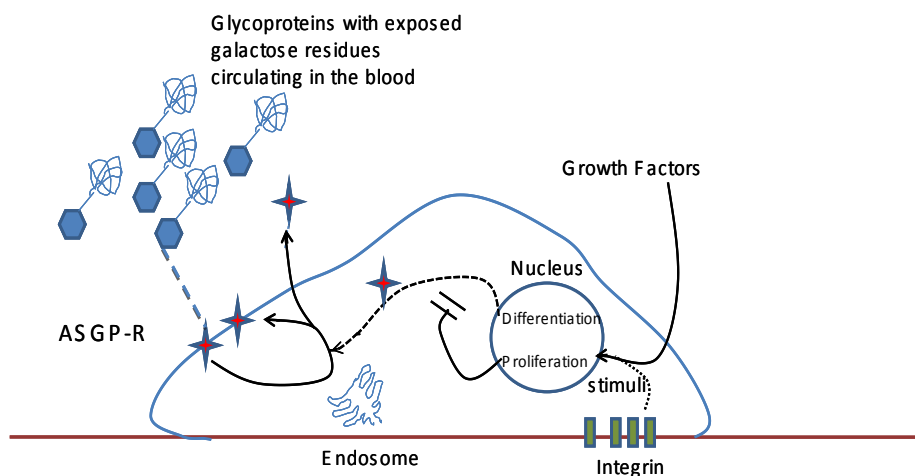


**Figure 1.1:** Schematic representation of a hepatocyte binding glycoproteins with exposed galactose residues via ASGP-R for internalisation by endocytosis. (Modified and adapted from (Hirose *et al.*, 2001)).
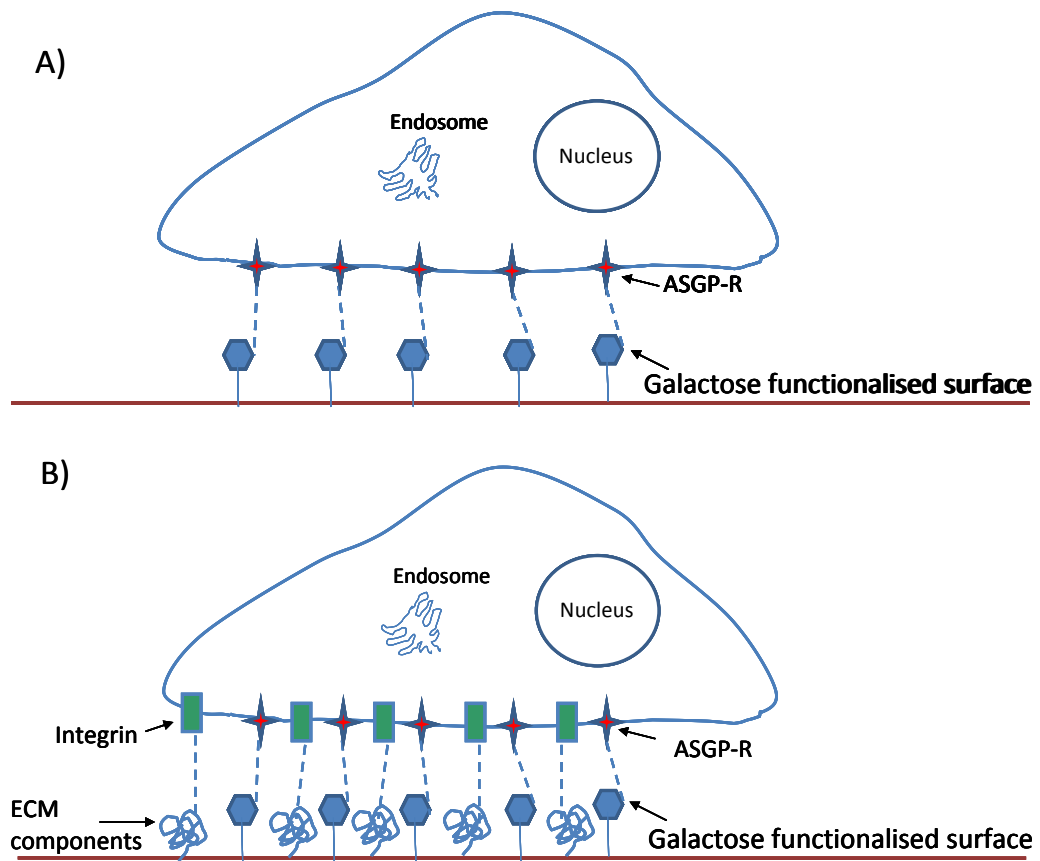
**Figure 1.2:** A schematic representation of a hepatocyte attaching to a galactose functionalised surface via ASGP-R. A) ASGP-R being employed as an adhesive ligand on a biomaterials surface. B) Integrin receptors participate in cell adhesion via ECM components secreted by hepatocytes after initial ASGP-R adhesion.

## Chapter 2.0 Literature Review

## 2.1 Introduction

The liver is one of few organs in the body capable of self-repair, yet when constant damage is caused by trauma, disease or substance abuse, regeneration can become impossible and the liver begins to fail. Therapies to treat liver failure have been in development for over fifty years and despite this, organ transplantation remains the most favoured course of action.

Tissue engineering is beginning to develop into a viable alternative therapy. The liver remains, however, a formidable challenge due to its unique architecture and multiple functions. Removal of hepatocytes from their *in-vivo* environment leads to de-differentiation and partial progression in the cell cycle (Berthiaume *et al.*, 1996, Wright and Paine, 1992, Mitaka, 1998). These changes are characterised by the loss of enzyme expression specific to the liver (Davila and Morris, 1999, Mitaka, 1998, Berthiaume *et al.*, 1996, Matsushita *et al.*, 1994). The encapsulation of hepatocytes within scaffolds offers the potential to maintain cell morphology; this may be of considerable benefit as studies have shown the shape of the cells is intrinsically linked with functionality. The ability to expand large numbers of functional hepatocytes *in-vitro* may benefit toxicity screening, where these cells could be used for high-throughput screening of new drug compounds without the use of expensive animal models.

This chapter highlights the strategies employed to engineer surfaces and materials to obtain desired interactions with cells and their ECM. Creating an accurate mimic of the ECM, remains a significant challenge to enable comprehensive repair of the body with tissue engineered products. The anatomy of the liver and the characteristics of the native cells are discussed and related to therapies currently in development.

**Part A: Anatomy of the liver and characteristics of the native ECM and cells**

**2.2 The Intact Liver**

**2.2.1 Structure and Function**

The liver is a large reddish-brown wedge-shaped organ located in the upper right part of the abdomen underneath the diaphragm, weighing in the region of 1.5 kg. The liver is known to be the largest visceral and dynamic organ in the human body. It is thought to regulate up to 500 bodily functions including metabolic, synthetic and detoxification processes. It is strategically interpositioned between the digestive system and the rest of the body. The liver is split into four principle regions; the left, right, caudate and quadrate lobes, Figure 2.1A. The division between the left and right lobes is discernible by the faliciform ligament. At the posterior edge of the faliciform ligament is the fibrous round ligament (Marieb, 1998, Ross *et al.*, 1989, Seeley and Tate, 1995). The small caudate lobe lies off the right lobe and left of the inferior vena cava, Figure 2.1A. The quadrate lobe is found between the left lobe and the gallbladder, Figure 2.1A.

The liver receives 75 % of its blood from the intestinal tract through the hepatic portal vein. This blood contains products of digestion including amino acids, carbohydrates and lipids, as well as any ingested drugs and toxins. The remaining 25 % of the blood supply comes from the hepatic artery (Guyton and Hall, 1996, Mitzner, 1974, Seeley and Tate, 1995). The liver metabolises digestive nutrients generating useable products that are released back into circulation or stored until needed. Toxic substrates are chemically modified by liver-specific enzymes such as P450, by either oxidation or hydroxylation reactions, rendering drugs inactive or making them easier to excrete as they become water soluble (Rang and Dale, 1991).

Within each liver lobe, connective tissue divides the lobe into around 100,000 liver lobules, which are the basic functional units with typical diameters between 0.8 - 2 mm, and several millimetres in length (Marieb, 1998, Martini, 2006, Guyton and Hall, 1996). The structure of the hexagonal liver lobule is shown in Figure 2.1B; each lobule is separated by the *interlobular septum*, consisting of connective tissue. The liver cells within the lobule are arranged in a series of irregular plates also known as hepatic cords, which radiate out from a central vein, in the shape of a wagon wheel. Each cellular plate is one cell thick, the hepatocytes, the

liver's parenchymal cells are lined by a single layer of endothelial cells and the channels between these layers are known as sinusoids, through which nutrient rich blood may flow, Figure 2.1B & 2.1C (Berry *et al.*, 1991).

**A**



**B**



**C**
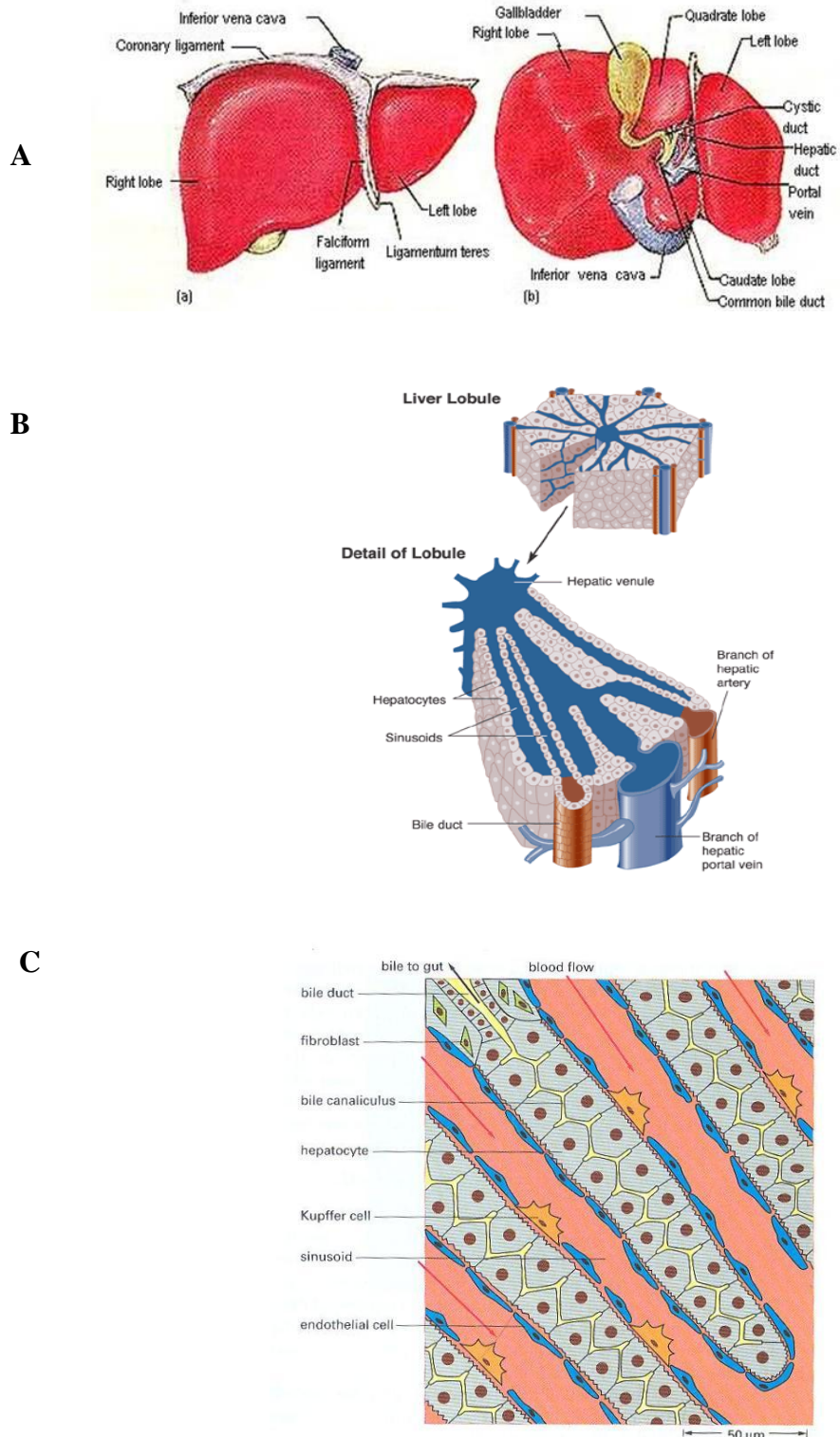
**Figure 2.1: Structure and cellular arrangement in the liver A)** Lobular arrangement of the liver, **B)** Cross section of a liver lobule, **C)** Cellular arrangement within the liver. (Reproduced from (Graaff, 1998, Cunningham and Van Horn, 2003, Alberts *et al.*, 1994b).

At the corner of each liver lobule are three structures, which together are termed the portal triad, they are a branch of the hepatic portal vein, a branch of the hepatic artery and a bile duct, Figure 2.1B. Blood from the two blood vessels of the portal triad, empty into the endothelial lined sinusoids, where the blood mixes and flows through the lobule to the central vein (Marieb, 1998). The way in which blood flows and circulates through the lobules gives rise to functional heterogeneity with a limited osmotic gradient (Mitzner, 1974, Braet and Wisse, 2002, Nakata *et al.*, 1960). Rather than each lobule acting on its own as a function unit undertaking all necessary processes, it has been determined that the liver is composed of functional sectors known as "Acini" (Rappaport *et al.*, 1954, Schiff, 1975). The acinus of a liver is split into three zones, each with unique location and functionality (Schiff, 1975, Jungermann and Sasse, 1978, Gebhardt, 1992).

Blood from the hepatic artery not only provides the liver with oxygen for the tissues, but brings cholesterol and other substances to the liver for processing. The liver produces half of the body's cholesterol, the rest is provided from ingested food (Marieb, 1998). Cholesterol is a major component of bile which aids digestion, in addition to this cholesterol is essential in the synthesis of adrenal hormones, estrogen, testosterone and angiotensin which takes place in the liver (Desimone and Cortese, 1992, Saltzman, 2004).

One of the liver's many functions is to produce bile; aiding digestion of foodstuffs through the emulsification of fat. Bile is composed of the breakdown products from haemoglobin from red blood cells, namely bilirubin and biliverdin, along with a range of salts, cholesterol, phospholipids and water (Marieb, 1998, Martini, 2006, Seeley and Tate, 1995). Bile is formed by the epithelial cells and excreted into bile canaliculi located between the opposing membranes of adjacent liver cells, Figure 2.1C. Bile exits the liver through hepatic bile ducts in the portal triad (Marieb, 1998, Guyton and Hall, 1996). At no point does bile enter the sinusoids or come into contact with the blood. In addition to this, the liver is also responsible for producing half of the body's lymph. Lymph is collected from the perisinusoidal spaces that drain into vessels that lie alongside the portal triad.

Another metabolic function which the liver performs is the regulation of glucose homeostasis, when the body is subjected to mild hyperglycaemia; the liver

takes up large amounts of carbohydrate from the blood and stores it as glycogen. The glycogen is broken down and released as the energy source glucose when needed to maintain blood sugar levels (Devlin, 1992, Butcher, 2003).

The liver also plays a crucial role in the destruction of aged red blood cells and the synthesis of many of the plasma proteins found within the blood. These can be split into two major categories: albumins and globulins. Albumins are large colloidal protein molecules. They influence osmotic pressure, fluid and plasma volumes exemplified by the secretion of angiotensin which helps in the regulation of blood pressure (Saltzman, 2004, Popper and Schaffner, 1957). The globulins aid in the transport of key substances including lipids, iron and copper. Additionally, globulins serve as immunoglobulins and a precursor to fibrin. The immunoglobulin IGF-1 is key in the stimulation of cell division and growth respectively (Saltzman, 2004). It is also possible for amino acids to undergo transamination within the liver to produce any required amino acids which is essential to haematological regulation. Furthermore the liver is responsible for the production of proteins associated with blood clotting including prothrombin and factors VII, IX and X (Saltzman, 2004).

## 2.2.2 Cell types of the liver

Two classes of cell types exist within the liver; parenchymal cells, more commonly referred to as hepatocytes, and non-parenchymal cells. The non-parenchymal cells act to support the function of hepatocytes and compromise of endothelial cells, Kupffer cells, Pit cells and Stellate cells. For the purposes of this report the review shall focus on hepatocytes.

## 2.2.2.1 Hepatocytes

Hepatocytes are responsible for the diverse functionality associated with the liver. Within the tissue, hepatocytes are the most abundant cell type accounting for 60-65 % of the cell population and approximately 90 % of the liver mass (Berry *et al.*, 1991, Greengar.O *et al.*, 1972). The hepatic cells are arranged in irregular sheets, also known as hepatic cords, with channels bordered by a single fenestrated layer of endothelial cells, which defines a series of sinusoids through which blood flows through the liver tissue. The "Space of Disse" provides a narrow gap between the endothelial layer and the hepatocytes (Berry *et al.*, 1991, Leeson and Leeson,

1970). Hepatocytes project large numbers of microvilli into the Space of Disse, where metabolic exchange takes place between the cells and the blood (Schiff, 1975, Berthiaume *et al.*, 1996, Moghe *et al.*, 1997, Alberts *et al.*, 1994b). The fenestrated endothelial layer controls the degree of interaction that the hepatocytes have with the nutrient rich blood flowing through the sinusoidal channels (Wisse *et al.*, 1996).

Within the Space of Disse, the hepatic cells are anchored into a unique basement membrane which consists of collagen type I and fibronectin, as the major components, with smaller amounts of collagen types III, IV, V and VI, and perlecan present (Martinez-Hernandez, 1984, Maher, 1998). Within the available literature, there is a degree of dispute about the presence of laminin in the hepatocyte basement membrane (Maher, 1998, Martinez-Hernandez, 1984, Schuppan, 1990, Griffiths *et al.*, 1991). However, despite the conflict of opinion, laminin is likely to be present within the liver basement membrane as it is a key component of ECM in connective tissues. It is possible that the overall distribution of this particular ECM component may be sparsely distributed in comparison to common basal laminae. The ECM of the liver will be discussed in detail in Section 2.2.3.

Hepatocytes have a distinctive polar morphology; many of the cells are binucleate with an additional set of chromosomes, known commonly as polyploidy (Ross *et al.*, 1989, Berry *et al.*, 1991). All of the cells are polyhedral in shape with three distinct plasma membrane surfaces. The lateral surfaces adjoin the neighbouring cells, through which cellular adhesion, signalling and binding the ECM occurs via filamentous actin found concentrated in the plasma membrane (Berry *et al.*, 1991, Berthiaume *et al.*, 1996, Ezzell *et al.*, 1993). The apical surface of the hepatocytes project into the bile canaliculus, with numerous microvilli; which aids excretion of the by-products of metabolism and bile. The polarity of the cells is aided by the ECM and cytoskeleton namely actin and myosin (Ezzell *et al.*, 1993).

## 2.2.3 The ECM of the Liver

All cells within the tissues of the body are surrounded by an ECM. The ECM is a dynamic 3-dimensional environment that plays a critical role in the way cells interact, develop and regenerate the tissues around them, Figure 2.2. The ECM can form a fibrous mesh surrounding cells as seen in cartilage or a continuous sheet which can induce cellular polarisation as seen in liver (Li *et al.*, 2003). The ECM

acts as a structural support and template architecture for cellular and tissue organisation. The ECM occupies a small percentage volume in the liver yet plays a disproportionately important role in liver function in both healthy and diseased states. The ECM has many molecular features including cell recognition motifs which mediate the attachment, survival, migration and remodelling of the cellular local environment.

### 2.2.3.1 ECM components

The ECM is composed of insoluble fibrillar proteins, such as collagen, laminin and elastin and a viscoelastic gel complex of proteoglycans and glycoaminoglycans, (GAGs). The ECM proteins, glycoproteins and glycans act as both signalling molecules and architectural elements to maintain the differentiated state of normal hepatocytes and non parenchymal cells. In a fibrotic or cirrhotic liver there are changes in the distribution, quantity and relative proportions of collagen and other ECM proteins. These changes result in altered cell phenotype, architectural distortion with abnormal blood flow, impaired diffusion and altered cell signalling.
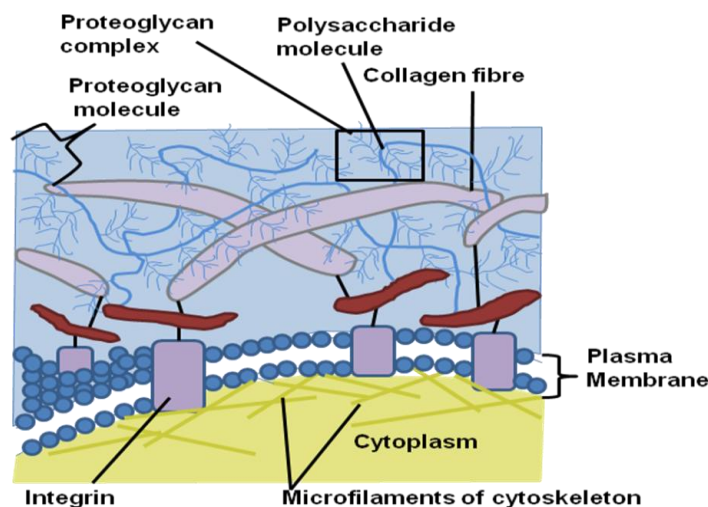


**Figure 2.2:** Schematic representation of the ECM. (Modified and adapted from (Campbell and Reece, 2007)).

Collagens are major structural proteins in normal and fibrotic liver. Ten different collagens have been identified in the adult liver; they are sub-divided into two groups, the fibrillar and non fibrillar. Collagens I, III, V and IV are the most abundant collagens in liver and are mechanically important, as they contribute tensile strength to the ECM (Schuppan *et al.*, 2001, Geerts *et al.*, 1989, Romanic *et al.*,

1991). Collagens IV, VI and VIII are known as network forming collagens. These collagens have interruptions in their helical chains which gives them flexibility. This flexibility allows them to make multiple associations forming networks rather than fibres, it also allows for them to interact with other proteins and macromolecules, in particular fibrillar collagens I and III.

Elastin and fibrillin are major components of fibres in the human body. They are responsible for mechanical properties of tissues in particular resilience. The function of different elastic fibres is not well known within the liver, however they do bind to multiple other ECM components in particular collagen and proteoglycans.

Laminins are a family of glycoproteins typically found in the basement membrane and associated with collagen IV, perlecan and enactin. They self assemble into mesh-like structures, and are architecturally significant in the basement membrane  (Martinez-Hernandez and Amenta, 1993, Hahn *et al.*, 1980).  Laminins interact with cell surface receptors to regulate additional functions including the development and differentiation of cells (Colognato and Yurchenco, 2000).

Fibronectin is the most abundant and widely distributed ECM glycoprotein with multiple binding domains including heparin binding domains, a collagen binding domain and a cell binding domain containing an Arginine-Glycine-Aspartic acid (RGD) motif. Assembly of fibronectin is driven by interaction with cell-surface integrins via the cell binding domain, signifying that it plays a particularly important role in the interaction of cells and the surrounding ECM (Martinez-Hernandez and Amenta, 1993).

Proteoglycans are proteins with GAG modifications which possess multiple functions within the ECM of the liver. Heparan, dermatan and chondroitin sulphate are all found within the liver. Proteoglycans are responsible for maintaining the structural integrity of the ECM and form a highly charged barrier to the passage of other molecules (Hahn *et al.*, 1980).  Proteoglycans also have a role in regulating growth factor signalling by binding to and sequestering many growth factors, consequently they are now recognised as signalling receptors (Roskams *et al.*, 1995, Tkachenko *et al.*, 2005).

Hyaluronic acid which does not bind to any of the component proteins is found in the ECM. Hyaluronic acid is a negatively charged carbohydrate polymer composed of repeating disaccharide units present in the ECM (McCourt, 1999). It is osmotically active causing water to be absorbed into the ECM. This osmotic swelling provides the ECM with its compressive strength (Hubbell, 2003). An ECM rich in hyaluronic acid is highly hydrated and promotes cellular migration. It makes up a minor component of the liver ECM, although it significantly increases in fibrotic liver (McCourt, 1999).

### 2.2.3.2 Location of ECM components

In a normal liver each separate region possesses different matrix and cellular components. The matrix surrounding the bile ducts and central venous region is similar to that of other epithelial organs, with a well organised basement membrane of collagen IV, entactin, laminin and perlecan (Martinez-Hernandez and Amenta, 1993). Whereas the Space of Disse, which lies between the epithelial cells and hepatocytes, has a unique matrix; lacking in continuous laminin, perlecan and enactin typically seen in basement membranes (Hahn *et al.*, 1980). Collagen IV is seen in discrete discontinuous deposits. With abundant amounts of fibronectin applied closely to the microvilli of the hepatocytes. Collagens III and VI are also present in this matrix composition, with collagen VI arranged homogenously and increasing in density from the portal to central regions of the liver (Loreal *et al.*, 1992).

### 2.2.3.3 ECM-Cell interactions

The localised architecture is determined by the cells through the production of specific proteins or through the secretion of enzymes, this allows for continuous remodelling of the ECM (Ramirez and Rifkin, 2003, Vu and Werb, 2000). The ECM provides the environment in which cells can organise themselves into cohesive tissue, consequently the ECM is often a barrier to cell migration. Matrix deposition in the normal liver is a dynamic process reflecting ongoing synthesis and degradation. Regulation of matrix deposition is important, as avoiding excess degradation is critical for avoiding liver tissue injury. Liver cells and their native ECM have a bidirectional relationship; almost all liver cells produce some matrix

and most in turn are phenotypically regulated by the ECM (Martinez-Hernandez and Amenta, 1993, Reid *et al.*, 1992).

Many of the functions of ECM molecules are mediated by their receptors; particularly the heterodimeric (α, β) transmembrane integrin family.  They are classified based on their capacity to interact with a specific ligand. Each integrin subunit has an extracellular domain, transmembrane domain and a cytoplasmic domain, Figure 2.3 (Masters and Anseth, 2004, Anselme, 2000, Takagi and Springer, 2002, Li *et al.*, 2003).  So far sixteen distinct α and eight β subunits have been identified, that make up twenty two known heterodimeric integrin receptors (E. Ruoslahti, 1991).  The organization of α and β subunits determines the ligand binding specificity and distribution of integrin hetreodimers for a variety of ECM proteins including fibronectin, vitronectin, laminin and collagen (Juliano and Haskill, 1993).  Usually one or more combinations of integrins can recognise the same ECM protein. However, integrin $\alpha_5\beta_1$ is unique as it only has the specificity to interact with fibronectin (Juliano and Haskill, 1993).  Matrix bound integrins initiate cell signalling through a variety of pathways and thereby regulate cell growth, differentiation and migration. In the liver they are important regulators of fibrosis and tissue remodelling. Integrin expression by the different cells of the liver reflects the specific composition of the underlying matrix and hepatocytes express a unique panel of integrins whilst biliary epithelial cells express integrins typical to most epithelial cells.
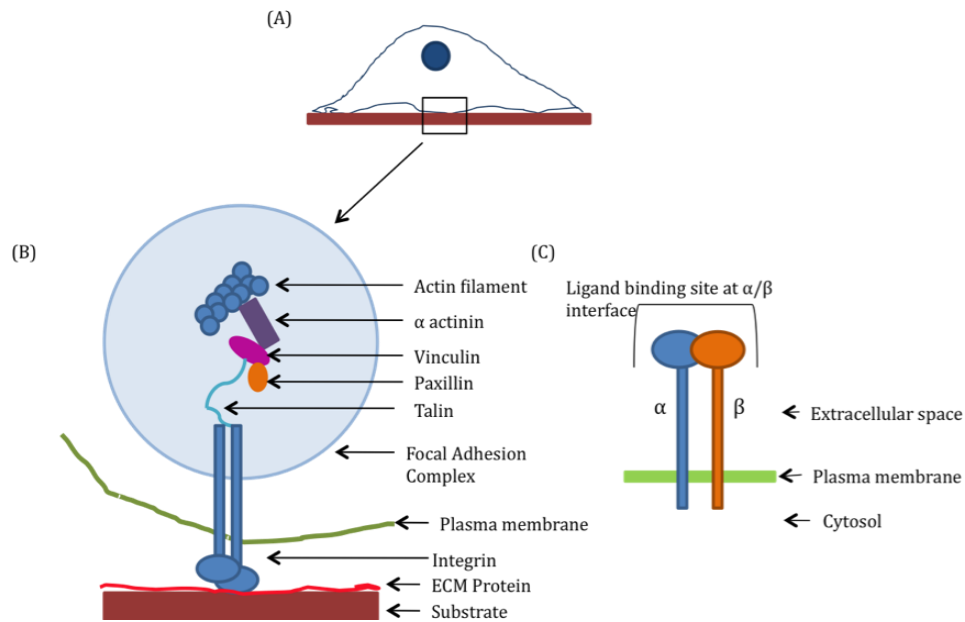
**Figure 2.3: A)** Cell coming into contact and forming focal adhesions with material**, B)** The interaction of inner and outer components of focal adhesion, **C)** Structure of the integrin subunits in their respective domains (Modified and adapted from (Alberts *et al.*, 1994a)).


At a site of cellular adhesion between a cell and the ECM, focal adhesions are formed comprising of clusters of integrins and ligands, Figure 2.3. The outer component of the focal adhesion interacts with ligand proteins in the ECM. The inner component of the focal adhesion is connected to an array of signalling proteins including vinculin, talin, paxillin and tensin, Figure 2.3B (Erkki Ruoslahti and Obrink, 1996, Anselme, 2000). These internal signalling proteins are known to interact with the actin filaments of the cellular cytoskeleton. Interactions between these proteins and the actin filaments can trigger biochemical signalling cascades which in turn can control the growth, proliferation, differentiation, locomotion and degree of gene expression within a cell, as previously mentioned (Johansson *et al.*, 1997). This type of "outside – in" signal transduction allows for the cell to gather information about their localised extracellular environment (Masters and Anseth, 2004, Alberts *et al.*, 1994c). Low numbers of focal adhesions have been shown to promote high motility in mammalian cells, whilst cell morphogenesis was shown to be associated with cells with increased numbers of focal adhesions (Kanda *et al.*, 2004). Clustering of integrins and ECM proteins promote cytoskeletal

reorganisation and signalling complexes after the assembly of actin filaments which in turn form large stress fibres (Giancotti and Ruoslahti, 1999). This causes further integrin clustering, enhancing matrix binding and integrin organisation. Organisation of the actin cytoskeleton is essential for maintaining cell shape and adhesion (Anselme, 2000).

Integrins may also be activated by an "inside – out" signalling cascade. Other receptors are similarly activated and induce a conformational change in the integrins and their ability to bind to ligands. The outer arrangement of the integrins on the cell surface may also change with this signalling cascade resulting in clustering of integrins and an increase in the number of recognition events. An example of the reorganisation of the cytoskeletal structures in "inside –out" signalling is in response to agonists such as $Mg^{2+}$ (Masters and Anseth, 2004, Hersel *et al.*, 2003, Takagi and Springer, 2002).

## 2.2.4 Asialoglycoprotein Receptors

The ASGP-R was initially discovered and characterised in mammalian liver by Ashwell and Morell (Ashwell and Morell, 1974). ASGP receptors are calcium dependent carbohydrate recognising surface receptors found on the cell surface membrane of hepatocytes. The main function of this lectin based receptor is to bind to galactosyl terminal glycoproteins and remove them from circulation by endocytosis (Hirose *et al.*, 2001, Cho *et al.*, 2007).

The ASGP-R can be regarded as a good indicator of the proliferative or differentiative state of hepatocytes (Hirose *et al.*, 2001). When hepatocytes are in a proliferative state the overall expression of ASGP-R is reduced and the receptor can be secreted into the local environment. During proliferation hepatocytes grow in response to stimuli, including signals from integrins which may prevent the transcription and thus the production of ASGP-R whilst in this state, Figure 2.4. When in a differentiative state, the hepatocytes express large numbers of the ASGP-R, Figure 2.4. It should be noted that the ASGP-R in its differentiated state can take up asialoglycoproteins via endocytosis and then recycle to reappear on the cell surface (Hirose *et al.*, 2001).
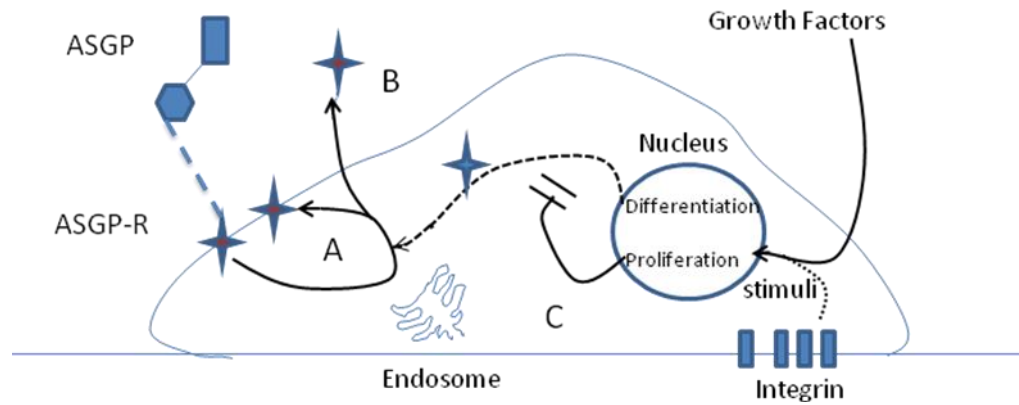
**Figure 2.4:** Mechanism for the regulation of hepatocytes: ASGP-R expression in proliferative and differentiative states. **A)** Recycling of ASGP-R onto the cell surface, **B)** In a proliferative state the hepatocyte receives signals from activated integrins resulting in shedding of ASGP-R, **C)** Expression of ASGP-R on the proliferative cell surface is decreased in response to activated integrins. (Modified and adapted from (Hirose *et al.*, 2001)).

While the ASGP-R on hepatocytes does not usually promote cell adhesion *in-vivo*, asialoglycoprotein ligands have been manipulated as adhesive ligands in order to induce hepatocyte adhesion to biomaterial surfaces (Kim *et al.*, 2004, Geffen and Spiess, 1992, Masters and Anseth, 2004). Hepatocyte adhesion may be guided through unique ASGP-R-carbohydrate interactions via galactose terminated ligands within a material. This mechanism has been exploited to create materials that induce hepatocyte specific adhesion to biomaterials or enable liver specific drug delivery, as will be discussed in Part C (Cho *et al.*, 2006, Gutsche *et al.*, 1994a, Kobayashi *et al.*, 1994, Du *et al.*, 2006).

It has been noted that the structure and density of the carbohydrate; monosaccharide or disaccharide; significantly affects the degree of attachment and morphology of hepatocytes. It was seen on sugar derivatized polystyrenes that the type of sugar attached to the polystyrene backbone influenced hepatocyte adhesion affinity. When the disaccharide sugars lactose or melibose are attached to the polystyrene backbone the terminal residues are β-galactose and α-galactose respectively. Hepatocytes show a higher affinity for the β-galactose residue compared to the α-galactose residue (Cho *et al.*, 2006, Kim *et al.*, 2003a). When the

monosaccharide form of galactose is attached to polystyrene, the hepatocytes have a higher affinity for this surface than either of the disaccharide derivatized materials. (Kim *et al.*, 2003b, Cho *et al.*, 2006, Park *et al.*, 2003).  Upon studying the morphology of the cells those hepatocytes cultured on the disaccharide derivatized materials were rounded in shape with no rearrangement of the actin cytoskeleton. Hepatocytes cultured on a high coating concentration (>50ng/ml) of the monosaccharide galactose derivatized material had spread out and flattened resulting in the formation of actin stress fibres after two days of culture (Kim *et al.*, 2003a). Ise *et al.* reported that hepatocytes attached to a galactose carrying polystyrene surface at a coating density below 20 ng/ml expressed low levels of ASGP-R and possessed higher proliferative capacities than cells on a coating density of 50 ng/ml or above (Ise *et al.*, 2001).  It has also been shown that the density of the galactose coating influences the mechanisms by which hepatocytes may attach. Hepatocyte adhesion to galactose derivatised surfaces results in rapid accumulation of ASGP-Rs in a patch at the site of adhesion (Weigel, 1980, Weisz and Schnaar, 1991).  At high coating densities on poly (N-p-vinylbenzyl-4-o-β-D-galactopyranosyl-D-gluconamide), (PVLA) (100 µg/ml), the ASGP-Rs on the cell surface membrane of hepatocytes are clustered within sites of focal adhesion as a large patch. This clustering prevents integrin receptors from taking part in the cell adhesion process (Kim *et al.*, 2003b).  At low PVLA densities (0.5 µg/ml), hepatocytes allow integrins to participate in the adhesion process within the space where ECM proteins have been secreted from hepatocytes during the culture process. The presence of integrin binding plays a significant role in turning spheroidal shaped cells into spread cells, and in "outside-in" signal transduction.

### 2.2.5 Conclusions

The native liver has a unique architecture and with multiple functions ranging from metabolic regulation to haematological regulation and bile production. Hexagonal liver lobules contain plates of parenchymal cells; with the hepatocytes encased by the ECM. The ECM contains cell recognition motifs which mediate cell survival, attachment, migration and remodelling of the local environment.  Specific carbohydrate recognising ligands are displayed on the surface of hepatocytes and these ASGP-Rs are now being exploited as guides for cellular adhesion onto galactose bearing polymer scaffolds, with an aim to specifically support the

attachment of hepatocytes and enable them to maintain typical hepatocyte cell behaviours.

## Part B: Modification of materials to control cell interactions

### 2.3.1 Overview

Cellular responses to a material can be influenced by engineering the chemistry, stiffness and topography of a surface, Figure 2.5. Each is an inter-related process where surface specific properties can be directed by changes to topography, chemistry and stiffness of a material.
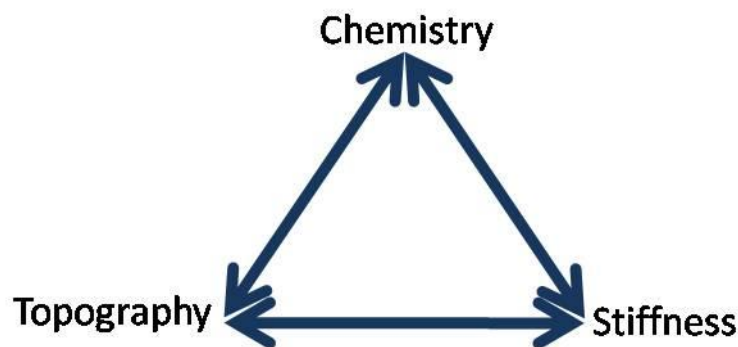


**Figure 2.5:** Schematic illustrating the inter-relation between chemistry, topography and stiffness.

### 2.3.2 Strategies to control protein adsorption and wettability

When an implant is placed in physiological conditions, proteins adsorb onto the surface within one second, creating a layer of organic matter known as a conditioning film, many proteins denature at the aqueous-solid interface as their conformation is disrupted (Ratner, 1996). Control of this interface is key to obtaining the desired cellular interactions for both traditional implants and tissue engineered mimics (Gray, 2004). The strength and type of adhesion seen depends upon the proteins adsorbed, the surface properties of the material, as well as any proteins secreted by cells (Brash, 1983, Neumann *et al.*, 1983, Masters and Anseth, 2004, Castner and Ratner, 2002). Cell adhesion to a surface is mediated by specific interactions which can either be adhesive; through integrins and other cell surface matrix receptors binding to insoluble ECM proteins, or non-adhesive; via serum albumin. Either way, the majority of cells bind to a component of the ECM.

Protein adsorption is a dynamic process, where small mobile proteins such as albumin attach to a surface first. These proteins can then be displaced by larger less mobile proteins with a higher affinity for the surface. This displacement cycle is known as "The Vroman effect" and occurs over the course of minutes to days depending on the size of the proteins involved (Vroman, 1962). Consequently, the composition of the film adsorbed onto the surface is likely to change over time depending on the affinity of a protein for the surface. In essence, the physical and chemical properties of the surface and the adsorbing protein influence the Vroman effect.

Surface-specific or non surface-specific interactions can be induced through surface modification and functionalisation of the biomaterial. Surface modification enables the materials' interfacial properties to be altered with no change to the underlying bulk properties (Cousins *et al.*, 2004, Lord *et al.*, 2006). There are three methods employed to alter the surface properties of a material; by changing the surface topography, by changing the surface chemistry or by altering the stiffness of the material, Figure 2.5. All approaches are interrelated as a change in surface chemistry can lead to nanoscale topographies being generated (Masters and Anseth, 2004, Taborelli *et al.*, 1995). In particular changes in chemical and topographical parameters have a profound effect on protein adsorption and final conformation, which in turn results in a variety of cell responses (Lewandowska *et al.*, 1989, Lewandowska *et al.*, 1988, Lewandowska *et al.*, 1992, Lord *et al.*, 2006, Taborelli *et al.*, 1995). In order to control cell response to a material, the surface properties must be controlled to obtain the desired protein response and consequently the desired cellular response.

Surface topography is known to affect protein adsorption (Stevens *et al.*, 2005, Masters and Anseth, 2004). Surfaces containing surface features such as grooves and ridges have been shown to align adsorbed proteins along them; additionally surface features can alter the conformation of an adsorbing protein. The composition and conformation of proteins in the conditioning film regulates how cells respond to a surface, due to the availability of binding sites on adsorbed proteins. Hence surface topography and changes to surface chemistry can affect the binding peptide ligands available for cellular interactions (Masters and Anseth, 2004, Stevens *et al.*, 2005, Clark, 1994, Allen *et al.*, 2006, Castner and Ratner, 2002).

Surface-specific or non surface-specific interactions can be induced through surface modification and functionalisation of the biomaterial, Figure 2.6. The simplest method to control the cell-interface interaction is to make the material hydrophobic or hydrophilic through the introduction of functional groups. Surface hydrophobicity is thought to affect the conformation of adsorbed proteins. On highly hydrophobic surfaces, proteins denature and spread causing structural rearrangement of the protein (Ostuni *et al.*, 2003, Masters and Anseth, 2004). A hydrophobic surface consists of non-hydrogen bonding apolar groups at the surface of the material such as $CH_3$ and $C_6H_5$, whereas a hydrophilic surface tends to have hydrogen bonding groups, i.e. OH, SH, $CONH_2$, or charged groups, i.e. $COO^-$, $NH_3^+$ at the surface. Consequently, the water in air contact angle of the material is greater than 90º for a hydrophobic surface and less than 90º for a hydrophilic surface.

Cell culture studies have shown that most cell types non specifically adhere to hydrophilic surfaces over hydrophobic surfaces with moderately hydrophilic surfaces (20-40º water contact angle) producing the most favourable cell responses (Grant *et al.*, 2005, Krasteva *et al.*, 2001, Ma *et al.*, 2003). Cells attach in large numbers, spread out and become confluent on hydrophilic surfaces, whilst on hydrophobic surfaces the cells tend to remain spherical, clumped together and remain easy to distinguish. The strength of cell adhesion may also be affected by surface hydrophobicity, Van Kooten *et al.* reported that fibroblasts adhered more firmly to substrata with high (~110º) contact angle than substrata with a low contact angle (~15º), although the authors state that the underlying surface chemistry is likely to have affected the data (Van Kooten *et al.*, 1992). It is noteworthy that hydrophobicity of a surface does not take into account the underlying surface chemistry, for example two different surfaces may possess the same wettabilities but have very different underlying surface chemistries (Allen *et al.*, 2006).

Taborelli *et al.* established that when albumin was adsorbed onto a hydrophilic $NH_2$ surface and a more hydrophobic $CH_3$ surface the overall height of the molecule was lower on the $NH_2$ surface than the $CH_3$ surface (1.6 ± 0.6 nm and 4.0 ± 1.3 nm respectively) as determined by Atomic Force Microscopy (AFM). The lower height conformation of the $NH_2$ surface promoted cell adhesion, whereas the $CH_3$ surface with the taller albumin height did not support cell growth (Taborelli *et al.*, 1995, Ranieri *et al.*, 1993).

Increasing Selectivity & Complexity

-Altering wettability
-Introducing functional groups (e.g. OH, COOH)
-Introducing biofunctional groups (e.g. RGD, saccharides)
-Introducing Biomolecules (e.g. proteins, sugars)
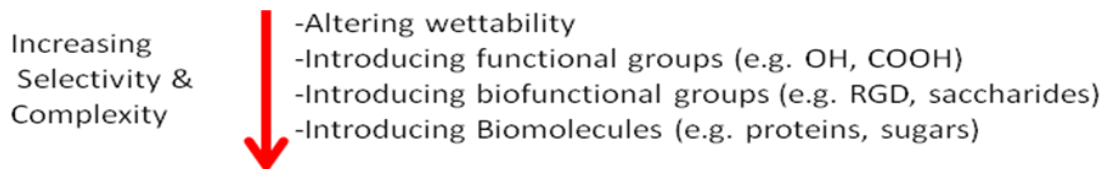
**Figure 2.6:** Methods of altering materials to direct cell behaviour.

The incorporation of functional groups onto a surface can be achieved using self assembled monolayers (SAMs), silanes and plasma modification discussed below, Section 2.3.3. The incorporation of a specific chemical functionality can result in a "chemical handle" being created on an inert surface such as PEG to which further chemical modifications can be made. It has been shown that more hydrophobic surfaces tend to adsorb larger amounts of protein than hydrophilic ones (Nath *et al.*, 2004, Masters and Anseth, 2004, Ostuni *et al.*, 2003). Conformational changes in the adsorbed protein such as denaturing and structural rearrangement are brought about by surfaces with very high hydrophobicity. Roach *et al.* showed that albumin (67 KDa), an anti-coagulant serum protein, adhered to hydrophobic $CH_3$ surfaces in greater amounts than to hydrophilic OH surfaces (Roach *et al.*, 2005). Proteins have been shown to adsorb more readily to a positively charged surface than a negatively charged one due to the effects of electrostatic repulsion (Masters and Anseth, 2004). Most proteins contain an overall negative charge at physiological pH, thus are more attracted to positively charged surfaces than those that are negatively charged. Proteins with differing charges adsorb onto surfaces with a variety of charges and hydrophobicities. It was observed that proteins readily adsorbed onto hydrophobic polystyrene surfaces, even in conditions of electrostatic repulsion (Arai and Norde, 1990a, Arai and Norde, 1990b). However, a greater degree of adsorption was seen where electrostatic attraction was present. In surfaces that were less hydrophobic, proteins bound to the surface with lower affinity. Consequently, this data highlights the greater role of electrostatic repulsion/attraction forces over very hydrophobic surfaces in controlling protein adsorption (Arai and Norde, 1990a, Arai and Norde, 1990b).

Surface charge is known to affect cell adhesion to substrates. Studies have shown that positively charged surfaces produce a higher degree of cell attachment than negatively charged surfaces (Sugimoto, 1981, Webb *et al.*, 1998, Maroudas,

1975). The reason for this is that cells contain a net overall negative charge (Vitte *et al.*, 2004, Sugimoto, 1981), thus a positively charged surface will partially counteract the repulsive barriers between the two, as described by Derjaguin-Landau-Verwey-Overbeek (DLVO) theory (Vitte *et al.*, 2004). Overall it is difficult to separate the effects of charge and wettability and their subsequent effect on cell adhesion and spreading.

### 2.3.3 Surface Modification

### 2.3.3.1 SAMs

Surface chemical modification of polymers can be used to create patterned surfaces to study the effects of protein adsorption and consequently mammalian cell behaviour (Ratner and Bryant, 2004). Various methods for the chemical modification of surfaces have been described (Dee and Bizios, 1996, Wang *et al.*, 2004). SAMs can be used to incorporate chemical adhesion ligands onto the surface of a material. SAMs are stable, highly ordered, single molecule thick films that can present specific functional groups to the surface at a very high density (Nath *et al.*, 2004, Mrksich, 2000, Castner and Ratner, 2002). When a gold surface is exposed to a solution of alkanethiols, a dense monolayer of alkanethiols will spontaneously self assemble. Sulphur atoms in the alkanethiols bond with the gold surface producing a densely packed, ordered monolayer of long chain molecules with a defined structure and chemistry which can be subsequently tailored to an application (Castner and Ratner, 2002, Nath *et al.*, 2004, Mrksich, 2000). The terminal group of the alkanethiols can be altered to present functional groups such as $NH_2$, COOH, OH, $CH_3$ at the surface interface. These groups consequently alter the overall wettability of the surface interface. The generalised structure of SAMs on a gold surface is shown in Figure 2.7. Stable cell adhesion is determined by the surface density of the adhesion ligands present on the material. The use of alkanethiolates on gold currently provides the best options to control the presentation of the ligands to the surface (Cousins *et al.*, 2004, Webb *et al.*, 2000, Mrksich, 2000). However SAMs are fragile due to their thinness and their lack of covalent bonding, so consequently can only be used as a model system to evaluate cell-surface and protein-surface responses *in-vitro* (Nath et al., 2004).
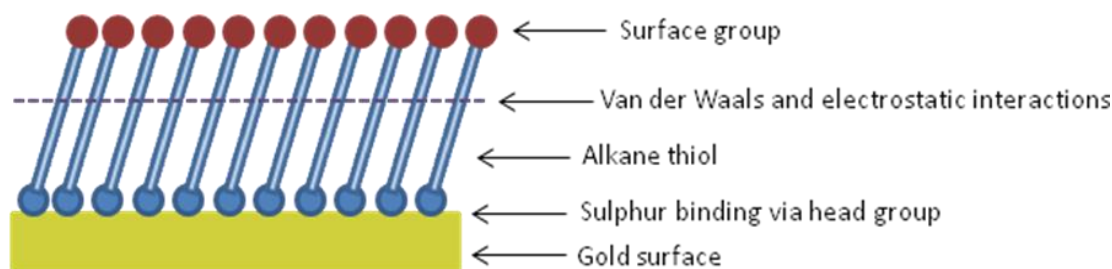
**Figure 2.7:** A schematic diagram of a self assembled monolayer, SAM, binding to a gold surface (Modified and adapted from (Ratner and Hoffman, 1996)).

Sigal *et al.* showed that protein adsorption onto SAMs of alkanethiols on gold with diverse wettabilities was dependant on the size of the protein. Small proteins (i.e. albumin, 67 KDa) were shown to only adsorb onto the least wettable surfaces tested. The larger proteins, such as fibrinogen (340 KDa), adsorbed onto all surfaces: to the greatest extent on the least wettable surfaces, with one notable exception of an ethylene glycol terminating SAM (Sigal *et al.*, 1998).

### 2.3.3.2 Silanes

Silane modification is used to modify hydroxylated or amine containing surfaces such as glass, silicon, alumina, quartz and metal oxides. Many different silanes are available to produce surfaces with a wide variety of functional groups. The production method is relatively rapid and results in the production of a stable surface (Castner and Ratner, 2002, Lewandowska *et al.*, 1989). This method has been reported as a potential way to control the behaviour of various cell lines, with differing chemical functionalities inducing varying cell responses. It has been shown that osteosarcoma cells on silane surfaces presenting $CH_3$, OH and $C_6H_5$ groups were slow to proliferate whereas growth was not affected on surfaces presenting COOH and $NH_2$ groups (Filippini *et al.*, 2001). The disadvantages of utilising silane groups for surface modification are the limited surface coverage compared to SAMs and the possibility of multiple layers forming during the modification procedure (Ratner and Hoffman, 1996). A silica surface with an epoxy terminating silane was coupled to PEG diamine molecules by Piehler *et al.* to create a passive background that resisted the adsorption of serum proteins. Consequently, biological ligands could be coupled to the terminal amine group of the immobilised PEG chains including thrombin inhibitors. The epoxy silane reaction resulted in surfaces that were not as

heterogeneous but possessed a higher density of immobilised PEG compared with amino-silane surfaces (Piehler *et al.*, 2000).

### 2.3.3.3 Plasma Modification

Plasma modification enables the surface chemical and physical properties to be altered covalently without affecting the underlying bulk properties (Hoffman, 1984). Additionally, low-powered systems may be able to alter the surface chemistry of a polymer with minimal effect to the surface roughness. By controlling the parameters associated with plasma deposition namely, power, excitation frequency, pressure, gas flow rate, and reactor geometry, the surface chemistry can be tailored for a particular application (Jones, 1993). Plasma treatment works by altering the molecular structure of the polymer in the outermost layers by replacing side chains or chains in the polymer backbone with moieties from the working gas (Jones, 1993, Hoffman, 1984). The wettability of polymeric materials can be increased by plasma treatment in atmospheres such as $O_2$, Ar, $N_2$ and $NH_3$, to incorporate chemical groups such as carboxyl, hydroxyl, amine and urea-type groups respectively. Biomedical applications for this technique include increasing the wettability of blood contacting devices such as catheters and blood bags and hence improving the efficacy of the devices (Gombotz and Hoffman, 1987).

### 2.3.4 Biofunctional groups

A more specific surface modification is to add biofunctional groups in the form of short peptides or saccharides onto the surface of the material. This type of modification interacts directly with specific ligand binding receptors on the cell surface e.g. integrins or lectins. There are many peptide sequences, typically from ECM resident proteins that have been used to influence cell attachment and function, including the aforementioned tripeptide RGD motif, an epitope found within fibronectin, and the penta-peptide isoleucine-lysine-valine-alanine-valine (IKVAV), which is an epitope within laminin (Masters and Anseth, 2004).

Typically, these surface modifications are conducted on non-adhesive, non-fouling materials, which are resistant to protein adsorption, the most commonly used is PEG or one of its derivatives to produce specific adhesion sites. RGD has been used extensively as a biological ligand to promote cell adhesion and has been shown

to be more effective than using the whole fibronectin molecule (Castner and Ratner, 2002, Hersel *et al.*, 2003, Sakiyama-Elbert and Hubbell, 2001). Around half of all known integrins are thought to bind to a variety of ECM molecules in a RGD dependent manner. Thus RGD is now used as a general motif to promote cell attachment via integrins (Hersel *et al.*, 2003).

To obtain the desired cell response, the type of ligand, spatial distribution and density all need to be considered as they have a collective influence on cell adhesion and migration (Sakiyama-Elbert and Hubbell, 2001). It was found that approximately $10^5$ copies/cell of the RGD tri-peptide were required to induce cell adhesion and focal adhesion formation. This value was considerably higher when using the entire fibronectin molecule to generate a similar effect (Massia and Hubbell, 1991). In a follow up to this work Hubbell *et al.* showed that the incorporation of the short peptide arginine-glutamic acid-aspartic acid-valine (REDV) onto a non fouling surface resulted in preferential attachment of endothelial cells (via integrin $\alpha_4\beta_1$) in comparison to other cells such as fibroblasts, smooth muscle cells and platelets. Hence by using specific ligands to modify the surface, surfaces can be activated for specific cell types although this is not found in the majority of cases (Hubbell *et al.*, 1991).

Recent studies have seen an increased use of patterned substrates to control cell adhesion and to examine downstream gene expression. The development of patterning at a sub-micron level has lead to studies of focal adhesion sites which are of the order of 50nm to 500nm. Focal adhesion sites form, enable cells to bind to the ECM via large clusters of integrins that link intra-cellularly to actin filaments and provide initiation sites for signalling pathways and anchor points for the cellular cytoskeleton as discussed previously. It has been proven by Koo *et al.*, that cell adhesion and signalling depends on the size of the nano-patterning and the density of the peptide, in this case RGD, within the patterns (Koo *et al.*, 2002).

Short peptide sequences generally lack receptor specificity (Keselowsky *et al.*, 2005, Hubbell *et al.*, 1991). However, the use of short peptide sequence is preferable over the use of entire proteins to allow for a higher density of immobilisation and hence functionality at a surface. Peptides also exhibit a higher degree of stability towards sterilisation, pH changes, purification, heat treatment and

storage. They are easier to characterise and are more cost effective than whole proteins (Hersel *et al.*, 2003, Ratner and Bryant, 2004, Sakiyama-Elbert and Hubbell, 2001).

**2.3.5 Biomolecules**

The most selective and complex modification to a material is to incorporate whole biomolecules such as proteins and polysaccharides. Surfaces modified in this way potentially allow for cells to bind to native proteins and sugars that would typically be found in the ECM. Various different molecules possess properties which are desirable for use in biomaterial coatings.

An example of biological molecule immobilisation involves the use of antibody attachment to a surface. If, for example an antibody raised against albumin is bound to a material surface this will then enable specific binding of albumin either by pre-adsorption or from the blood stream when implanted. Immobilisation of the antibody can be achieved by utilising the well known avidin-biotin interaction in combination with commonly available biotin-tagged antibodies. Avidin is immobilised onto a material surface then coupled to biotinylated antibodies to induce the interaction. Attachment of albumin to an anti-albumin surface can bring about a reduction in platelet attachment, spreading and an inhibitory effect to bacterial adhesion (McFarland *et al.*, 1998, An *et al.*, 1995). Attaching biomolecules in this way reduces the likelihood of a protein denaturing upon interaction with a surface and additionally offers a degree of spatial control over the attached molecule. The methodology is dependent on two separate protein-ligand interactions; if either loses its functionality then the surface is no longer viable.

Surfaces displaying glycans can be prepared by immobilising the sugar molecule onto a spacer molecule, such as PEG, acrylic acid or cyanuric chloride to preserve the chemical functionality and availability of the sugar molecule by ensuring the function critical groups are not involved in the attachment process (Gotoh *et al.*, 2004, Yoon *et al.*, 2002, Kim *et al.*, 2000, Steffen *et al.*, 2000). For example, lactose (galactose β1-4 glucose) was covalently immobilised onto silk fibroin using cyanuric chloride as a spacer. The material was then evaluated as a potential scaffold to induce hepatocyte attachment and culture. It was noted that solutions with a higher density of lactose present performed better than the silk

fibroin control, Table 2.1 (Gotoh *et al.*, 2004). Direct glycoconjugation of sugars to a polystyrene derivative has been used to introduce oligosaccharides into vinyl strain monomers. These materials form soluble micelle structures in water and therefore can be used to coat materials at varying densities to regulate cellular differentiation and cell-cell interactions (Hayashi *et al.*, 2004). The type of sugar selected can be matched to the optimised cell function required, allowing for unique specificity of the coating.

| Paper | Surface Type | Material/Chemical functionality | Cell Type | Comments |
|---|---|---|---|---|
| Taborelli *et al.* (1995) | SAMs | NH$_2$ & CH$_3$ | N/A | Albumin adsorbed on NH$_2$ had a lower height than CH$_3$ surface determined by AFM. NH$_2$ promoted cell adhesion whereas CH$_3$ surface did not. |
| Sigal *et al.* (1998) | SAMs | Various including CH$_3$, OH, OCH$_3$ and EG | N/A | Variety of proteins adsorb to surfaces. Small proteins only adsorb to least wettable surfaces. Large proteins adsorb to all surfaces with exception of EG terminated SAM. |
| Van Kooten *et al.* (1992) | Bulk material | PMMA, TCP, Glass, FEP-Teflon | Human Skin fibroblasts | Cells adhered to the hydrophobic surfaces stronger than the hydrophilic surfaces. |

| Roach *et al.* (2005) | SAMs | OH & CH$_3$ | N/A | Albumin adsorbed to CH$_3$ surface in greater amounts than OH surface. Fibrinogen is adsorbed by a multistep process including conformational change. |
|---|---|---|---|---|
| Arai *et al.* (1990) | Various | PS(-), PS(+), POM, α-Fe$_2$O$_3$ (+),α-Fe$_2$O$_3$ (-) | N/A | RNase(-), LSZ(-), MGB(++) and α-LA(+) adsorbed to surfaces. Hydrophobic surfaces adsorbed all proteins regardless of electrostatic repulsion. Overall adsorption is lower on hydrophilic surfaces than hydrophobic surfaces |
| Filippini *et al.* (2001) | Silane | NH$_2$, COOH, CH$_3$, C$_6$H$_5$, OH | Osteosarcoma cells | Proliferation of cells is slowed by CH$_3$, OH and C$_6$H$_5$ surfaces. COOH and NH$_2$ surfaces had no effect. |

| Piehlar *et al.* (2000) | Silane | Epoxy-PEG-biomolecule | N/A | Biological ligands coupled to the terminal $NH_2$ of the immobilised PEG chains inc. thrombin inhibitors. Epoxy silane reaction resulted in surfaces that were not heterogeneous but possessed a higher density of immobilised PEG compared with amino-silane surfaces. |
|---|---|---|---|---|
| Gombotz & Hoffman (1987) | Plasma deposition treatment | $O_2$, Ar, $N_2$ and $NH_3$ plasmas. | N/A | Increases the wettability of blood contacting devices thus improving the efficacy of the devices |
| Massia & Hubbell (1991) | Peptide-polymer hybrid | RGD modified glass | Human foreskin fibroblasts | $10^5$ copies/cell of the RGD tri-peptide were required to induce cell adhesion and focal adhesion formation |

| McFarland *et al.* (1998) | Plasma glow treatment | Albumin modified polymers | Platelets | Albumin attached to a surface via antibodies. Decrease in platelet adhesion and spreading seen on albumin surfaces. |
|---|---|---|---|---|
| Gotoh *et al.* (2004) | Glyco-conjugate | Silk fibrion- cyanuric chloride spacer- lactose | Hepatocytes | Solutions with a higher density of lactose present performed better than the silk fibroin control. |

**Table 2.1:** Overview of types of surface modification available, the chemistry and associated biological responses. EG=ethylene glycol, PS = polystyrene, RNase = ribonuclease, MGB = myoglobin, POM=polyoxometalate, $Fe_2O_3$= haematite, LSZ = lysosyme, α-LA = α-lactoalbumin, PMMA=poly(methylmethacrylate), TCP= Tissue culture plastic.

**2.3.6 PEG based surfaces and hydrogels**

PEG and PEG-based hydrogels (Zourob *et al.*, 2006) have been used to provide a well defined platform from which fundamental studies have been undertaken. PEG based materials resist non-specific protein adsorption and interactions, and can be chemically altered for specific applications such as the inclusion of adhesive regions and biodegradable linkages, enabling cells to be entrapped at tissue-like densities. The mass transport properties of PEG based materials can be tailored by adjusting polymer chain lengths and density(Tsang *et al.*, 2007). Consequently, PEG based scaffolds have been widely utilised because of their hydrophilicity, biocompatibility and ability to be chemically modified for precise applications. Methods for chemically tailoring synthetic hydrogels and surfaces were discussed above in Section 2.3.3, ranging from simple changes in wettability to highly specific alterations using biomolecules and artificial proteins to obtain specific cell attachment and the control of cell-substratum interactions.

In order to evaluate cellular responses to chemically modified surfaces, the surface must be designed to resist non-specific adsorption of biomolecules. Non-specific adsorption of organic matter, i.e. proteins, platelets or bacteria, to surfaces can prevent specifically regulated cell behaviours by the surface and are never found in nature. Thus non-specific interactions must be prevented in order to provide surfaces that either control the conformation and orientation of proteins so that the body will specifically recognise them, or prevent protein adsorption completely. The latter of these two surfaces are known as "non-fouling" (Masters and Anseth, 2004, Castner and Ratner, 2002, Mrksich, 2000, Mrksich, 2002). Methods to prevent protein adsorption and create non-fouling surfaces include specific biomolecule coatings or using materials such as PEG.

PEG provides a boundary layer which prevents protein and hence cellular interactions with an underlying substrate material (Kingshott *et al.*, 2002, Harder *et al.*, 1998). Protein adsorption is regulated between a balance of steric repulsion, Van der Waal's forces and hydrophobic interactions between a protein and a surface. The steric repulsion of biomolecules by PEG is dependent on the degree of salvation of the PEG chains also known as osmotic repulsion and the conformational entropy of the PEG chains or elastic repulsion (Harder *et al.*, 1998, Jeon *et al.*, 1991, Jeon and

Andrade, 1991). At a given molecular weight of PEG, there is a specific grafting density above which proteins and other biomolecules will be repelled. However, Whitesides group, (Harder *et al.*, 1998), showed that overpacking of SAMs capped with ethylene glycol groups resulted in fibrinogen adsorption to the surface. It is thought that this occurred as the functional groups were so tightly packed they lost their helical structure required to maintain their hydration, thus allowing adsorption to occur (Kingshott *et al.*, 2002, Harder *et al.*, 1998). Graft density of PEG can be affected by chain length, as longer chains are more disordered with larger helical coils thus the interaction strength between PEG molecules and limiting graft density is increased (Kingshott *et al.*, 2002, Masters and Anseth, 2004, Sofia *et al.*, 1998). Additionally, longer PEG chains are generally thought to resist protein adsorption better than shorter ones (Prime and Whitesides, 1991). The longer the length of the PEG chain the larger the area occupied per attachment site, nullifying low-graft densities (Masters and Anseth, 2004, Elbert and Hubbell, 1996, Sofia *et al.*, 1998).

Polyethlene glycol acrylamide (PEGA) is a non-fouling copolymer platform compatible with organic solvents and aqueous conditions, making it an ideal material for chemical modification and biological assays respectively(Meldal, 1992, Halling *et al.*, 2005). The material prevents non specific cell adhesion and provides an ideal environment for enzyme catalysis reactions (Todd *et al.*, 2007, Zourob *et al.*, 2006). The material is optically transparent which allows for ease of assessment of results.

PEG and other non-fouling materials, such as poly(vinyl alcohol) (PVA), and poly(hydroxyethyl methacrylate) (pHEMA), may be functionalised using a variety of methods including end point attachment (Piehler *et al.*, 2000), plasma deposition (Castner and Ratner, 2002), graft polymerisation (Masters and Anseth, 2004) and silanation (Jo and Park, 1999).

**2.3.7 Conclusions**

Enhancing material biofunctionality to provide favourable protein adsorption and hence cellular responses can take on differing levels of complexity and specificity from relatively simple changes in the hydrophilicity of the material to a material functionalised with charged groups, peptides or whole biomolecules. Including specific chemical and physical cues can result in controlled and specific cell adhesion and consequently more tissue typical cell behaviour.

# Part C: Systems that mimic the hepatic environment

## 2.4 Tissue Engineered Constructs

Due to the complexity of the liver the literature on liver tissue engineering does not fall into a single category; multicellular aggregates, scaffolds, bioreactors, microtechnology with cell patterning and *in-situ* regeneration all contribute to this diverse field. In the interests of this report the use of scaffolds will be the key focus for discussion. As mentioned earlier, the survival, growth and proliferation of hepatocytes is regulated by their local surroundings and more specifically by the ECM. Culturing hepatocytes *in –vitro* frequently results in a loss of viability and down-regulation of liver specific functions such as albumin and urea synthesis, and dedicated enzymes such as CYP1A. Consequently, maintenance of such functionalities is essential for hepatocytes grown *in-vitro* culture conditions.

### 2.4.1 Non-Galactosylated Scaffolds

The initial development of scaffolds for use in liver tissue engineering occurred in the early 1990's. Cima–Griffiths *et al.* evaluated hepatocyte behaviour and functionality on synthetic polymers; polylactic co-glycolic acid (PLGA) and PLGA-polylactic acid (PLA) blends against Matrigel™ and collagen type I. It was determined that these synthetic materials could support hepatocyte growth and functionality over five days in culture. The rate of albumin secretion by cells on the PLA-PLGA polymer blend material doubled over the course of 5 days whilst the collagen type I control decreased by 60 % (Cima *et al.*, 1991).

The use of foams and sponges has been investigated extensively with collagen and alginate foams being widely utilised. Ranucci *et al.* produced a range of porous collagen foams by freeze drying with pores of 10 μm, 18 μm and 82 μm on which hepatocytes were cultured, Table 2.2. It was observed that cells were compacted and cuboidal in shape in the smallest pores, with positive vinculin staining indicative of cell-to-cell contacts and a high degree of albumin production, 40 pg/cell/day. The 18 μm porous foam resulted in cell spreading and decreased albumin levels, 4 pg/cell/day. The largest pores, 82 μm, enabled formation of an extensive cellular network, with increased albumin secretion 26 pg/cell/day and positive E-cadherin staining. The larger pores resulted in larger cell aggregates within the foam to form; however, the level of albumin synthesis is not comparable

(Ranucci *et al.*, 2000). Alginate sponges with pores ranging in diameter from 100-150 µm were evaluated as a 3D matrix for hepatocyte growth (Glicklis *et al.*, 2000). It was determined that this scaffold allowed the seeded cells to maintain their viability and metabolic rate; however the cells did not proliferate. The cells did form spheroids within the sponge over the course of seven days, reaching an average size of 100 µm. It was shown that albumin secretion rates increased over the initial seven days of culture to a maximum of 60 µg albumin/$10^6$ cells/day compared to the control collagen dishes were albumin secretion was negligible (Glicklis *et al.*, 2000). The urea secretion rates were seen to be comparable between the alginate sponges and collagen type I coated dishes (~100 µg urea/$10^6$ cells/day) (Glicklis *et al.*, 2000). Hence long term functionality studies shows that alginate scaffolds can perform as well as traditional aggregate cell cultures.

The use of porous microspheres has been popular in drug delivery systems but they also have demonstrated an ability to be used for tissue engineering applications to deliver bioactive molecules such as growth factors to specific sites (Mathiowitz and Langer, 1987, Newman and McBurney, 2004, Cao and Shoichet, 1999, Oe *et al.*, 2003). The use of microspheres allows for versatile modification in a controllable manner. Growth factors can be incorporated into the microspheres to regulate cell growth and promote vascularisation, additionally microspheres can be assembled into a variety of shapes. Mooney *et al.* utilised work from Cima-Griffith *et al.* to use PLGA in the form of microspheres to deliver epidermal growth factor (EGF), Figure 2.8A. EGF was shown to stimulate hepatocyte growth in a dose dependant manner, Figure 2.8B & C. This study resulted in improved engraftment of transplanted hepatocytes *in vivo* (Mooney et al., 1996). Poly(3 hydroxybutyrate-co-3-hydroxyvalerate) (PHBV) microspheres are biocompatible, biodegradable and can be produced in a variety of  sizes to suit the intended application (Sendil *et al.*, 1999, Hu *et al.*, 2003). Zhu *et al.* demonstrated the potential use of PHBV microspheres for producing liver tissue engineered constructs. Microspheres with a range of diameters between 100-300 µm were produced with a rough external topography and internal pores between 10-20 µm from the processing method. The highest seeding efficiency was achieved on the smallest of the microspheres, with cells bridging across the individual microspheres after four days of culture, Table 2.2. By day seven the albumin secretion from the microspheres was between two to four times

higher than the two dimensional positive control (Zhu *et al.*, 2007). The P450 activity of the cells showed a steady increase over the course of the study, there was no significant difference between the microspheres, however, the data was significantly higher than the poly(L-lysine) film used as the positive control. Compared to the 2D positive control the overall proliferation and improved hepatic function of cells grown on microspheres shows them to have excellent potential as a liver construct.
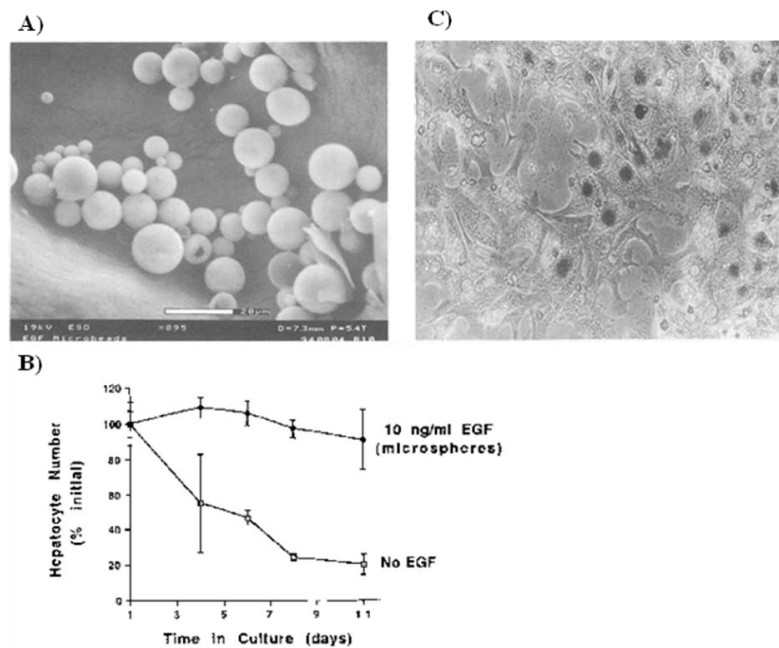


**Figure 2.8:A)** PLGA microspheres containing EGF, **B)** Percentage change in number of cells over 11 days culture in media containing 10 ng/ml EGF from microspheres and media not containing EGF **C)** Micrograph of hepatocytes growing in presence of 10 µg/ml EGF released from the microspheres (Modified and reproduced from (Mooney *et al.*, 1996)).

Bio-characteristics of GAGs include the binding and modulation of growth factors and cytokines as well as playing a role in the adhesion, migration and differentiation of cells. Heparin has been shown in the past to improve the maintenance of albumin synthesis when hepatocytes are cultured on collagen gels (Fujita *et al.*, 1987). It is possible that contact with GAGs within the ECM may be necessary to maintain differentiation *in-vitro*. Cell differentiation is improved when there is good cell communication with the ECM (Lecluyse *et al.*, 1994). Heparin coatings are used to enhance blood compatibility of many biomaterials. The

immobilisation of GAGs such as heparin and chondroitin-6-sulphate on collagen films and gels with and without a cross-linking reagent was evaluated by Kataropoulou *et al*. The viability of primary hepatocytes on the cross-linked collagen films was higher than that of the collagen film alone with the cells retaining their morphology. In contrast, cross-linking GAGs into collagen gels decreases cell viability, Table 2.2. It was also observed that heparin on both the films and the gels decreased the glucuronidation pathway within the cells making it unfeasible for use in an artificial liver device. Whereas cross-linked chondroitin 6 sulphate on collagen films improved the glucuronidation metabolic pathway in primary hepatocytes, Table 2.2 (Kataropoulou *et al.*, 2005, Grant *et al.*, 2005). The use of GAGs within surfaces is at an early stage of research, however this approach may provide a means to maintain or even increase the expression of hepatocyte specific functions in a monolayer culture environment.

Semler *et al.* illustrated the importance of the mechano-sensitive nature of hepatocytes on polyacrylamide gel discs, in addition to their ability to bind to modified surfaces. Rigid substrates (G´=5.6 kPa) yielded reduced liver specific activities, whilst compliant gels (G´=1.9 kPa) resulted in the cells remaining spheroidal as there is little mechanical stimuli for the cells, Table 2.2 (Semler *et al.*, 2005, Wells, 2008). Encapsulation of hepatocytes in photopolymerisable PEG illustrated the effect of micro-environmental stimuli on the fate of cells(Semler *et al.*, 2005, Underhill *et al.*, 2007, Tsang *et al.*, 2007, Wells, 2008).

| Paper | Material | Cell Type | Comments |
|---|---|---|---|
| Cima-Griffiths *et al.* (1991) | PLGA and PLA-PLGA polymer blends | Primary hepatocytes (Rat) | Materials support growth and functionality over 5 days. Rate of albumin secretion by cells on the PLA-PLGA polymer blend material doubled during culture period whilst the collagen type I control decreased by 60 %. |
| Rancucci *et al.* (2000) | Collagen foams | Primary hepatocytes (Rat) | Freeze-dried foams with 3 pore sizes (10, 18 & 82 $\mu$m). Smaller pores resulted in compact cells and positive vinculin staining. Large pores resulted in extensive cellular network. Albumin secretion not comparable between scaffolds. |
| Glicklis *et al.* (2000) | Alginate sponges | Primary hepatocytes (Rat) | Pores ranging in diameter from 100-150 $\mu$m. Viability & metabolic rate of cells maintained over 14 days. Spheroid formation seen. Albumin secretion increased with formation of spheroids – better than collagen type I control. Urea synthesis between materials was comparable. |

| | | | |
|---|---|---|---|
| Mooney *et al.* (1996) | PLGA microspheres containing EGF | Primary hepatocytes (Rat) | EGF was shown to stimulate hepatocyte growth in a dose dependant manner. ~70 % of EGF is released after 5 days. Improved engraftment of transplanted hepatocytes *in vivo*. |
| Zhu *et al.* (2006) | PHBV microspheres | Hepatoma cell lines, Hep3B & HepG2 (Human) | Range of diameters 100-300 μm. Internal pores 10-20 μm. Highest seeding efficiency on smallest microspheres. Albumin secretion 2-4 times higher than 2D positive control on Day 7. |
| Kataropoulou *et al.* (2005) | GAGs (heparin & chondroitin-6-sulphate) in collagen gels | Primary hepatocytes (Rat) | Incorporation of heparin in collagen decreased cell viability & glucuronidation pathway. Chondroitin − 6-sulphate on collagen films increased glucuronidation pathway. |
| Semler *et al.* (2004) | Polyacrylamide gel discs | Primary hepatocytes (Rat) | Hepatocytes shown to be mechano-sensitive. Rigid substrates resulted in flattened cells with reduced liver specific activities. Compliant gels resulted in spheroidal cells as there is little mechanical stimuli. |

**Table 2.2:** Summary table of key attributes of non-galactosylated tissue scaffolds that mimic the hepatic environment.

**2.4.2 Galactosylated Scaffolds**

As discussed in Part B, it is essential to regulate cell-to-material interactions in natural and synthetic mimics for applications in whole-cell biological evaluation platforms and tissue engineering. A method of enhancing hepatocyte adhesion to surfaces is to use galactose mediated hepatocyte recognition mechanisms, first described by Ashwell & Morell (Ashwell and Morell, 1974). As introduced above, ASGP-R found on the hepatocyte cell surface recognises and binds to galactose moieties, Section 2.2.4. This specificity has led to the development of several galactose carrying polymers and gels. The initial synthetic polymer of choice was PVLA, as this polymer contains β-galactose in the oligosaccharide side chains which in turn are covalently bound to a polystyrene backbone, Figure 2.9A. It was reported by Kim *et al.* that using PVLA as an artificial ECM regulated cell proliferation, morphology and differentiation, and that these behaviours were distinct in comparison to hepatocytes grown on natural ECM. It has been shown that hepatocyte adhesion to PVLA is mediated by galactose specific interactions between ASGP-R of the cells and the galactose residues seen in the polymer. The hepatocyte morphology observed is dependent on the galactose density available to the cells; at a high density of 100 µg/ml PVLA the hepatocytes displayed a spherical appearance whereas at a low density of 0.5 µg/ml PVLA the cells appeared spread out on the surface of the material, Table 2.3 (Kim *et al.*, 2004, Kim *et al.*, 2003b).

ECM-hepatocyte contact regulates cell behaviours i.e. proliferation, migration and survival. However the precise mechanisms by which hepatocyte-ECM interactions control cellular behaviour are unclear. Therefore the nature of cell adhesion signalling is based on current knowledge of potential mechanisms available in the literature. Focal adhesion kinase (FAK) is known to be a key molecule involved in the formation of focal contacts via integrin signalling. FAK mediates cellular functions such as growth, survival, spreading and migration. When cells bind to the ECM via integrins, autophosphorylation is triggered at the Tyr-397 residue of FAK. Therefore the phosphorylation of FAK can be used as an indicator of integrin binding to an ECM mimic. Kim *et al.* compared phosphorylated FAK (pFAK) expression on hepatocytes cultured on PVLA as a synthetic galactose carrying ECM against a naturally occurring ECM protein; fibronectin. The results showed that although the rate of adhesion was almost identical for both surfaces, pFAK was not

detected in the cells cultured on PVLA even at 12 hours post seeding whereas it was present at all time-points taken on the fibronectin surface, Figure 2.9B. The down regulation of pFAK in hepatocytes cultured on PVLA is likely to be the result of differences in cellular adhesion. It has also been seen that hepatocytes attached to PVLA surfaces did not exhibit localised vinculin, actin and pFAK at the point of focal adhesion, Figure 2.9C. On the other hand hepatocytes grown on collagen exhibited localisation of pFAK, and vinculin, Figure 2.9C. This is indicative that hepatocytes grown on PVLA with ASGP-R mediated adhesion do not initiate integrin mediated signalling (Kim *et al.*, 2003b).
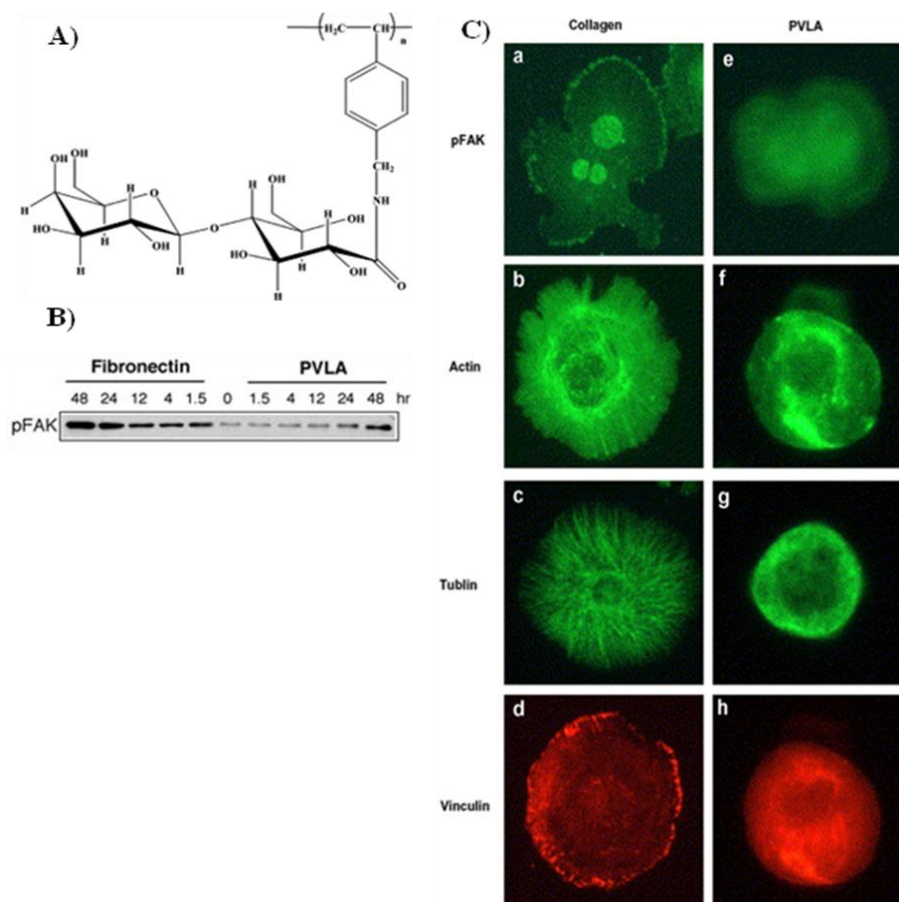


**Figure 2.9: A)** Structure of poly (N-p-vinylbenzyl-4-o-β-D-galactopyranosyl-D-gluconamide) (PVLA) **B)** Western blot analysis of FAK phosphorylation **C)** Focal adhesion and cytoskeletal proteins of attached hepatocytes onto collagen and PVLA (Modified and reproduced from (Kim *et al.*, 2003b, Cho *et al.*, 2007)).

In a similar strategy, Quirk *et al.* conjugated galactose onto poly (D, L- lactic acid) (PLA) via the amine functionality.  The surfaces were evaluated in a co-culture system of hepatocytes and hepatic stellate cells. Attachment of hepatocytes was enhanced twofold on the galactosylated PLA compared to unmodified PLA using the highest galactose concentration. It was determined that attachment to the surface of the material was predominately by ASGP-R, as blocking the receptors with unbound galactose in the media resulted in a reduction in levels of attachment.  The PLA and modified PLA surfaces bound similar numbers of hepatic stellate cells, confirming the specific targeted nature of the galactosylated surface to hepatocytes via the ASGP-R-galactose bond (Quirk *et al.*, 2003).

Natural polymers have also been galactosylated in an aim to create synthetic matrices to host hepatocytes growth.  Galactose moieties have been covalently coupled with alginate and the hepatocytes then consequently entrapped within the galactosylated alginate capsules. The results show that cells entrapped in the galactose bearing alginate showed better viability and improved albumin and urea synthesis compared to those in alginate scaffolds alone (Yang *et al.*, 2001). Galactosylated chitosan (GC) has been used in conjunction with alginate to form a hybrid scaffold for cellular attachment, where hepatocyte aggregation was observed in the presence of EGF owing to the galactose specific recognition event between the galactose in the chitosan and ASGP-R of the hepatocytes.   Park *et al* illustrated that this system had good hepatocyte adhesion to the scaffold however some cell loss was seen due to poor mass transfer within the spheroids of cells that formed, Table 2.3 (Park *et al.*, 2003). The cellular response was seen to vary depending on the galactose density used in functionalised chitosan; at high concentrations (5 µg/ml) the hepatocytes were round in shape and formed spheroids after 24 hours in culture in the presence of EGF, whereas at low concentrations (0.05 µg/ml) the cells were flat and spread out in the presence of EGF (Park *et al.*, 2003).  Many researchers try to promote spheroid formation of hepatocytes within tissue engineered ECM mimics as the structure represents the tight cell-to-cell contact seen in the liver. Tight cell-to-cell contact reproduces the tight junctions and bile canaliculi seen in the ultrastructure and morphology of a liver lobule. Consequently, liver specific functions such as albumin secretions and detoxification functions are maintained. However, the efficacy of hepatocyte spheroids in clinical applications is limited due

to poor mass transport of nutrients, oxygen and key metabolites into and out of these large cell aggregates (Glicklis *et al.*, 2004). Cell loss from these spheroids is problematic in forming and maintaining these structures since the spheroids detach easily from surfaces (Du *et al.*, 2006).

Galactosylated chitosan has been electrospun to form a nanofibrous mesh with an average diameter of ~160 nm. These nanofibrous scaffolds provide hepatocytes with an ECM like environment which enables higher expression of liver specific functions including albumin secretion, urea synthesis and cytochrome P450 maintenance than that of hepatocytes cultured on galactosylated chitosan films. Hepatocytes on electrospun GC were seen to have formed as flat aggregates that interacted closely with the nanofibres compared to 3D spheroidal aggregates seen on GC films, Table 2.3. The nanofibrous scaffolds also have a greater degree of mechanical stability compared to spheroid hepatocyte aggregates (Feng *et al.*, 2009, Chu *et al.*, 2009).

Encapsulation of hepatocytes within galactosylated alginates was shown by Yang *et al.* although the presence of EGF and insulin was shown to be vital in the maintenance of spherical cell morphologies, with the degree of attachment correlating to the concentration of galactose moieties. Those cells in spheroidal form exhibited greater degree of cellular differentiation and higher levels of P450 metabolites rather than cellular monolayers, Table 2.3 (Yang *et al.*, 2002, Kim *et al.*, 2003b).

Galactose moieties have been coupled with gelatin to form three-dimensional porous sponge matrices. The survival rate of hepatocytes on this sponge substrate was longer than the survival rate of hepatocytes cultured on a collagen type I monolayer. In addition, the cells on the matrices formed spheroids which helped to maintain secretion of serum albumin and synthesis of urea, Table 2.3 (Hong *et al.*, 2003). However, with the lack of a vascular network in the matrix, mass transfer limitations are experienced in the large spheroid colonies formed (Glicklis *et al.*, 2004).

Berthiaume *et al.* showed that three dimensional matrices were more effective at inducing differentiated hepatocyte functions than two dimensional ones. Collagen ECM based sandwich scaffolds cause hepatocytes to re-arrange their

cytoskeleton and adopt *in-vivo* like morphology and functions (Berthiaume *et al.*, 1996, Ezzell *et al.*, 1993, Selden *et al.*, 2000). The use of a synthetic sandwich culture has recently been developed, by sandwiching a hepatocyte monolayer between a top layer of porous polyethylene terephthalate (PET) track-etched membrane (which was modified with glycine-arginine-glycine-aspartic acid-serine (GRGDS)) and a bottom layer of galactosylated PET film. This culture system provided ECM based functionalities to the hepatocytes, which in turn induced the formation of hepatic polarity. Cell-to-cell interactions were promoted with differentiated functions such as albumin and urea synthesis maintained to a higher level than that of a traditional collagen sandwich culture, over the course of 14 days, Table 2.3. This synthetic system has the potential to replace the ECM based sandwich culture system for relevant applications in liver tissue engineering and drug development (Du *et al.*, 2008).

| Paper | Material | Cell Type | Comments |
|---|---|---|---|
| Kim *et al.* (2004) | PVLA | Primary hepatocytes (Mouse) | Hepatocyte morphology dependant on galactose density. 100 μg/ml PVLA resulted in spheroidal morphology, whereas 0.5 μg/ml resulted in flattened cells |
| Yang *et al.* (2002) | Galactosylated Alginate | Primary hepatocytes (Mouse) | Improved cellular viability, albumin, P450 & urea synthesis compared to alginate alone. Greater degree of cellular differentiation |
| Park *et al*. (2003) | Galactosylated Chitosan (GC) | Primary hepatocytes (Mouse) | Good hepatocyte adhesion & mechanical strength. Spheroid formation in the presence of EGF. Some cell loss seen due to poor mass transport within spheroids |
| Feng *et al.* (2009) | Electrospun galactosylated chitosan | Primary hepatocytes (Rat) | Nanofibrous mesh ~160 nm diameter fibres. High levels of liver specific functions maintained; albumin, urea, P450. Flat aggregates formed with better mechanical stability than cells on GC films |

| Hong *et al.* (2003) | Gelatin sponges | Primary hepatocytes (Mouse) | Gelatin crosslinked with galactose. Cell survival was greater than that of cells grown on Collagen type I. Spheroidal cell formations seen which maintained albumin & urea synthesis. |
|---|---|---|---|
| Du *et al.* (2008) | PET sandwich culture with GRGDS on top &galactosylated PET as bottom layer | Primary hepatocytes (Rat) | Provides ECM based functionalities, induces cell polarisation. Albumin & Urea synthesis maintained to higher levels than traditional collagen sandwich culture. |
| Quirk *et al.* (2003) | Galactosylated PLA discs | Primary hepatocytes (Rat) | Selective hepatocyte adhesion via the ASGP-R. Presence of soluble galactose in media reduces attachment levels. Modified surface is unable to bind additional cell numbers of stellate cells due to lack of specificity. |

**Table 2.3:** Summary table of key attributes of galactosylated tissue scaffolds that mimic the hepatic environment.

### 2.4.3 Conclusions

There is little doubt in current literature that both the specific chemistry and mechanical environment of the ECM influence both hepatocellular behaviour and phenotype. Thus, both factors must be considered in the overall design of hepatocellular constructs for cell culture and *in-vitro* liver model applications. It has been shown that natural materials such as collagen, alginates and the use of GAGs as biological cues can produce comparable results without having to utilise specific cell receptor guides. The asialoglycoprotein receptors found on the cell surface membrane of hepatocytes recognise and can bind to galactose containing moieties. This unique specificity has led to the development of several galactose carrying polymers and gels based on natural and synthetic materials. Engineering surfaces and materials to obtain desired interactions with cells and their ECM remains a considerable challenge. For example, while simple functions of the liver can be maintained using current tissue engineered systems, other more complex functions seen in the tissue are lost.

## Chapter 3.0:  Synthesis and characterisation of galactose functionalised PEGA hydrogel surfaces

### 3.1 Introduction

There are powerful reasons both clinical and commercial for the development of systems that can augment the hepatic structure and function. The important role of the ECM in liver development and maintenance has led to the use of natural and synthetic biomaterials in order to mimic this environment.  Synthetic polymeric hydrogels can be customised in terms of material chemistry, stiffness and structure to maximise cell survival, proliferation and tissue formation. Synthetic hydrogels can be altered for specific applications, e.g. maximising cell-cell interactions and have the ability to entrap large amounts of water, comparable to that of native tissue. Many cell lines including chondrocytes, fibroblasts and hepatocytes have all been successfully immobilised in and on PEG based gels (Ratner and Bryant, 2004, Raeber *et al.*, 2005, Underhill *et al.*, 2007). The diffusion properties of hydrogels can be customised by adjusting polymer chain lengths and densities to suit the intended application (Peppas *et al.*, 2000, Lutolf and Hubbell, 2005, Kloxin *et al.*, 2009).

The use of a co-polymer of PEG and acrylamide, PEGA, is being used as a starting point to develop a unique platform which will promote hepatocyte viability and hepatocyte specific functions. Hepatocytes are anchorage dependant cells. The hepatocyte plasma membrane displays the ASGP-R which has a unique affinity for galactose. This hepatocyte specific binding interaction was exploited in the hydrogels described in this thesis through the incorporation of galactose moieties. The use of ASGP-R as an adhesive ligand for hepatocytes has been utilised before in both natural and synthetic biomaterials. It is hoped that applying this well-defined carbohydrate recognition system to hydrogels may result in a system that will preferentially support the attachment of hepatocytes and enable them to maintain normal cellular functions.   It has also been shown that the density of the galactose coating influences the mechanisms by which hepatocytes may attach. The use of ASGP-R to initially bind the cells followed by integrin binding is most likely to induce phenotypically normal hepatocyte behaviour which has been shown to require tight cell-cell contacts.

This chapter describes the synthesis of surface supported PEGA hydrogel, and its subsequent modification to incorporate galactose moieties through covalent coupling. A range of surfaces were manufactured and characterised. The three systems prepared were; PEGA, PEGA with galactose moieties in the form of lactobionic acid (LA) and PEGA with a control sugar in the form of D-glucuronic acid (GA).

## 3.2 PEGA surfaces

All chemicals and reagents, unless otherwise stated were purchased from Sigma Aldrich Company Ltd. (Gillingham, UK) and were used as received.

The development of PEGA surfaces resulted in a material which was compatible with both organic solvent conditions for chemical modification and aqueous conditions required for biological assays (Meldal, 1992, Halling *et al.*, 2005). PEGA itself provides an optically transparent non-biofouling platform which has so far been used to pattern surfaces to prevent non-specific cell adhesion, suitable environments for enzyme catalysis and enzyme responsive surfaces (Todd *et al.*, 2007, Zourob *et al.*, 2006).

### 3.2.1 Production of PEGA surfaces

PEGA hydrogel surfaces were prepared as shown in Figures 3.1 & 3.2. The monomers mono and bis – acrylomido PEG ($M_w$=1900) (Polymerlabs, UK) were mixed in a 1:1 ratio w/w with dimethylacrylamide and dissolved in dimethylformamide (DMF) and less than 1 % Irgacure 784 (Ciba, Basel, Switzerland) e.g. 0.5g $PEGA_{1900}$ monomers, 0.5g dimethylacrylamide, 1.5ml DMF and 0.02g Igracure 784. The solution was stirred for at least five hours in the dark using a magnetic stirrer. To produce PEGA surfaces, a few drops of the PEGA solution were spin coated onto epoxy functionalised glass slides (Genetix, Hampshire, UK) for 10 seconds at 1000 RPM. Protective polyethylene sheets were placed over the surface to prevent drying of the hydrogel. The surfaces were exposed to UV light (365nm) for approximately 50 seconds.

### 3.2.2 Modification of PEGA Surfaces

Galactose moieties were bulk immobilised by mixing saccharides and coupling agents with PEGA macro-monomers prior to polymerisation. 4-O-β-D-galactopyranosyl-D-gluconic acid, hereafter referred to as LA, was pre-dissolved in dimethyl sulfoxide (DMSO) and then added to the monomer mixture along with two crosslinking agents, N-hydroxysuccinimide ester (NHS) and 1-ethyl-3-[3-dimethylaminopropyl] carbodiimide hydrochloride (EDC). For example; 0.1 mmol LA was pre-dissolved in 0.5 ml of DMSO and added to 0.5 g PEGA$_{1900}$ monomers, 0.5g dimethylacrylamide, 1 ml DMF and 0.02 g Igracure 784, 23 mg NHS and 41.3mg EDC. The solution was stirred for at least five hours in the dark using a magnetic stirrer. A control sugar, GA was introduced in an identical manner to PEGA. To produce PEGA crosslinked surfaces with either LA or GA, a few drops of the PEGA solution were spin coated onto epoxy functionalised glass slides (Genetix, Hampshire, UK) for 10 seconds at 1000 RPM. Protective polyester sheets were placed over the surface to prevent drying of the hydrogel. The surfaces were exposed to UV light (365 nm) for approximately 50 seconds, Figures 3.1 & 3.3.

### 3.2.3 Fourier-Transform Infrared Spectroscopy (FTIR)

FTIR spectra were measured using a Nicolet 5700 FTIR spectrometer to obtain the transmission spectra of the PEGA based gels and the reaction constituents. Samples were scanned in either solid or liquid form. A background scan was collected prior to the sample data being taken. The scan settings used were 64 scans per sample and a resolution of 4 cm$^{-1}$. This technique was used to determine if sugar had been chemically incorporated into PEGA by examining the bond stretching and bending.

### 3.2.4 Dansyl Chloride Labelling

The homogeneity of the PEGA surfaces was characterised using dansyl chloride labelling of primary amines, and analysis by fluorescence microscopy. Surfaces were rinsed in ethanol, methanol and DMF before being immersed in 2 ml of dansyl chloride solution and left in the dark for one hour. The dansyl chloride solution was freshly prepared as follows; 10 ml DMF, 180 mg Dansyl chloride and 125µl N' N- diisopropylethylamine (DIPEA). Surfaces were then rinsed in DMF,

ethanol and distilled water and subsequently viewed by fluorescence microscope (Eclipse 50i, Nikon, Melville, USA) using the Lucia software.

### 3.2.5 Fmoc-Phe labelling

PEGA coated quartz slides with varying concentrations of LA and GA (0- 0.2 mmol), were manufactured, as described in Section 3.2.2. Fluorenyl-9-methoxycarbonyl (Fmoc) protected Phenylalanine (Bachem Ltd, St. Helens, UK) (5x molar equivalence) was then coupled onto PEGA coated quartz surfaces in the presence of (2-(1H-Benzotriazole-1-yl)-1,1,3,3-tetramethyuronium hexafluorophosphate) (HBTu) (4.9x molar equivalence) and N,N-Diisopropylethylamine (DIPEA) (10x molar equivalence) in DMF. Fmoc amino acid coupling was carried out by immersion in solution for 2 hours in the first instance followed by rinsing with DMF, methanol, ethanol and DMF again, then immersion in fresh solution overnight. The surfaces were then rinsed as described above. This reaction pathway produced Fmoc- amino acid PEGA surfaces containing sugars, shown schematically in Figure 3.1.

The amount of Fmoc amino acid attached to the PEGA surfaces was then quantified using UV-visible spectroscopy. UV-visible spectroscopy was carried out at room temperature on a Jasco V-660 Spectrophotometer fitted with a thin film sample holder. The loading of Fmoc groups was quantified by measuring the absorbance at 301 nm, which could be correlated with the amount of free amines left in the PEGA material following sugar incorporation. A standard curve of known Fmoc-Phe concentrations was used to determine the molar extinction coefficient and the degree of loading of Fmoc-Phe on the PEGA surfaces.
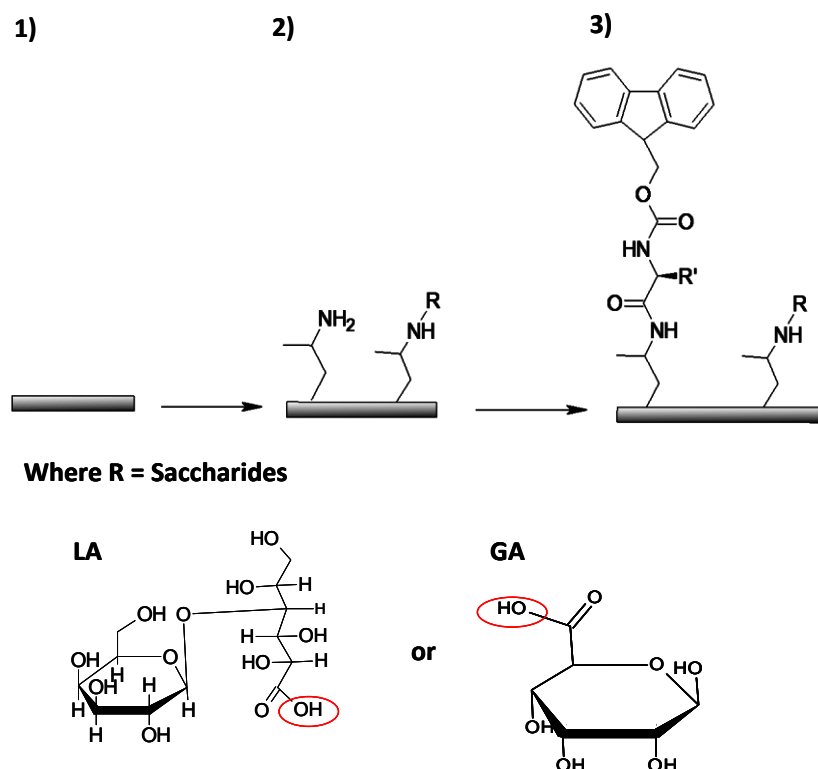
**Figure 3.1: Schematic representation of surface preparation: 1)** Glass Substrate **2)** UV cured PEGA monolayer with varying sugar concentrations, **3)** Attachment of Fmoc-Phe to remaining free amine groups by solid phase peptide synthesis, where R' is the peptide side group. Red circle on the sugars indicates groups lost during bonding process.

### 3.2.6 Interferometry

PEGA coatings were examined using an interferometer (Microxam Interferometer, Phase Shift, Tuscan, Arizona, USA) using x 10 magnification, a measurement area of 810 x 615 μm and a spatial sampling of 1.1 x 1.3 μm. The glass/polymer interface was exposed using a scalpel to remove half of the PEGA coating. The interface was then examined to determine the depth of the layer.

### 3.2.7 Protein Adsorption Assay

PEGA surfaces were incubated in 2 ml cell culture medium containing 10 % foetal bovine serum (FBS) at 37ºC, 5 % $CO_2$ and 95 % humidity for 24 hours. Epoxy functionalised glass slides and tissue culture plastic were used as control materials. The medium was removed and the samples rinsed in 1 ml distilled water on a shaker for 15 minutes. The samples were then transferred to fresh wells where the adsorbed

protein was then desorbed by treatment with 6M urea on a shaker for 60 minutes at room temperature. The urea/protein solution was quantified using the Quant-iT protein assay kit (Molecular Probes, Paisley, UK) using the manufacturers protocol. All reagents were equilibrated to room temperature prior to use. The Quant-iT protein reagent was diluted 1:200 in the Quant-iT protein buffer, 190 µl of this working reagent was loaded into each well of a 96 well plate, to which 10 µl of the desorbed urea/protein sample was added. The fluorescence of the product was measured using a fluorescence plate reader (Fluostar OPTIMA, BMG LABTECH, Germany) at 495/585 nm. Sample protein concentrations were determined using a standard curve of known protein bovine serum albumin/urea concentrations. Three samples of each surface were produced for testing. The experiment was repeated six times.

## 3.3 Results and Discussion

The PEGA monomers consist of acrylamide, a bis-acryloamido PEG crosslinker and a mono-acrylamide PEG. UV polymerisation results in the formation of a hydrogel consisting of acrylamide backbone crosslinked with poly (ethylene glycol) (PEGA$_{1900}$), Figure 3.2. The polymer carries PEG linkers with pendant primary amines groups, which can be used for chemical functionalisation. The overall reaction schematic is shown in Figure 3.2.
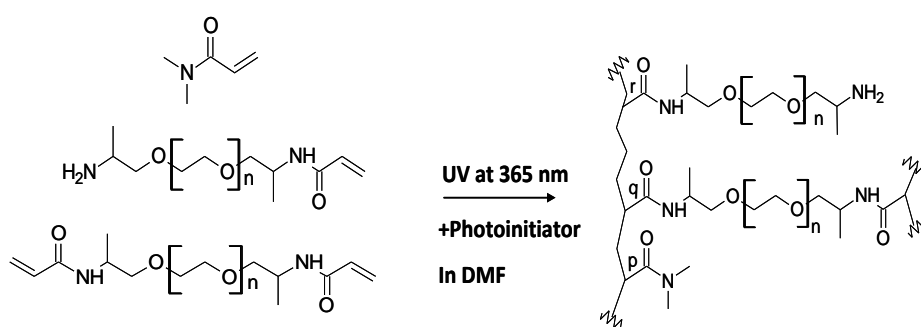


**Figure 3.2:** Synthesis of PEGA.

Coupling of LA or GA within PEGA was performed using EDC and NHS as coupling agents. The synthesis scheme is shown in Figure 3.3. The sugars were bound to the free pendant amine at the end of the PEGA linkers. EDC induces the activation of carboxylic acid groups to give activated *O*-acyl urea ester groups, and the amide-type crosslinks can be formed through the reaction of these activated

carboxylic groups with amine group containing materials. Based on the cross linking concept shown in Figure 3.3, the activated carboxylic acid of the sugars was formed using EDC in the presence of nucleophile NHS, and subsequently bound to the free amines within PEGA. The presence of either sugar within the PEGA gel was confirmed by FTIR spectra.
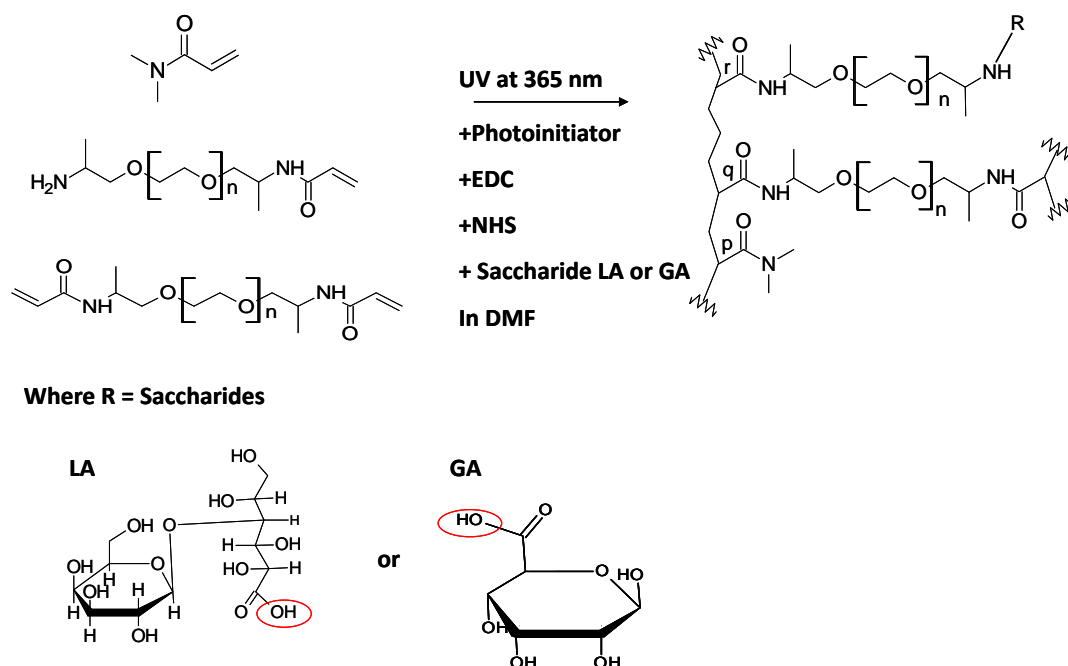


**Figure 3.3** Synthesis of PEGA with sugars LA or GA. Red circle on the sugars indicates groups lost during bonding process.

FTIR spectra were measured using a Nicolet 5700 FTIR spectrometer to obtain the transmission spectra of the PEGA based gels and the reaction constituents. Figure 3.4 (A-C) shows the FTIR spectra of, polymerised PEGA, unmodified LA and polymerised PEGA+LA respectively. Figure 3.5 (A-C) shows the FTIR spectra of polymerised PEGA, unmodified GA and polymerised PEGA+GA respectively.

LA exhibited a broad OH absorption occurring in the region between 3500 and 2800 cm$^{-1}$, and a distinctive band at approximately 1740 cm$^{-1}$ which is associated with carbonyl stretching (C=O) of carboxylic peaks, Figure 3.4. A primary alcohol stretching bond, (C-O) was observed at 1020 cm$^{-1}$, Figure 3.4. (Haslam and Willis, 1972, Rabek, 1980, Williams and Flemming, 1996).

PEGA was seen to exhibit a broad OH absorption occurring in the region of 3500 and 2800 cm$^{-1}$ with a smaller OH peak between 2960 and 2870 cm$^{-1}$ attributed

to carboxylic acid bond stretching, Figure 3.4 (Rabek, 1980). A characteristic absorption of Amide I was observed at 1670 $cm^{-1}$. The significant absorption at 1100 $cm^{-1}$ can be attributed to the presence of C-N bonds within the material, Figure 3.4 (Rabek, 1980, Haslam and Willis, 1972, Williams and Flemming, 1996).

In the FTIR spectra of PEGA+LA, the carbonyl stretching of LA almost disappears due to the amide bond formation between carboxylic groups of LA and the amine groups of PEGA. The peaks of amide I of PEGA+LA slightly shifted from 1670 $cm^{-1}$ to a split peak between 1670 and 1620 $cm^{-1}$, which when compared to PEGA indicates a conformational change in PEGA after reaction with LA, Figure 3.4. Furthermore the OH stretching peak becomes broader and deeper, which indicates that the intramolecular hydrogen bonding within the polymer chains has increased due to the introduction of LA into the PEGA chains (Williams and Flemming, 1996). This is further mirrored by a broader absorption peak at around 1100 $cm^{-1}$, associated with the C-N bonds in the material indicating the potential formation of amide bonds within the material, Figure 3.4.
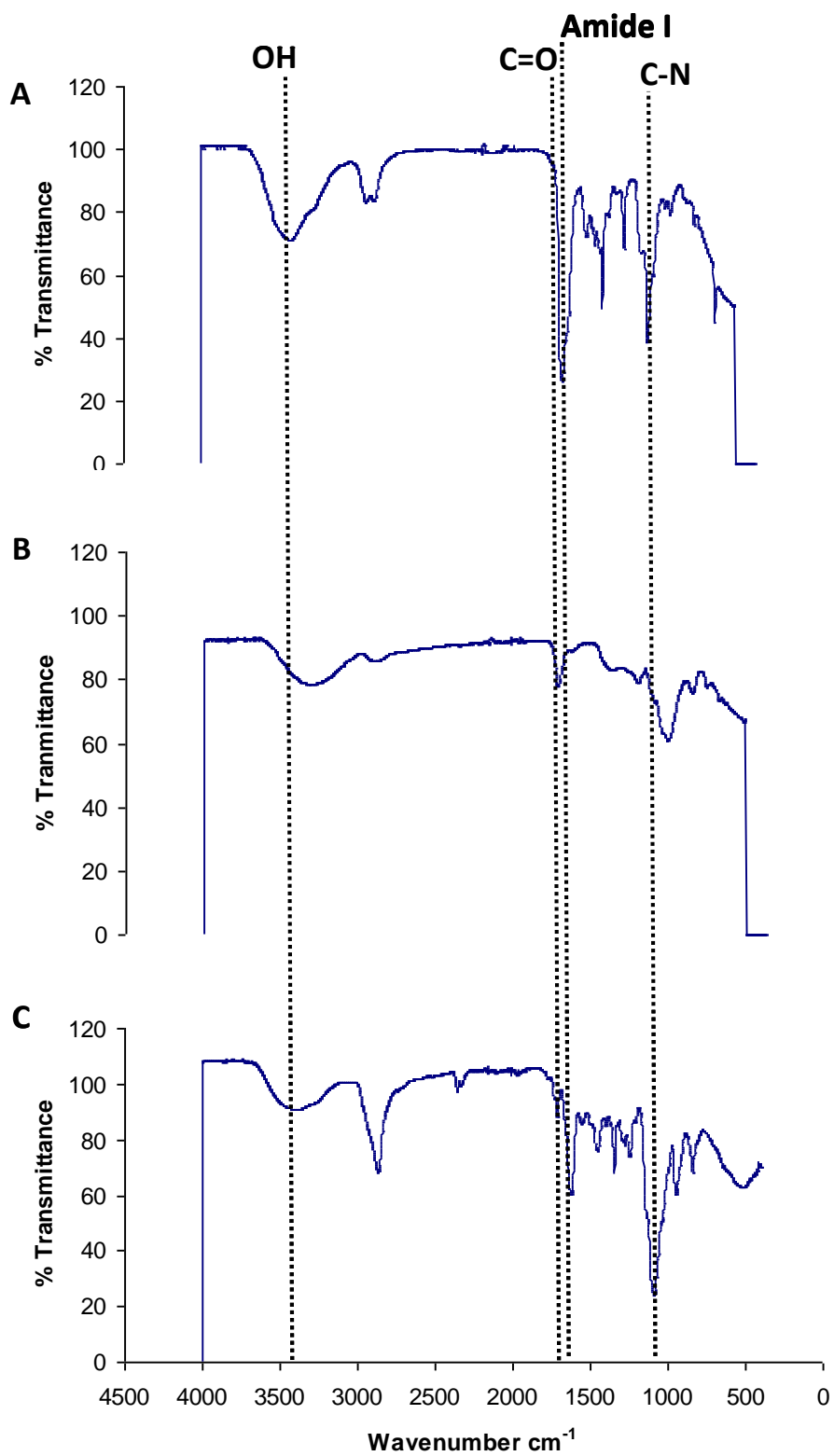
**Figure 3.4:** FTIR spectra: **A)** polymerised PEGA, **B)** unmodified lactobionic acid, **C)** polymerised PEGA+LA (0.1mmol).
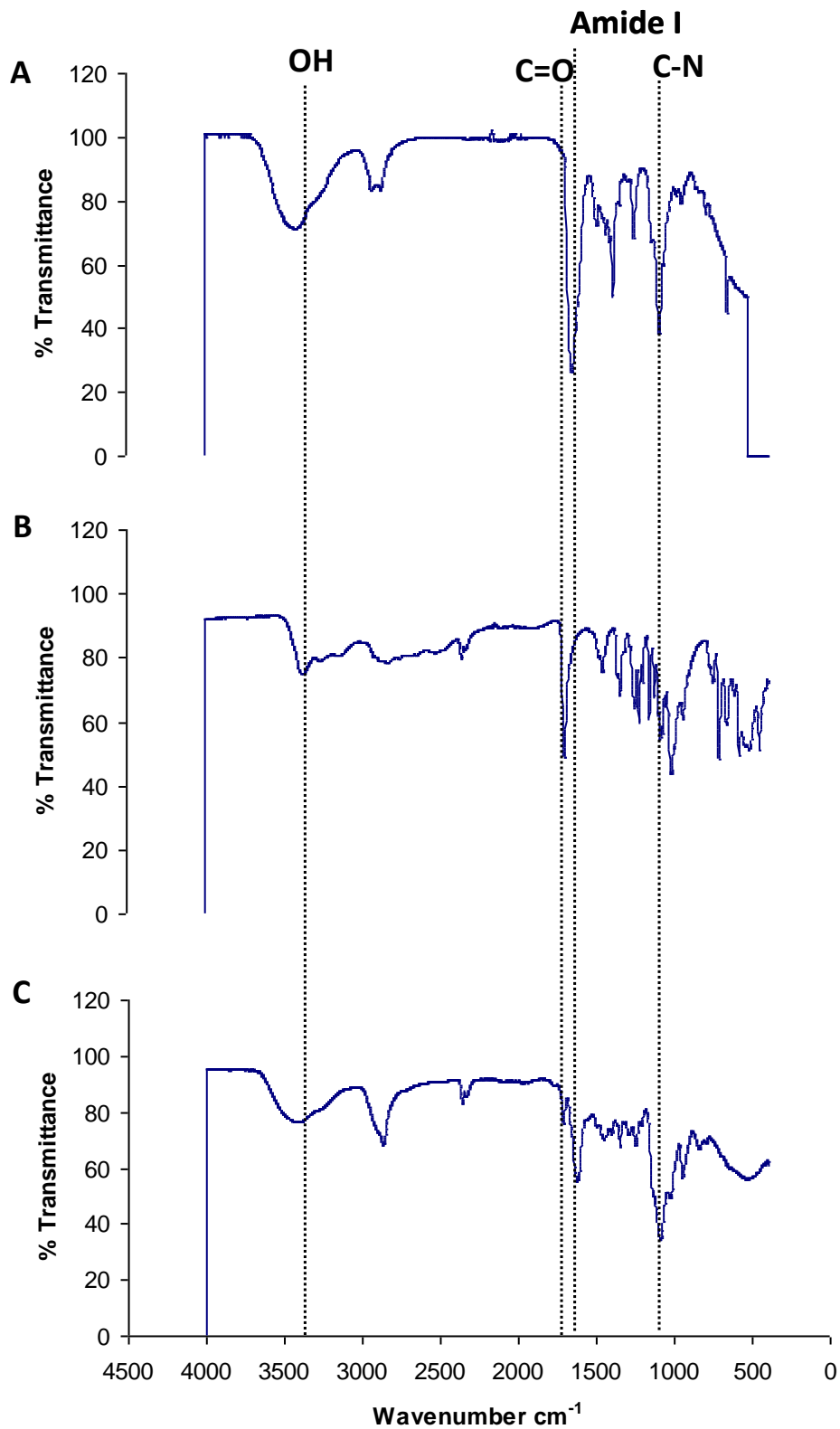
**Figure: 3.5:** FTIR spectra: **A)** polymerised PEGA, **B)** D-glucuronic acid, **C)** polymerised PEGA+GA (0.1mmol).

GA also exhibited a broad OH absorption occurring in the region between 3500 and 2800 cm$^{-1}$, due to hydrogen bonding, Figure 3.5. Carbonyl containing compounds show a very characteristic absorption in the range of 1600-1800 cm$^{-1}$ (Williams and Flemming, 1996, Rabek, 1980). In the case of GA, a distinctive band at approximately 1740 cm$^{-1}$ was identified, which is thought to be associated with carbonyl stretching (C=O) of carboxylic peaks, Figure 3.5. A primary alcohol stretching bond, (C-O) was also observed at 1020 cm$^{-1}$, Figure 3.5. Nearly all organic molecules absorb strongly close to 3000 cm$^{-1}$ due to C-H stretching vibrations associated with alkyl groups. The position of this C-H stretch is shifted by the presence of adjacent multiple bonds (Rabek, 1980, Williams and Flemming, 1996, Haslam and Willis, 1972). When GA is incorporated into PEGA, the carbonyl stretching of GA almost disappears due to the amide bond formation between carboxylic groups of GA and the amine groups of PEGA. The peaks of amide I of PEGA+GA slightly shifted from 1670 cm$^{-1}$ to a split peak between 1670 and 1620 cm$^{-1}$, which when compared to PEGA, indicates a conformational change in PEGA after reaction with GA, Figure 3.5.
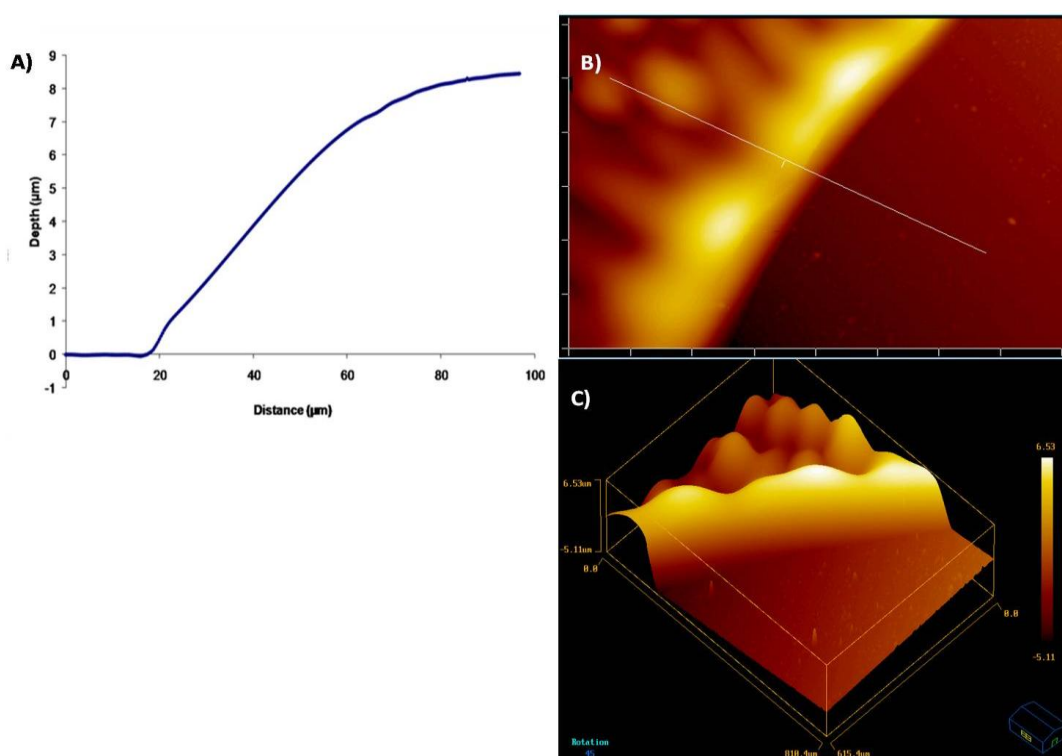


**Figure 3.6: A)** Depth of PEGA profile generated by interferometry, **B)** 2D image of PEGA-glass interface generated by interferometry, **C)** 3D image of the PEGA-glass interface generated by interferometry.

The thickness of the PEGA layers was determined using interferometry. The PEGA monolayer was removed from half of the sample and the interface was examined. The distance between the PEGA monolayer and the underlying glass substrate was assumed to be the thickness of the PEGA coating, and was determined to be approximately 8 microns, Figure 3.6. The depth of the PEGA coating was unaffected by the presence of the sugars chemically crosslinked into the hydrogel. The surface of the PEGA hydrogel was seen to have slight variations in the height, i.e. an inherent roughness of the order of approximately a micron, which may be an artefact of the spin coating and UV polymerisation steps. This surface roughness may in turn influence cellular behaviour and morphology.

The distribution of chemically reactive primary amines was determined qualitatively using dansyl chloride staining and quantitatively using Fmoc-Phe loading experiments. When labelled with dansyl chloride, unmodified PEGA surfaces showed a homogeneous distribution of chemically active primary amines at the micron scale. The micrographs in Figures 3.7 and 3.8 show fluorescent images of unmodified PEGA, with varying concentrations (0.01-0.2 mmol) of LA and GA sugars respectively. The images acquired from "PEGA only" are bright blue given that there are numerous free amine groups in the structure. As the concentration of the sugars incorporated into PEGA increases fewer free amine groups are available, so the images appear darker. The graphs in Figure 3.7A and 3.8A show the pixel intensity versus the distance across the surface for both sugars. The data is indicative that each of the surfaces investigated were chemically homogeneous at the micron level as the pixel intensity i.e. fluorescence was similar across each surface.
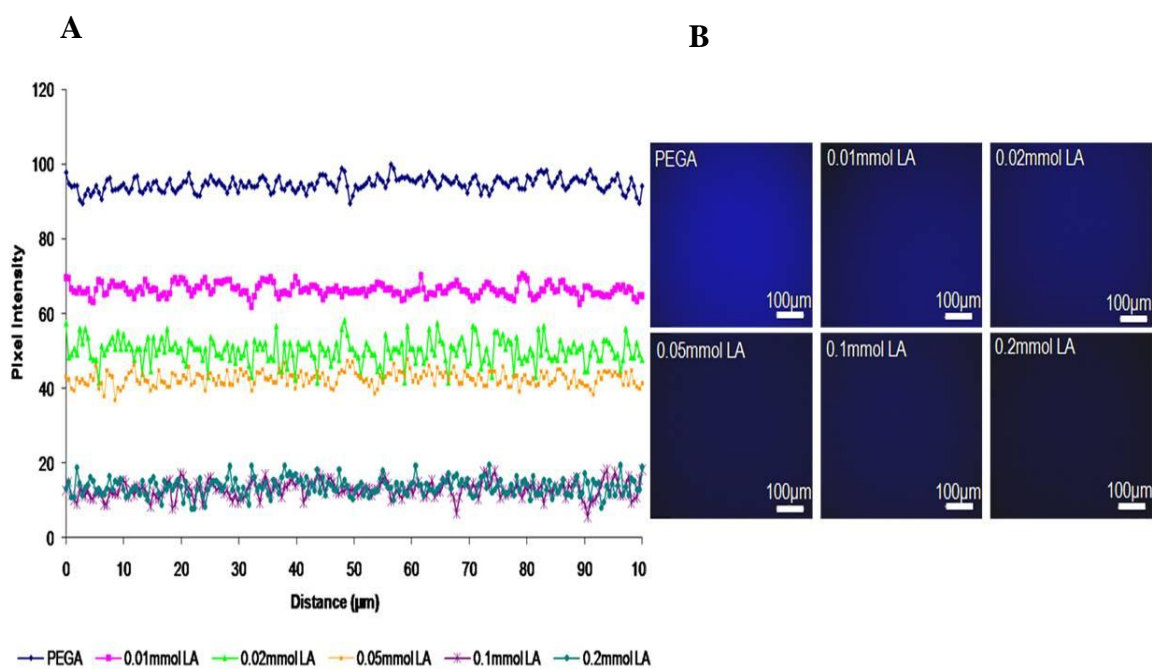
**Figure 3.7: A)** Pixel intensity versus the distance for surfaces containing LA, **B)** Corresponding dansyl chloride fluorescent micrographs.
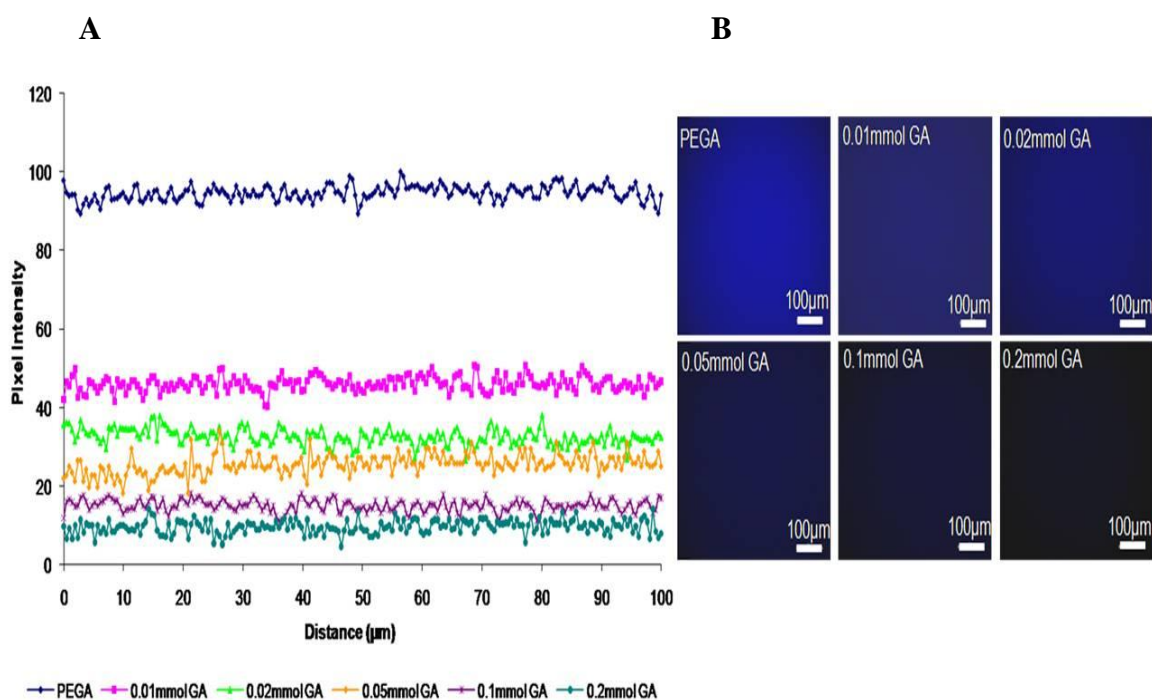


**Figure 3.8: A)** Pixel intensity versus the distance for surfaces containing GA **B)** Corresponding dansyl chloride fluorescent micrographs.

The conjugation of Fmoc-Phe to each model sugar surface allowed for the concentration determination of chemically reactive primary free amines. Utilising

standard amide coupling chemistry, Fmoc-Phe was used to label the remaining free amines present on each sugar surface. Figure 3.9 shows that as the concentration of sugar increases within the PEGA the number of reactive free amines decreases, as seen with the dansyl chloride staining. The data suggests that the GA control sugar ($M_w$=194.1), exhibited the same number of available amines as LA ($M_w$=358.3), suggesting that the size of the sugar molecule i.e. monosaccharide (GA) vs. disaccharide (LA), does not affect the overall reactivity. Figure 3.9 illustrates that as the sugar concentration in PEGA is reduced the percentage free amine available in the material plateau's towards 100 %. PEGA had an average concentration of 0.02 mmol Fmoc-Phe on each surface tested. Consequently, it was assumed that unmodified PEGA had 100 % free amines available on the monolayer surface. The coupling efficiency of Fmoc-Phe onto the free amines had previously been determined to be >95 % (Zourob *et al.*, 2006).
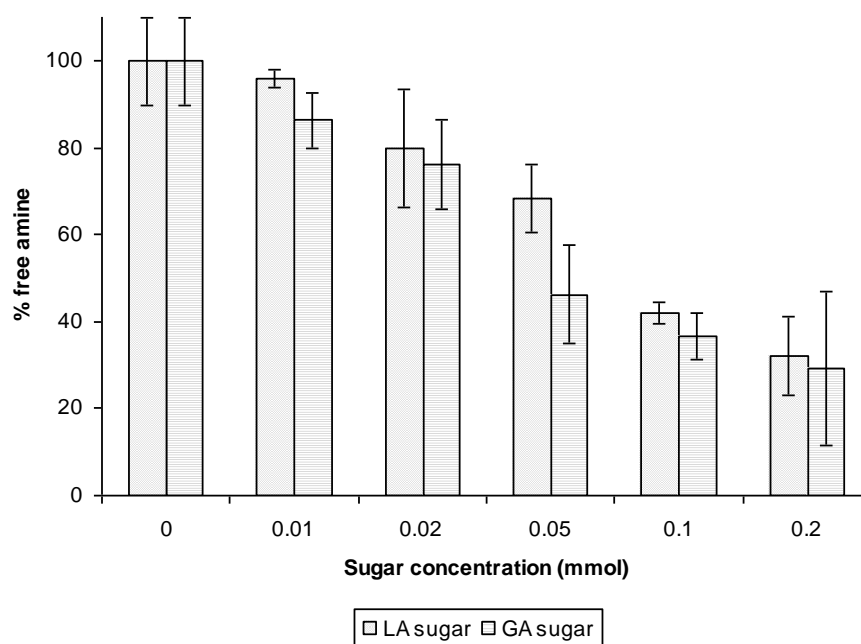


**Figure 3.9:** Effect of sugar loading on percentage free amines available in PEGA.

The amount of adsorbed protein on PEGA surfaces was determined using the QuantiT™ assay kit and is shown in Table 3.1. There was no significant difference, as determined by student t-test, in the amount of protein adsorbed between unmodified PEGA, PEGA+LA (0.1 mmol) and PEGA+GA (0.1 mmol) surfaces ($p$>0.05). This suggests that any cellular interaction on the sugar PEGA surfaces

would be down to specific interactions with the incorporated LA or GA sugar PEGA surfaces rather than by interactions with an adsorbed protein layer. The total amount of protein on the PEGA surfaces was higher than non-fouling PEG surfaces, as quoted by Benesch *et al.* and Todd *et al.*, (~8 ng/mm$^2$ and 12.6 ± 1.0 ng/mm$^2$) for serum protein adsorption (Benesch *et al.*, 2001, Todd *et al.*, 2009).  It is likely that the hydrated nature of the PEGA structure entrapped proteins within its structure, resulting in an increased amount of adsorbed protein compared to traditional two dimensional monolayer systems.

| Sample | Protein Adsorption ng/mm$^2$ ± (S.D.) | Adhesive to hepatocyte cell line FL83B |
|---|---|---|
| Epoxy coated glass | 68.9 (3.0) | Yes |
| PEGA | 24.0 (1.0) | No |
| PEGA+LA (0.1 mmol) | 23.3 (5.0) | Yes |
| PEGA+GA (0.1 mmol) | 23.8 (5.0) | Yes |

**Table 3.1:** Amount of protein adsorbed from serum containing cell media over 24 hours at physiological conditions, using a fluorescence assay kit. Data is expressed as the mean value ± standard deviation, (n=9).

### 3.4 Conclusions

PEGA has been effectively functionalised with a galactose carrying saccharide (LA) or a control saccharide (GA), in order to create a hydrogel surface which may provide a suitable substrate for the adhesion, growth and maintenance of hepatocytes. Analysis by FTIR and dansyl chloride labelling showed that the saccharides LA and GA had been successfully immobilised within the PEGA structure with no effect upon the protein adsorption. The coverage of sugar groups was determined by dansyl labelling and fluorescence microscopy, as well as UV-visible spectroscopy analysis of labelled amines. It was determined that increasing the sugar concentration within the PEGA resulted in a decrease in the number of free amines available within the hydrogel. The lactobionic acid carries a galactose moiety which should be available to interact with the ASGP-R present on the hepatocyte

plasma membrane. D-glucuronic acid was chosen as a control sugar of similar structure to galactose but is not recognised by the ASGP-R.

## Chapter 4.0: Hepatocyte cell line response to a galactose functionalised hydrogel surface

### 4.1 Introduction

The use of PEG based hydrogels has been developed for hepatocyte cell culture enabling the development of biological platforms on which hepatocellular functions can be evaluated. The development of biomaterials which allow for the attachment, function and viability of cultured hepatocytes would improve options available for both clinical and commercial applications. As discussed earlier in Chapter 2, cells are influenced by the chemical composition of the surfaces on which they are grown. In particular, cellular adhesion and liver specific cell phenotypes are better maintained on hydrophilic materials. One strategy used to improve cell attachment and retention of *in-vivo* phenotype is to immobilise bioactive molecules that are recognised by cell surface receptors within scaffolds. Many recent studies have focused on regulating cell adhesion through immobilised short chain peptide derivatives in particular, RGD, a cell-binding epitope found within fibronectin. However, integrin-fibronectin interactions can be found in most cell types not just hepatocytes. This study focuses on how hepatocytes can be selectively recruited to a hydrogel surface that contains well-defined carbohydrate ligands that interact with the ASGP-R lectin that is uniquely expressed by hepatocytes.

Carbohydrate–receptor interactions are often associated with specific recognition by cells. Carbohydrate recognising receptors are found on many cell surfaces, of particular importance here is the interaction of hepatocytes with galactose/N-acetyl-β-galactosamine containing ligands via ASGP-R. It has been shown previously that galactose carrying polymers can be used to bind hepatocytes through a hepatocyte specific receptor mediated mechanism. A co-polymer of PEG and acrylamide, PEGA hydrogel containing covalently bound galactose, was developed to mimic the ASGP-R-carbohydrate interaction. Although ASGP-R is a non adhesive cell surface receptor *in vivo*, (Section 2.2.4), PEGA functionalised with galactose can be used to guide hepatocyte adhesion through the unique ASGP-R-carbohydrate interaction (Kim *et al.*, 2003b, Masters and Anseth, 2004, Cho *et al.*, 2007).

This chapter describes the cellular evaluation of three systems; PEGA, PEGA with galactose moieties in the form of lactobionic acid (LA) and PEGA with a control sugar in the form of D-glucuronic acid (GA). The surfaces were evaluated in terms of hepatocyte attachment, viability and functionality.

## 4.2 Materials and Methods

All chemicals and reagents, unless otherwise stated were purchased from Sigma Aldrich Company Ltd. (Gillingham, UK) and were used as received.

### 4.2.1 Maintenance of cell cultures

Mouse hepatocyte cell line FL83B (ATCC, VA, USA) was grown in Kaighn's modification of Ham's F12 medium with L-glutamine (F12-K) supplemented with 10 % foetal bovine serum (FBS) and 1 % antibiotics (Penicillin-Streptomycin) by volume, and maintained at 37ºC in a humidified 5 % $CO_2$ atmosphere. The cells were removed using 0.05 % trypsin in Ethylene diamine tetra-acetic acid (EDTA) solution at sub-confluency, and the medium was replaced every 48 hours. The FL83B cell line tends to undergo apoptosis once cells reach confluence, therefore cultures were passaged when sub-confluent.

### 4.2.2 Light Microscopy

To observe the potential effect of sugars within PEGA hydrogel surfaces over a period of 7 days, FL83B hepatocytes were seeded at a density of $6\times10^4$ cells/ml onto either 1) tissue culture plastic (TCP), 2) glass, 3) PEGA, 4) PEGA+LA (0.1 mmol), and 5) PEGA+GA (0.1 mmol). The media was aspirated and replaced with 2 ml of fresh pre-warmed media every other day.

The cells were cultured in a humidified incubator for 7 days. The morphology of the cells was examined at time-points 1, 3 and 7 days using a Leica inverted microscope with digital camera and Spot advanced software.

### 4.2.3 Live/Dead Assay

A Live/Dead Viability/Cytotoxicity assay kit for mammalian cells (Invitrogen, Paisley, UK) was used to assess cell viability at 1, 3 and 7 days. The samples were seeded with hepatocytes at a density of $6 \times 10^4$ cells/ml onto either: 1)

glass, 2) PEGA 3) PEGA+LA (0.1mmol), or 4) PEGA+GA (0.1mmol). Briefly, the media was aspirated from the samples and the surfaces were rinsed twice with pre-warmed PBS. A working solution of 2 µl/ml ethidium homodimer-1 and 0.5 µl/ml Calcein AM was prepared in PBS. The ethidium homodimer-1 was added first to the PBS then vortexed to mix, followed by the addition of Calcein AM. Calcein AM is a fluorogenic esterase substrate that is hydrolysed to a green fluorescent product. Green fluorescence is an indication that the cells are alive, with an intact cell membrane and have esterase activity. Conversely, Ethidium homodimer-1 is a red fluorescent nucleic acid stain that can only enter cells if the cell membrane has been compromised typically but not always seen when a cell dies. Each sample was covered with live /dead working solution for 10 minutes in the dark, after which the excess dye was removed. The reagents do not fluoresce until they are in contact with the cells. Each of the samples was then visualised under the fluorescence microscope (Nikon Eclipse 50i).

### 4.2.4 DNA assay

To determine the cell number on each sample surface, FL83B hepatocytes were seeded at a density of $6 \times 10^4$ cells/ml onto either: 1) tissue culture plastic (TCP), 2) glass, 3) PEGA, 4) PEGA+LA (0.1 mmol), or 5) PEGA+GA (0.1 mmol). At each time point, days 1, 3 and 7 of culture, the cell culture media was aspirated from the samples and the wells were rinsed twice with pre-warmed PBS. The samples were then transferred into new 6 well plates. 1 ml of distilled water was then added to each well. The well plates were then frozen overnight in the -80ºC freezer. The sample plates were then freeze-thawed three times to lyse the DNA from the cells on the sample surfaces. 50 µl of each sample was pipetted into a Nunc clear flat bottom 96-well plate, and 50 µl of Tris-NaCl-EDTA (TNE) buffer was added to each well followed by 100 µl of Hoechst stain working solution (1 in 50 dilution from Hoechst stock solution (1 mg/ml of Hoechst 33258 in distilled water) with TNE buffer). The plate was tapped to allow for the components to mix then the fluorescence is measured using a Fluorostar Optima Fluorescence plate reader (BMG Latech) at a wavelength of 355nm excitation and 460 nm emission. In order to assess cell numbers a calibration curve of hepatocytes was prepared up to a density of $1 \times 10^6$ cells. The experiment was repeated six times, the data presented is representative of the results.

## 4.2.5 Immunocytochemical Staining

FL83B hepatocytes were seeded at a density of $6 \times 10^4$ cells/ml onto either: 1) tissue culture plastic (TCP), 2) glass, 3) PEGA 4) PEGA+LA (0.1 mmol), or 5) PEGA+GA (0.1 mmol). The cells were cultured until day 4 when the media was removed, the cell were washed twice with PBS and then fixed using 4 % paraformaldehyde (PFA) for ten minutes. The cells were then stained for either; f-actin, vinculin or pFAK with the nuclei being counter stained with 4, 6 diamidino-2-phenyladole (DAPI), a fluorescent stain that binds strongly to DNA.

For f-actin staining, the cells were fixed using 4 % PFA, blocked with 1 % goat serum, 1mg/ml bovine serum albumin (BSA) in 0.1 % Triton X-100 in PBS for 30 minutes. The block was removed and the cells incubated in the dark with rhodamine phalloidin (Invitrogen, Paisley, UK) (5μl stock in 200μl block) for 20 minutes. The samples were washed 5 times with phosphate buffered saline (PBS) before being mounted in Prolong Gold antifade reagent with DAPI (Invitrogen). The samples were imaged with a fluorescence microscope (Nikon Eclipse 50i).

For Vinculin staining, cells were fixed with 4 % PFA, and then blocked with 1 % goat serum, 1mg/ml BSA in 0.1 % Triton X-100 in PBS for 30 minutes at room temperature. Samples were incubated with the primary mouse monoclonal anti-vinculin antibody (Sigma Aldrich, Gillingham, UK) at 1:400 dilution for 1 hour at room temperature (RT). The sample wells were rinsed 5 times with PBS, then samples were incubated with the secondary antibody, goat anti-mouse Alexa Fluor 546 IgG (red) (Invitrogen, Paisley, UK) at a 1:1000 dilution for 45 minutes. After removal of the secondary antibody, the samples were washed again 5 times with PBS before being mounted in Prolong Gold antifade reagent with DAPI (Invitrogen, Paisley, UK). The samples were imaged with a fluorescence microscope (Nikon Eclipse 50i).

For phosphorylated focal adhesion kinase (pFAK) staining, cells were fixed with 4 % PFA, then blocked with 1 % goat serum, 1mg/ml BSA in 0.1 % Triton X-100 in PBS for 30 minutes. The block was removed and the cells incubated in the dark with primary antibody; rabbit polyclonal to FAK [phospho Y397], (Abcam,

Cambridge, UK) (1 µl stock antibody in 500 µl block solution). The sample wells were then rinsed 5 times with PBS, before being incubated with the secondary antibody goat anti-rabbit Alexa 486 IgG (green) (Invitrogen, Paisley, UK) at a 1:1000 dilution for 45 minutes. Post removal of the secondary antibody, the samples were washed again 5 times with PBS before being mounted in Prolong Gold antifade reagent with DAPI (Invitrogen, Paisley, UK). The samples were left to cure in the dark at room temperature prior to imaging and storage. The samples were imaged with a fluorescence microscope (Nikon Eclipse 50i).

### 4.2.6 Urea assay

Urea is primarily produced by the liver and is the main end product of protein catabolism in animals. Urea determination is very useful to assess if hepatocytes are functioning as a primary method for the removal of ammonia in culture. To observe if cells grown on PEGA hydrogel surfaces could synthesise urea, FL83B hepatocytes were seeded at a density of $6 \times 10^4$ cells/ml onto either: 1) tissue culture plastic (TCP), 2) glass, 3) PEGA, 4) PEGA+LA (0.1 mmol), or 5) PEGA+GA (0.1 mmol). At each time point, days 1, 3 and 7 of culture, the cell culture media was aspirated from the samples and the wells were rinsed twice with pre-warmed PBS. The samples were then transferred into new 6 well plates. 1 ml of fresh media containing ammonium chloride (2 mM) was added to each well. A sample of media was taken immediately at the addition of the ammonium chloride spiked media and then again after 2 hours incubation at 37ºC. A QuantiChrom Urea assay kit (Bioassay Systems, CA, USA) was used to measure urea directly in the cell media without any pre-treatment. A chromogenic reagent in the kit forms a coloured complex specifically with urea. The intensity of the colour is directly proportional to the urea concentration in the sample. The kit components were equilibrated to room temperature. Sufficient working reagent for all the samples was prepared by combining reagents A and B together in equal proportions. Once prepared the working reagent was used within 20 minutes. Cell media samples were assayed directly. 50 µl distilled water which acts as a blank, 50 µl 5mg urea/dL urea standard and 50 µl samples were transferred in triplicate into separate wells of a 96 well plate. 200 µl of the working reagent was pipetted into each well and the plate was lightly tapped to mix. The plate was then incubated at room temperature for 50 minutes. The

optical density of the samples was then read at 405 nm using a plate reader. Using this data the urea concentration (mg/dL) of the sample can be calculated as:-

$$[Urea] = \frac{(ODsample - ODblank)}{(ODs \tan dard - ODblank)} \times n \times [STD] \quad \textbf{Equation 4.1}$$

where:- Optical Density (OD) sample, OD Blank and OD Standard are the optical density values of sample, water and standard respectively, n is the dilution factor (= 1) and [STD] = 5 mg/dL the urea standard concentration. Note: 1 mg/dL urea equals 167μM. The experiment was repeated three times, the data presented is representative of the results.

**4.2.7 Flow cytometry**

A sub-confluent culture of FL83B mouse hepatocytes was used to assess the cell line for the presence of ASGP-R. The media was removed from the flask and the cells were rinsed twice with pre-warmed sterile PBS. 3ml of EDTA based dissociation buffer (Invitrogen, Paisley, UK) was added and the flask was returned to the incubator at 37ºC for 10 minutes. Any cells which did not detach from the tissue culture plastic were removed with a cell scraper. The dissociation buffer was pipetted up and down to dislodge all the cells, and the cells were then transferred into a falcon tube. A sample of the cell suspension was retained for a cell count, and the remainder was then spun for 5 minutes at 2000 RPM to create a cell pellet. The supernatant was then carefully removed and the cell pellet was resuspended in the appropriate volume of PBS to obtain 2 million cells per ml in eppendorf tubes. The sample was divided into two eppendorf tubes; one tube for the negative control and the other to test for the presence of ASGP-R using a fluorescein isothiocyanate (FITC) conjugated monoclonal antibody to rat ASGP-R antibody (Hycult Biotechnology, The Netherlands). The cell samples were spun down in a bench top centrifuge for one minute at 5000 RPM and the supernatant was then removed. 100 μl of FTIC conjugated monoclonal antibody to rat ASGP-R, diluted 1 in 10 with fluorescent activated cell sorter (FACS) buffer (0.2 % BSA , 0.1 % Sodium Azide in PBS) was added to the eppendorf and the cells were carefully resuspended. Cells being used for the negative control were resuspended in FACS buffer without any antibody present. The cells were incubated on ice for 30 minutes in the dark, after which the cells were spun at 5000 RPM for one minute and the supernatant removed.

The cells were then washed with 900 µl of PBS (non-sterile) per eppendorf, and then spun at 5000 RPM for one minute. The supernatant was then carefully removed and the cells resuspended in 250 µl of PBS. The samples were kept at 4ºC until they could be analysed by flow cytometry.

The FACs machine (BD FACSCalibur Flow Cytometer) with Cell Quest Pro software was used to evaluate the cell population. Cells were gated using the forward Vs Sidescatter graph. 10,000 events in the cell gate were counted and the fluorescence in the FL1 or FL2 regions was registered and plotted against the cell count. The experiment was repeated twice and the data presented in this thesis is representative of the results.

### 4.2.8 Polymerase Chain Reaction (PCR)

A cell pellet was created from appropriate samples and cell culture to assay the presence of liver specific genetic markers. The culture medium was removed and the cells were washed twice in pre-warmed PBS. An appropriate amount of trypsin; 3 mls for a T-75 flask and 1 ml for a 6 well plate were used to detach the cells from the tissue culture plastic and samples respectively. The trypsin was then neutralised with F12-K medium, three times the amount of trypsin added. The cells were transferred to falcon tubes and centrifuged for 5 minutes at 1500 RPM, to create a cell pellet. The supernatant was then removed and the cells were resuspended in 1ml of media and transferred to eppendorf tubes. The cells were spun down again using a bench top centrifuge and the supernatant was removed. The cell pellets were labelled and stored at -80ºC, until the ribonucleic acid (RNA) was extracted from the cells.

Primary hepatocytes isolated from male Black 6 mice (purchased from Lonza, UK) were resurrected from liquid nitrogen storage by fast thawing in a 37 ºC water bath. The cells were transferred to 10 mls cold media and resuspended. The cells were centrifuged for 3 minutes at 700 RPM. The supernatant was then removed and the cells were resuspended in 1ml of pre-warmed media and transferred to eppendorf tubes. The cells were spun down again using a bench top centrifuge and the supernatant was removed. The cell pellets were labelled and stored at -80ºC, until the ribonucleic acid (RNA) was extracted from the cells.

The liver was dissected from a 2.8 month old male Black 6 mouse, (a kind gift from Dr. Brian Bigger) and segments were snap frozen in liquid nitrogen. The liver tissue was stored at -80ºC, until the ribonucleic acid (RNA) was extracted.

A commercially available RNA extraction kit, RNeasy minikit (Qiagen, Crawley, UK) was used to extract the RNA from prepared frozen cell pellets and snap frozen liver tissue as per the manufacturer's instructions. The quantity of RNA (in terms of ng/µl) was determined for each sample using the NanoDrop (Jenway Genova, UK). The extracted RNA was then stored at -80ºC until use.

Reverse transcription of RNA was used to generate complementary deoxyribonucleic acid (cDNA) for the PCR reactions. 1 µg of total RNA in a total volume of 20 µl RNAse free water was pipetted into a PCR strip tube. The tube was placed into the PCR machine and heated at 65ºC for 3 minutes before being held at 4ºC. A master mixture of total volume of 20 µl was assembled containing: 2 µl oligodT (0.5 µg/µl –Promega), 8 µl RT buffer, 4 µl dNTP (2.5 mM stock – Promega), 0.8 µl AMV transcriptase (Promega) and 5.2 µl RNAse free water. 20 µl of mastermix was then added to the PCR strip tube containing the RNA. The mixture was incubated in the PCR machine at 42ºC for one hour, followed by 98ºC for five minutes before being transferred to ice (4ºC). When finished the strip tubes were placed in the microfuge and spun for several seconds. 40 µl of cDNA was then transferred from the PCR strip tube into a microfuge tube for storage at -20ºC. 1µl of this cDNA was used per PCR reaction.

Reverse Transcription PCR (RT-PCR) was used to look at genes of interest. Primers for the genes of interest arrived freeze dried and were resuspended to 1 µg/µl concentration using nuclease free water and vortexing to resuspend the material, to create a stock solution. A 1 in 10 dilution of this stock primer solution, in water was used to obtain a working dilution. For one PCR reaction a 20 µl PCR mastermix was made containing; 10 µl Biomix Red (a commercial PCR master mix containing dNTPs, enzymes, buffer and loading dye),1 µl of the forward primer sequence of the gene of interest, 1 µl of the reverse primer sequence of the gene of interest and 7 µl of water. For each PCR reaction 19 µl of the PCR master mix was pipetted into a PCR strip tube, to which 1 µl of cDNA was added. The lid was placed on the tube, labelled and briefly microfuged to bring the entire mixture down to the

bottom of the tube. The tube was then loaded into the PCR machine and run at for 35 cycles at an annealing temperature of 60ºC for all genes except GAPDH. The GAPDH housekeeping gene was processed for 25 cycles at an annealing temperature of 60ºC.

A DNA agarose gel was prepared to run the PCR samples in. 1.5g of agarose and was dissolved in 150 ml of 1 x Tris-acetate-EDTA (TAE) buffer using a microwave. When the agarose was fully dissolved, the solution was cooled slightly from boiling in a beaker of water. The gel mould was assembled and a comb placed in the mould. The comb created channels in the gel into which the PCR samples were loaded. The agarose solution was poured into the mould and left to set at room temperature. Once the gel was set, the ends of the mould and the comb were removed and the gel was immersed in the gel tank containing 1 x TAE. Each channel was then systematically loaded first with a 10 µl of a 1 kB DNA ladder, followed by 10 µl of each PCR reaction. The gel was then run for 60 minutes with an applied voltage of 100 V. Subsequently, the gel was imaged using the transilluminator to determine whether the genes of interest were present in the sample of cDNA.

The genes of interest were GAPDH (housekeeper gene), asialoglycoprotein (ASGP), α-fetaprotein, (αFP) albumin and cytokeratin 18, (CK18), which are liver specific markers with the exception of GAPDH.

The hepatocyte cell line used, primary hepatocytes and liver tissue were evaluated for the genes of interest. Subsequently, the cell line was seeded onto the sample surfaces, grown in culture for six days then harvested for RT-PCR.

**4.3 Results and Discussion**

Data was collected from all the sample materials in the study as described in Section 4.2. The cell attachment, morphology, proliferation and genetic results are discussed in turn below.

**4.3.1 Cell attachment and morphology**

The degree of cell attachment was qualitatively assessed for mouse hepatocyte cells after 1, 3 or 7 days incubation. At each time-point samples were discarded after testing. Each of the candidate materials; glass, TCP, PEGA,

PEGA+LA and PEGA+GA, were examined at each time-point to evaluate cell behaviour using complementary techniques; light microscopy, live/dead staining and immunochemical staining of actin cytoskeleton, vinculin and pFAK.

The attachment and distribution of hepatocytes was observed on the candidate materials. Figure 4.1 outlines the morphology of the attaching cells at days 1, 3 and 7 using light microscopy. Figure 4.2 outlines the viability of the cell at days 1, 3 and 7 using live/dead viability assay.

Hepatocytes on the glass surface were seen to increase in number over 7 days in culture and were confirmed to be viable by live/dead staining, Figures 4.1 & 4.2. Few cells were seen to attach to the PEGA surface, confirming the non-fouling nature of the material, Figure 4.1 (Todd *et al.*, 2007). This was additionally confirmed by the live/dead assay which showed the majority of the cells on this surface stained red, Figure 4.2. Care must be taken in interpreting images from the live/dead viability assay, as dead cells may have detached from the surfaces and influence the degree of the viability seen on a surface. Cells attached to the PEGA+LA material and increased rapidly in cell number until a complete monolayer of viable cells was evident on Day 7, Figure 4.2. The cells generally took on a cuboidal epithelial morphology in culture forming tight cell-cell contacts, which is consistent with previously observed morphologies by Breslow *et al.,* Figure 4.1. (Breslow *et al.*, 1973). The PEGA+GA substrate produced an increase in cell number over the course of the culture period and performed to a similar level as the glass, Figures 4.1 & 4.2.
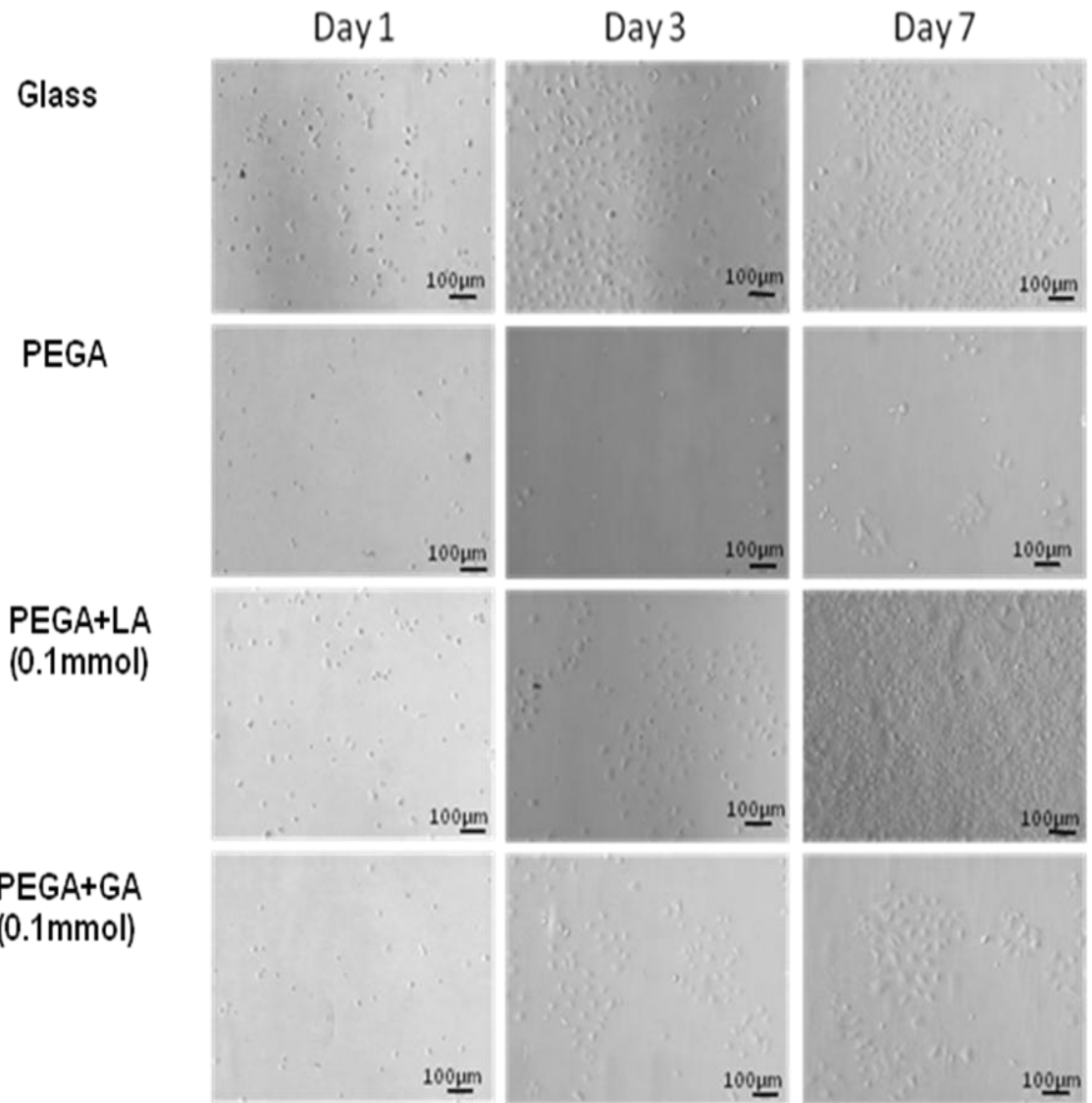
**Figure 4.1:** Light microscopy of hepatocyte cell line FL83B growing on substrate surfaces over the course of 7 days.
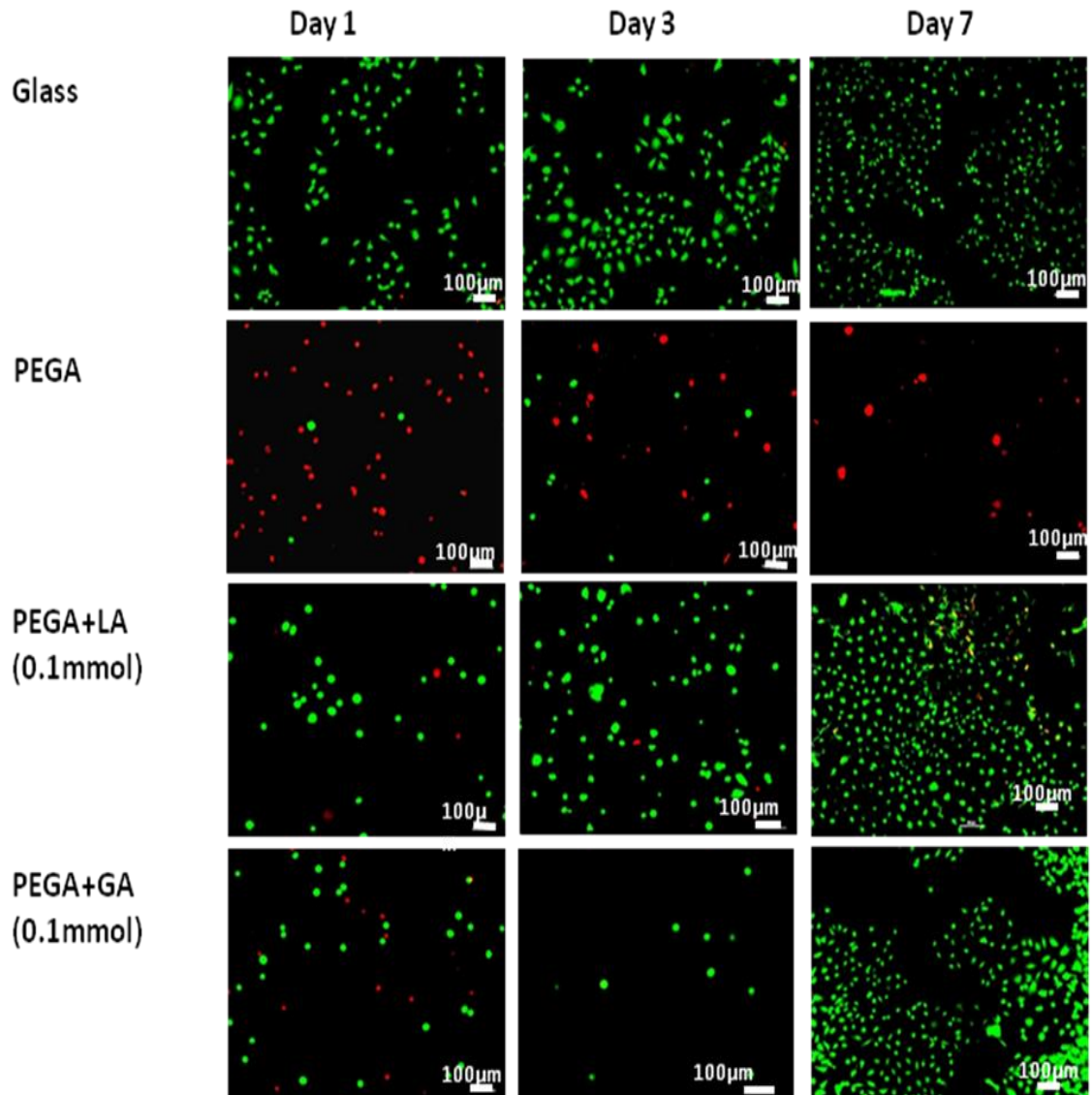
**Figure 4.2:** Live /Dead staining evaluating the cellular viability of hepatocyte cell line FL83B grown on selective surfaces (Glass, PEGA, PEGA+LA and PEGA+GA) over the course of 7 days. Green fluorescence is an indication that the cells are alive, whilst red fluorescence is a sign that the cells have either died or are not viable.

Cell adhesion to the ECM induces reorganisation of cytoskeletal components and influences cell morphology. Vinculin and f-actin are major cytoskeletal proteins involved in integrin mediated signalling and cell spreading (Critchley, 2000, Kim *et al.*, 2003b). Cell line hepatocytes cultured on TCP, PEGA+LA and PEGA+GA were stained for vinculin, pFAK and f-actin, Figure 4.3. Hepatocytes were extensively spread on TCP with the vinculin and pFAK localised at the points of focal contact. However, there was little to no reorganisation of actin filaments and vinculin in

hepatocytes on the PEGA+LA surfaces. The vinculin and pFAK were seen to be internalised on the galactose carrying surface with little evidence of clustering at the cell membrane, Figure 4.3, suggesting the presence of ASGP-R mediated binding. Interestingly, the hydrogel surface containing the control sugar PEGA+GA showed vinculin and pFAK localised in clusters at sites of cell-matrix adhesion and there was a more polarised actin cytoskeleton suggesting the presence of integrin binding, Figure 4.3. When integrin binding occurs to the ECM autophosphorylation occurs at the Tyr-397 residue of FAK resulting in the initiation of focal adhesions (Schaller *et al.*, 1994). The staining observed here reveals that integrin mediated signalling may not be activated in cells attaching to the PEGA+LA surface. It has previously been shown that hepatocytes can bind to galactose carrying polymers via ASGP-R, inhibiting the phosphorylation of FAK (Cho *et al.*, 2006, Gutsche *et al.*, 1994b). Selective adhesion of hepatocytes via this mechanism was shown to drive internalisation of cytoskeletal and focal adhesion components (Kim *et al.*, 2003b, Cho *et al.*, 2006). Therefore, the patterns observed in this study may indicate that PEGA+LA adhesion is primarily mediated via ASGP-R, and does not initiate integrin mediated signalling components.
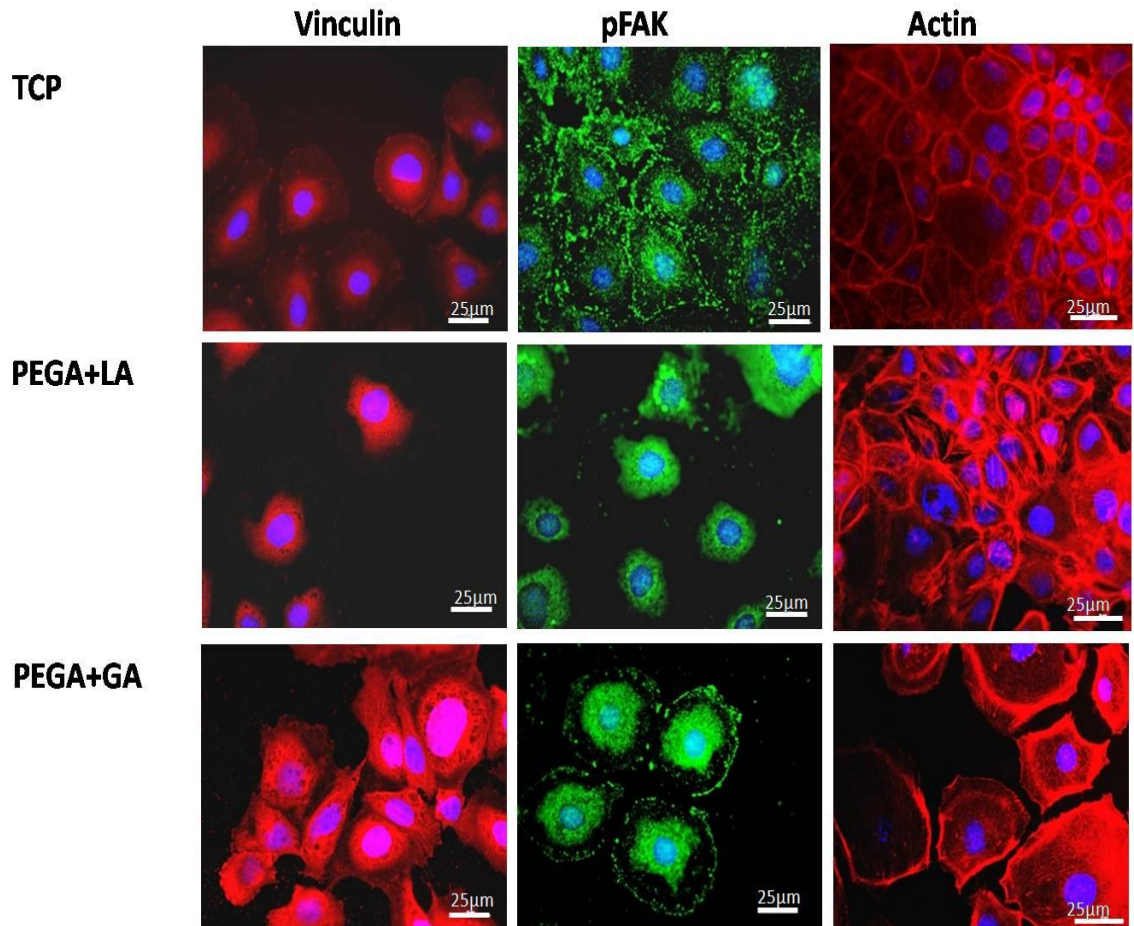
**Figure 4.3:** Fluorescence micrographs of immunocytochemical staining of day 4 hepatocyte cell line for vinculin (red), pFAK (green) and actin (red); grown on either TCP, PEGA+LA or PEGA+GA. Nuclei are counter stained blue.

### 4.3.2 Cell Proliferation and metabolic activity

DNA assays were conducted on all the samples in order to quantify the degree of proliferation. Standard calibration curves were prepared for hepatocytes by assaying known number of cells.

The mean fluorescence values for each material were recorded and the number of cells present calculated using three independent samples per material per time-point, and the data was plotted accordingly. The mean cell number values measured for each material tested for 1, 3 and 7 days are summarised in Figure 4.4 and are highlighted in white, grey and dark grey respectively.

Figure 4.4 shows a general increase of cells in the hepatocyte cultures on most of the substrate materials at different time-points in a 7 day period. Glass and PEGA substrates appeared to be the exception to the general trend observed with all the other materials in the study where the cell number remained constant over 7 days, Figure 4.4. The mean number of cells on the glass cover slips did slightly decrease from 2.27 x $10^4$ cells/cm$^2$ to 1.52 x $10^4$ cells/cm$^2$ after 3 days in culture before increasing to 2.09 x $10^4$ cells/cm$^2$ at the 7 day time-point, Figure 4.4. The mean number of cells on the non- fouling PEGA substrate did slightly increase from 4.99 x $10^3$ cells/cm$^2$ to 5.23 x $10^3$ cells/cm$^2$ after 3 days in culture before increasing to 6.31 x $10^3$ cells/cm$^2$ at the 7 day time-point. The constant but low levels of cell numbers suggest that hepatocytes do not proliferate well on these substrates. This is further confirmed by the lack of metabolic activity seen on this material in terms of urea synthesis.
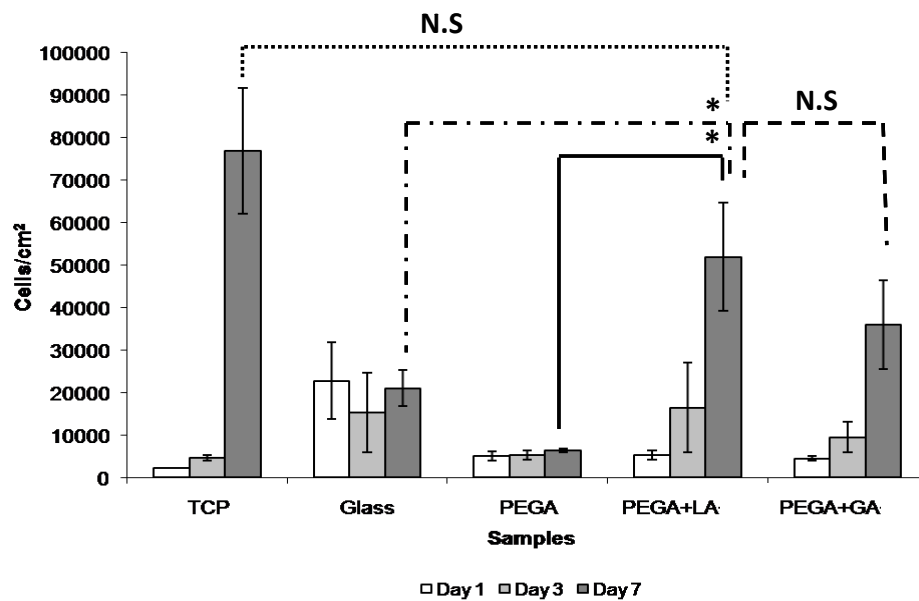


**Figure 4.4:** DNA assay, determined by Hoechst labelling, illustrating proliferation of cell number over 7 days for TCP, Glass, PEGA, PEGA+LA and PEGA+GA. Data is expressed as the mean cell number ± standard deviation, (n=6). Degree of significance is determined by Student t-test with a two tailed distribution and equal variance. * = ($p$<0.05). N.S = Not Significant.

Hepatocytes grew well on TCP over the course of 7 days, with cell numbers increasing from 2.18 x $10^3$ cells/cm$^2$ after one day in culture to 7.69 x $10^4$ cells/cm$^2$ after 7 days of incubation. The presence of sugars either LA or GA incorporated into

PEGA hydrogel surfaces had a marked effect on the cellular proliferation observed. Cell numbers increased steadily over the course of the culture period and after 7 days incubation PEGA+LA and PEGA+GA had mean cell numbers of 5.29 x$10^4$ cells/cm$^2$ and 3.60 x $10^4$ cells/cm$^2$ respectively. The PEGA+LA and PEGA+GA surfaces after 7 days in culture performs statistically significantly better than both glass and PEGA substrates, ($p$<0.05) Figure 4.4. PEGA+LA is comparable to TCP in terms of cellular proliferation ($p$>0.05); however PEGA+GA is not, ($p$<0.05) Figure 4.4.

Urea synthesis is a key function of hepatocytes; enabling the transformation of ammonia into urea. Typically it had been shown that synthesis of urea by *in-vitro* cultured hepatocytes on galactosylated surfaces is maintained for longer than on non-galactosylated substrates (Yang *et al.*, 2002, Hong *et al.*, 2003). Despite this the cells do lose their functionality over time (Du *et al.*, 2006, Fan *et al.*, 2009). Three independent samples per material per time-point were used to determine urea synthesis in culture, and the data was plotted accordingly. The mean urea secretion values measured for each material tested with hepatocytes for 1, 3 and 7 days are summarised in Figure 4.5 and are highlighted in white, grey and dark grey respectively.

The generalised trend of the data shows that urea synthesis decreases over time. All samples showed a decrease in mean urea synthesis from Day 1 to Day 3 of incubation with the exception of TCP. TCP, glass and PEGA showed a decrease in urea synthesis on day 7 of culture, Figure 4.5. The decrease in urea synthesis on TCP from 0.42 mg/dL on day one to 0.15 mg/dL on day 7 of culture suggests a loss of metabolic function despite of a significant increase in cell numbers over the course of seven days. Initially, the glass substrate supported the most substantial urea synthesis of all the samples, with 0.96 mg/dL seen after one day in culture, which can be correlated to high viable cell numbers, this decreased to 0.41 mg/dL at Day 3, the synthesis of urea then plateaued as the day 7 value (0.39 mg/dL) was not significantly different from the day 3 value, ($p$>0.05) Figure 4.5. Urea synthesis on the PEGA surface is negligible which can be correlated to low viable cell numbers. The average urea synthesis on the PEGA+LA did decrease from 0.94 mg/dL to 0.44 mg/dL after 3 days in culture before significantly increasing to 0.68 mg/dL at the 7 day time-point, ($p$<0.05) Figure 4.5. The presence of galactose within the PEGA resulted in a significant increase in urea synthesis compared to all other materials on

day 7, ($p<0.05$), Figure 4.5. A similar trend was also observed for the PEGA+GA material. The increase in urea synthesis on the PEGA+LA and PEGA+GA surfaces at the day 7 time-point suggests that the cells may have conditioned their local environment forming a functional architecture in which liver specific functions may be maintained.
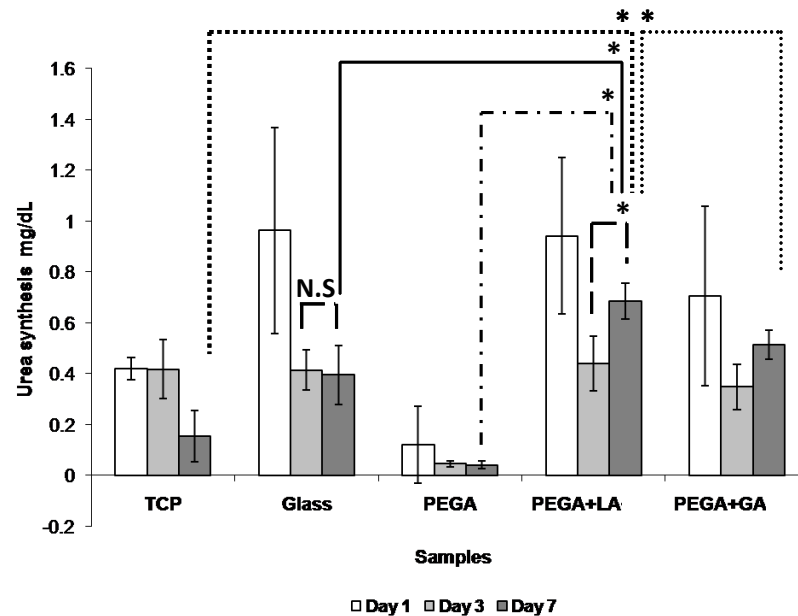


**Figure 4.5:** Urea synthesis over the course of 7 days for TCP, Glass, PEGA, PEGA+LA and PEGA+GA. Data is expressed in terms of mean urea synthesis (mg/dL) ± standard deviation, (n=6). Degree of significance is determined by Student t-test with a two tailed distribution and equal variance. * = ($p<0.05$) N.S = Not Significant.

### 4.3.3 RT-PCR and flow cytometric detection of liver specific markers

RT-PCR was used to assay for liver specific markers; α-FP, ASGP, albumin and CK18, and compared against primary cells and a section of liver tissue. Additionally, live hepatocytes were labelled to detect ASGP-Rs on the surface of the cells by flow cytometry.

Within the population of FL83B hepatocytes there appeared to be two sub-populations containing different levels of cell-surface ASGP-R. Although the majority of cells contained no detectable ASGP-R, ~29 % of the cells were immunopositive for the receptor, Figure 4.6. The ASGP-Rs detected by the antibody

are at the cell surface, the cells were not permeabilised prior to staining, and therefore the receptors should be available to bind to galactose.
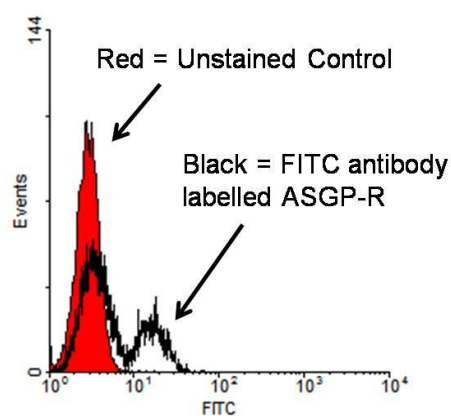


**Figure 4.6:** Flow cytometry of ASGP-R of a typical cell population of hepatocytes. Data shows a split population of cells with 29 % positive for ASGP-R.

Initially, a population of FL83B cells was analysed for the expression of liver specific genes. The cells were found to express, α-FP, albumin and CK18. The cells did not show any expression of ASGP-R. Primary cells taken from a fresh preparation were positive for all markers except α-FP, which is only present in foetal liver tissue (Berry *et al.*, 1991), Figure 4.7. Although this was not a quantitative assay, there was some suggestion that the level of expression of ASGP-R in primary cells was not as high as that in liver tissue. This is in agreement with previous studies which have suggested that the receptor is down-regulated in primary cells when placed *in-vitro* culture. These observations suggest that although there is a residual level of ASGP-R on the surface of some FL83B cells within the population; message RNA for ASGP-R is not being actively transcribed. The next aim of this study was to determine whether exposure of the FL83B cells to the various test surfaces, in particular the PEGA+LA surface, altered ASGP-R expression. Consequently, cells were seeded onto the sample surfaces, grown in culture for six days then harvested for RT-PCR, Figure 4.8. On evaluation, it was clear that the cells did not switch on ASGP-R expression. The previous marker genes were also run, which verified that the cells were still expressing the liver specific markers of CK18, albumin and α-feta protein. The expression of albumin was relatively weak in all of the samples suggesting that this function may be down regulated at the point of cell collection.

Consequently, it can be seen that the cells are actively functioning as liver cells and maintaining liver specific functions such as urea synthesis. However, ASGP-R expression is not maintained by the FL83B hepatocyte cell line in culture.
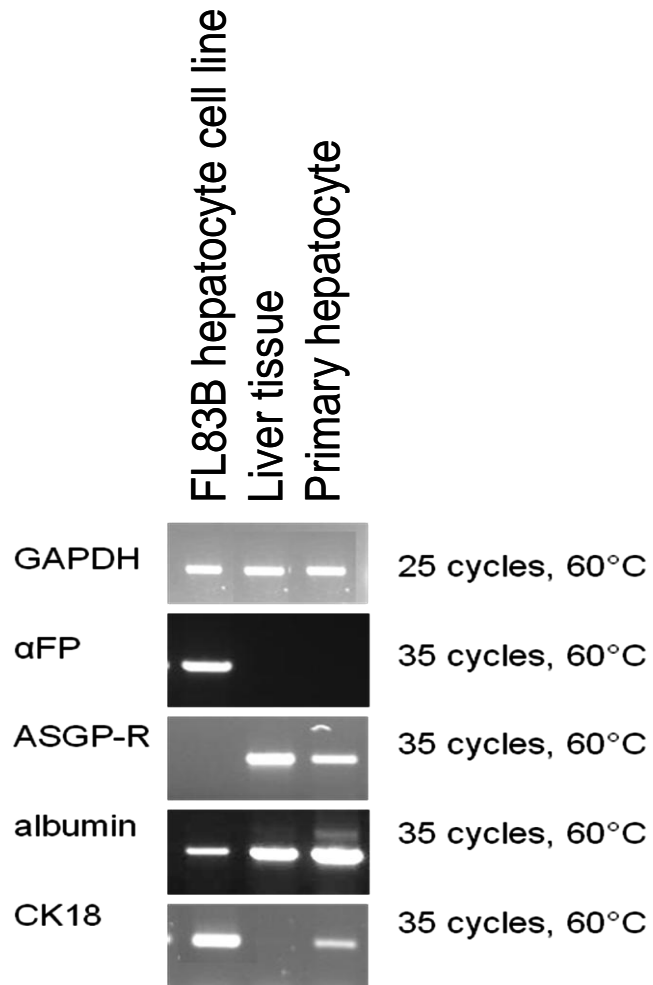


**Figure 4.7:** Initial evaluation of hepatocyte cell line by PCR for liver specific genes. Liver tissue and primary liver cells were used as sample controls and GAPDH was used as the loading control.
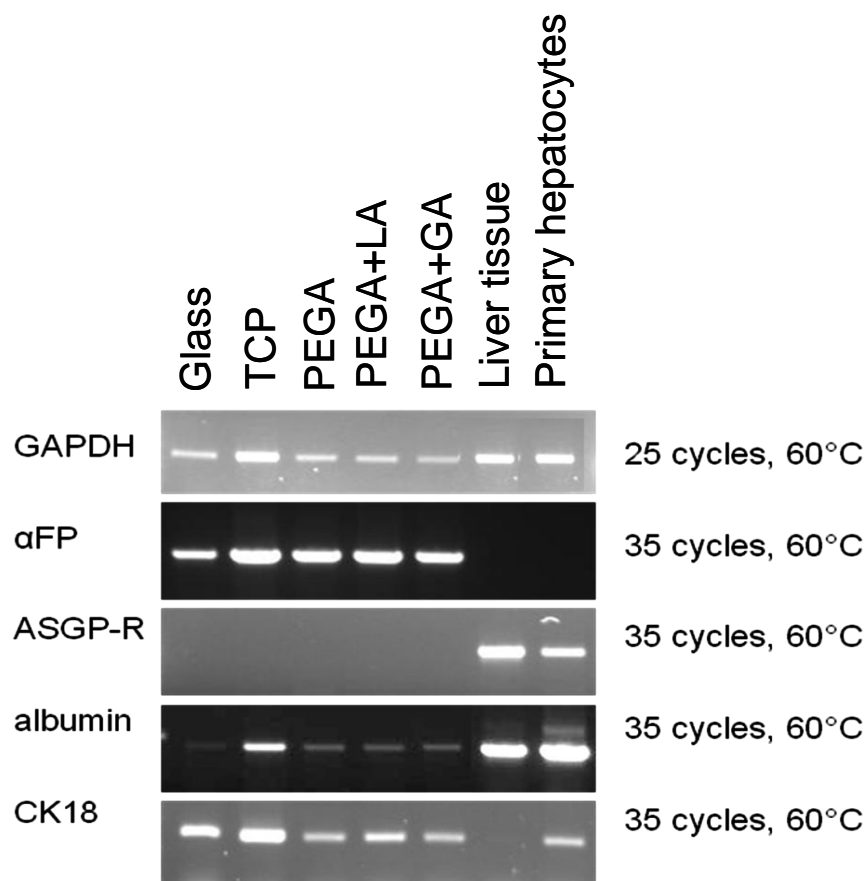
**Figure 4.8:** Evaluation of hepatocyte cell line by PCR on substrate surfaces after six days culture, to determine whether the presence of galactose switched on ASGP-R. Liver tissue and primary liver cells were used as sample controls and GAPDH was used as the loading control.

## 4.4 Conclusions

Sugar functionalised PEGA hydrogel surfaces were evaluated as platforms on which to grow and direct liver cell behaviour. A PEGA hydrogel displaying a galactose moiety (PEGA+LA) was prepared to guide cellular adhesion via the unique ASGP-R – galactose interaction. The control materials; glass, TCP, PEGA hydrogel and PEGA+GA (control sugar) were also evaluated. It was observed that unmodified PEGA retained its non-fouling properties and did not support cellular adhesion and growth. The presence of saccharides in the form of LA and GA within PEGA resulted in good hepatocyte adhesion and proliferation and maintained some liver specific functions e.g. urea synthesis. Although initial analyses, by immunocytochemical staining, suggested that the ASGP-R-galactose system was

functional in providing an optimal surface for hepatocyte growth, further investigations using flow cytometry and RT-PCR, proved that the cellular attachment was unlikely to be via the designed mechanism. Due to the low levels of ASGP-R detected at the plasma membrane in a small sub-population of the cells and the lack of active transcription of the ASGP-R message detected by RT-PCR, it is unlikely that the cells are attaching to the galactose modified surfaces by ASGP-R. Consequently, the attachment mechanism to this surface remains unclear, but it is likely to involve the preferential binding of ECM components by the saccharides which would then enable cell adhesion either via integrins or other cell-matrix receptors. The presence of LA and GA saccharides within the PEGA material clearly had a supportive effect on hepatocyte culture and merits further investigation.

## Chapter 5.0 Surface characterisation of sugar functionalized poly(ethylene glycol) monolayers

### 5.1 Introduction

Exploiting the interaction between cell surface receptors and biological ligands can lead the development of dynamic biomaterials that can actively and selectively stimulate desired cellular functions in relation to tissue growth and healing. In this regard, PEG – based biomaterials have been used to provide a well defined platform from which fundamental studies have been undertaken. PEG based materials resist non-specific protein adsorption and interactions, thus PEG based scaffolds have been used to systematically introduce selected cell attachment motifs, especially those from matrix adhesion proteins i.e. RGD present within fibronectin and other ECM-resident proteins, and study how this influences cell attachment and function, see Section 2.3.7 (Todd *et al.*, 2009, Benoit and Anseth, 2005, Kloxin *et al.*, 2009). This study focuses on utilising simple sugars to create a bioactive surface which hepatocytes may interact with, by exploiting the ASGP-R as an adhesive ligand via galactose moieties.

It was shown in Chapters 3 and 4 that bioinert PEG based hydrogel surfaces (polyethylene glycol) acrylamide – PEGA when modified with sugars LA or GA, promote hepatocyte attachment, proliferation and maintenance of essential functions. Limitations of the above system were firstly that the highly hydrated PEGA surfaces could not be easily chemically analysed due to the high water content within the material, thus preventing traditional ultra high vacuum techniques from being used. Additionally, the PEGA based systems are fragile and prone to adhesive failure from the glass substrates. However, the use of PEG monolayers provides a chemically stable platform which can be modified and analysed using ultra high vacuum techniques such as XPS and ToF-SIMS.

This chapter describes the production of PEG monolayers, and their subsequent modification using stepwise amide coupling chemistry to immobilise the two candidate sugars; LA and GA. A range of surfaces were manufactured and characterised using water contact angle, protein adsorption assays, XPS and ToF-SIMS. The reaction conditions were varied in terms of number of coupling cycles and the solvent used.

### 5.2 PEG surfaces

All chemicals and reagents, unless otherwise stated were purchased from Sigma Aldrich Company Ltd. (Gillingham, UK) and were used as received.

### 5.2.1 Preparation of surfaces

Borosilicate glass coverslips (Chance glass Ltd, Malvern, UK, 12mm diameter, No 2 thickness) and all other glassware used were cleaned prior to use by immersion in piranha solution (strongly corrosive), a 3:7 mixture of hydrogen peroxide solution and concentrated sulphuric acid, for 30 minutes, followed by rinsing in copious amounts of deionised water and drying in an oven at 100ºC overnight.

### 5.2.2 Silanation and PEG coupling

PEG monolayers were produced with reference to methods described by Piehler *et al.* and Todd *et al.* (Piehler *et al.*, 2000, Todd *et al.*, 2009). Glass coverslips were modified with (3-glycidyloxypropyl) trimethoxysilane (GOPTS) by incubation in 100 % GOPTS at room temperature for one hour, then washed in dry acetone and dried under nitrogen gas flow. Following this, the surfaces were immediately treated with pure PEG-diamine (Polypure, Norway, n=18) by melting a layer of the pure PEG powder on the surface at 75ºC for 48 hours, after which the surfaces were thoroughly washed with distilled water and dried under atmospheric conditions overnight.

### 5.2.3 Modification of PEG monolayers

LA and GA sugar modified surfaces were produced via coupling to the terminal amine groups on PEG surfaces. 0.2 mmoles of sugar were coupled to the amine rich PEG surfaces in the presence of (2-(1H-Benzotriazole-1-yl)-1,1,3,3-tetramethyuronium hexafluorophosphate) (HBTu) (4.9x molar equivalence) and N,N-Diisopropylethylamine (DIPEA) (10x molar equivalence) in DMF or DMSO. Two different solvents were investigated to determine if solvent selection affected the efficiency of the sugar coupling, as was the number of coupling cycles used: single, double or triple coupling. Immersion in the solution for 2 hours in the first instance (single coupling) followed by rinsing with ethanol, methanol then the

coupling solvent DMF or DMSO. Immersion in fresh solution overnight resulted in double coupled surfaces, which were then washed in the same way as the single coupled materials. Triple coupling was achieved by immersion in the solution for two consecutive 2 hour intervals, changing the solutions and rinsing the surfaces between incubations, as described above, followed by overnight coupling in fresh solutions. The overall surface production scheme can be seen in Figure 5.1.
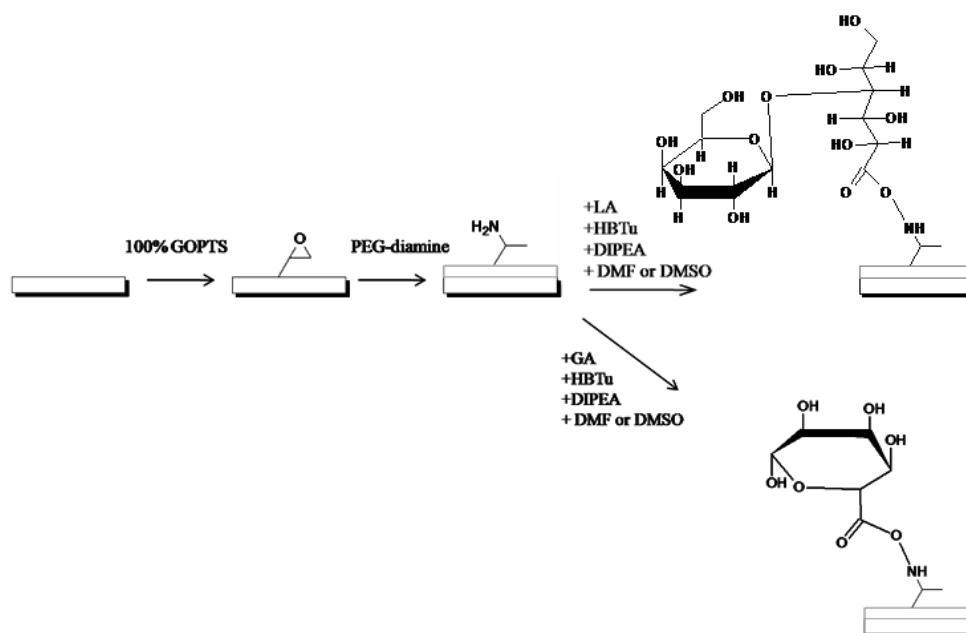


**Figure 5.1:** Schematic representation illustrating surface production.

## 5.2.4 Water Contact Angle

Wettability studies were conducted on all the candidate and control materials by measuring "water in air" contact angles. This was achieved by placing each sample into the holder of the Krüss DSA100 water contact angle meter (Krüss GmbH, Hamburg, Germany) and dispensing a 5 µl droplet of deionised water from a syringe needle onto the surface of the PEG monolayers and the control materials. The contact angle meter produced digital images of deionised water droplets on the surfaces, as well as measuring the angle of the static "water in air" droplets formed on the materials. All measurements were performed at room temperature. For each sample, ten contact angles from different regions of the candidate surface were measured and averaged.

### 5.2.5 Protein Adsorption

PEG surfaces were incubated in 1ml cell culture medium containing 10 % foetal bovine serum (FBS) at 37ºC, 5 % $CO_2$ and 95 % humidity for 24 hours. Glass coverslips, tissue culture plastic and GOPTS modified glass coverslips were used as control materials. The medium was then removed and the samples rinsed in 1 ml distilled water on a shaker for 15 minutes. The samples were then transferred to fresh wells where the adsorbed protein was then desorbed by treatment with 6M urea on a shaker for 60 minutes at room temperature. The urea/protein solution was quantified using the Quant-iT™ protein assay kit (Molecular Probes, Paisley, UK) using the manufacturers protocol. All reagents were equilibrated to room temperature prior to use. The Quant-iT™ protein reagent was diluted 1:200 in the Quant-iT protein buffer, 190 µl of this working reagent was loaded into each well of a 96 well plate, to which 10 µl of the desorbed urea/protein sample was added. The fluorescence of the product was measured using a fluorescence plate reader (Fluostar OPTIMA, BMG LABTECH, Germany) at 495/585 nm. Sample protein concentrations were determined using a standard curve of known protein bovine serum albumin/urea concentrations. Three samples of each surface were produced for testing. The experiment was repeated six times.

### 5.2.6 XPS

XPS and ToF-SIMS are complementary surface analysis techniques. ToF-SIMS provides qualitative information molecular information whilst XPS provides elemental and functional information. XPS is used routinely used as a surface analysis technique for metallic and polymeric materials. This technique has a depth resolution of around 1-10 nm (Istone, 1995, Briggs, 1998). When a surface is bombarded with a photon source, electrons contained within the material can be ejected, provided that the energy of the incoming photon is greater than that of the binding energy holding the electron within its orbital; this principle is recognized as the "photoelectric effect" (Istone, 1995, Briggs and Seah, 1990). Ejected electrons are known as photoelectrons and can come from both the core and valance orbitals of an atom. Electrons from the core orbitals, "core electrons", possess discrete energy values constitute the major portion of XPS spectra and do not participate in chemical bonding. The valance orbital is only partially filled with electrons in the outer shell

orbitals which are involved in chemical bonding and have broad energy values(Briggs and Seah, 1990, Briggs, 1998). The energy needed to move core electrons to the outermost shell orbital is used to identify the atomic origin. For example, C1s core level has a binding energy of ~285 eV and O1s has a binding energy of ~530 eV. The binding energy (BE) of photoelectron is given by the equation (Istone, 1995, Briggs, 1998):

$$BE = h\upsilon - KE - W \qquad \textbf{Equation 5.1,}$$

where, $h\upsilon$ is the energy of the incident photon beam, KE is the kinetic energy of a photoelectron and W is the work function. BE can be determined from $h\upsilon$, which is known from the X-ray source used.  KE is determined experimentally. The work function (W) is defined as the minimum energy barrier that an electron has to overcome to allow photoemission to occur, however in practical applications, this value is generally ignored. By calculating the peak area for the elements of interest from the XPS spectra, the atomic concentrations and percentages can be determined. Information about chemical functionalities and oxidation states can also be gathered from XPS spectra. The variation in binding energy and the energy level of the specific atom being studied with respect to the chemical environment surrounding it can result in a shift in the binding energy (Briggs and Seah, 1990).

In the case of polymeric and/or non-conducting samples, photoemission results in sample charging, this in turn increases the apparent binding energy values of core levels. The charging effect is balanced out by flooding the surface of the sample with low energy electrons using an electron flood gun. However, this process results in over compensation; the effect is apparent from the C1s core level binding energy being one or two eV lower than 285 eV. Thus prior to data processing, charge correction is employed by choosing the peak in the spectrum for which the correct binding is known. Conventionally polymeric surfaces are charge corrected with respect to binding energy of the aliphatic hydrocarbon C1s at 285 eV (Istone, 1995, Briggs, 1998).

A typical XPS instruments set up consists of an X-ray source, the source manipulator, UHV chamber, the electron transfer optics, an electron detector and kinetic energy analyser. The electrons generated during photoemission has relatively low kinetic energy (0-1500 eV), thus electrons can not travel large distances in

matter. Photoelectrons that emerge only from the material without the loss in kinetic energy comprise the peaks in XPS spectrum. The use of ultra high vacuums in the region of $10^{-9} - 10^{-10}$ Torr help reduce photoelectron scattering by removing air molecules.

XPS was used to acquire quantitative information on the chemical species available on the surface both during treatment steps and after coupling of sugar molecules. Samples were mounted onto stainless steel sample holders using double sided adhesive tape. Samples were analysed using the Kratos AXIS ULTRA (Kratos Analytical Ltd, Manchester, UK) with a monochromatic Al kα X-ray source (148.6 eV) operated using a 10 mA emission current and a 15 KeV anode potential. The instrument was used in FAT (fixed analyser transmission) mode, with a pass energy of 80 eV for wide scans and a pass energy 20 eV for high resolution scans. The take off angle for the photoelectron analyser was set normal to the sample surface and the monochromatic beam set at 60º to the lens (in magnetic lens mode). The base pressure in the analysis chamber was maintained not more than $10^{-9}$ Torr. Sample charging was prevented by using a charge neutraliser.

The wide scan and high resolution spectra of C1s, O1s and Si2p were collected for all samples. N1s and S2p wide scans and high resolution spectra were collected for the PEG monolayer samples. Curve fitting of C1s peak was performed using a Gaussian-Lorentzian peak shape function with a straight base line throughout the analysis. The high resolution scans were charge corrected to the main C1s peak (C-C, C-H) at 285 eV. Data analysis was carried out using CASA XPS software with Kratos sensitivity factors to determine the atomic percentage values from the peak areas.

**5.2.7 ToF-SIMS**

ToF-SIMS was used to analyse the chemical modifications to PEG surfaces. ToF-SIMS is a highly sensitive surface analysis technique and is used to obtain chemical information on the surface of materials. The principle of this technique involves bombarding the target surface with a beam of accelerated ions, for example $Ar^+$, $Ga^+$, $Cs^+$ or $Bi^+$. This beam collides with atoms and molecules in the surface and can ionise them, forming secondary ions. Secondary ions are accelerated into a mass spectrometer and their time of flight between the surface and the detector is

measured, Figure 5.2. The time taken for a secondary ion to reach the detector is proportional to the mass of the ion. The number of ions with a particular ratio of mass to charge (m/z) is recorded and presented in a spectrum (Belu *et al.*, 2003, Vickerman and Briggs, 2001, Schueler *et al.*, 1990).
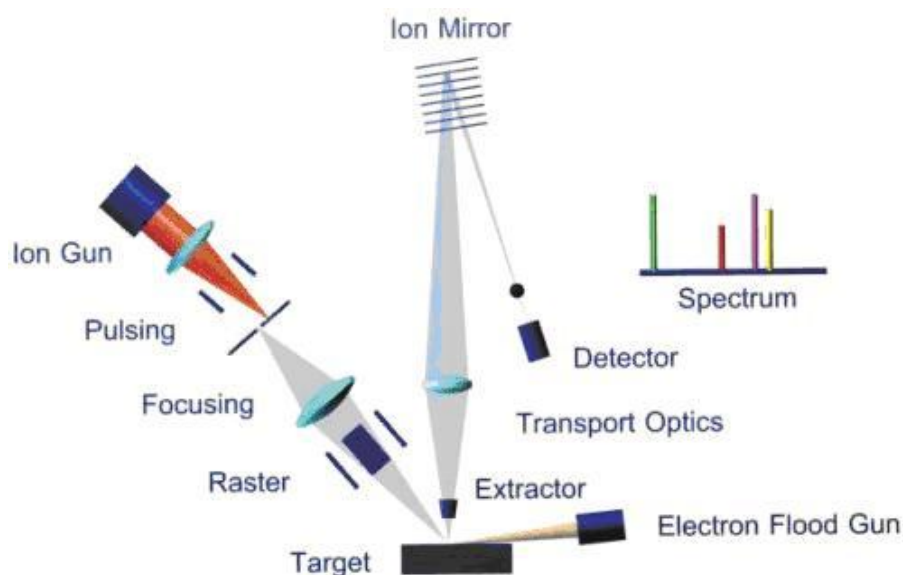
**Figure 5.2:** Schematic representation of ToF-SIMS set up. (Copyright Ion-Tof GmbH).

Secondary ion mass spectrometric analysis was carried out using a SIMS IV time of flight (ToF-SIMS) instrument (ION-TOF, GmbH, Munster, Germany) operated by Dr David Scurr, University of Nottingham. Similar to other SIMS instruments, it consists of four basic parts: a primary beam source, a sample holder, a mass spectrometer and an ultra high vacuum system, Figure 5.2. The instrument is fitted with an electron flood gun, for charge compensation, which is essential for non-conducting samples like polymers (Belu *et al.*, 2003, Vickerman and Briggs, 2001). A Bismuth liquid metal ion source was used to produce a primary beam using an acceleration voltage of 25 kV, a pulsed target current of 1 pA and post acceleration of 10 kV. Large scale images were acquired by rastering the stage under the pulsed primary ion beam, using a raster size of $256 \times 256$ over an area of $500 \times 500$ $\mu m^2$. All doses were kept well below the static limit, with a maximum dose of $10^{12}$ ions per $cm^2$ for both combined polarities. Acquisition of full raw datasets allowed for the retrospective construction of spectra from the imaged area. Positive

spectra were normalised to the total ion intensity for comparison between samples. All data analysis was carried out using the software supplied by the instrument manufacturer, IonSpec and IonImage (version 4.0) were used for spectroscopy and image analysis respectively. For each treatment, duplicate samples were analysed. The treatments analysed were: piranha cleaned glass, glass coverslips modified with GOPTS, PEG monolayers and PEG monolayers modified with either LA or GA.

## 5.3 Results and Discussion

### 5.3.1 Surface analysis

The surface modifications carried out in the study are confined to the monolayer. Consequently, the treated layer is prone to contamination and post-chemical reactions. Moreover, the chemical reactions that proceed to near completion in solution do not always do so at a surface due to steric considerations. Therefore, analysis of the modified surfaces to confirm the success of the proposed reaction shown in Figure 5.1 is essential if the biological response is to be reliably correlated with chemically-induced changes.

In the present study, complementary surface techniques with varying surface sensitivities namely: - "water in air" contact angle measurements, ToF-SIMS and XPS were used to confirm the changes in surface chemistry before and after functionalisation. The total amount of protein adsorbed from solution was quantified using a fluorescence labelling assay.

### 5.3.2. Water contact angle

The static "water in air" contact angle is a measure of the hydrophobic/ hydrophilic nature of the surfaces, with more hydrophilic surfaces having smaller water contact angles. For each sample, a total of ten independent static contact angles were measured from different regions of the candidate surface and averaged; the results of which are given in Table 5.1.

| Sample | Average contact angle $\theta_c$ degrees±(S.D.) |
|---|---|
| Piranha cleaned glass | 53.6 (11.6) |
| GOPTS | 67.1 (6.3) |
| PEG | 27.5 (4.7) |
| PEG+LA double coupling (DMF) | 26.3 (1.8) |
| PEG+GA double coupling (DMF) | 24.2 (6.0) |

**Table 5.1:** Static water contact angles. Data is expressed as the mean value ± standard deviation (n=10).

Water contact angle is a simple way to determine if surface modification has influenced the hydrophilicity of the material. The piranha cleaned glass exhibited an average water contact angle of 53.6° whereas silanation of the glass (GOPTS) resulted in an increase in the water contact angle to 67.1° attributed to the presence of epoxy groups within the silane molecule. The PEG monolayer exhibited an average contact angle of 27.5°, Table 5.1, which agrees with data presented by Piehlar *et al.* from which the modification technique was based (Piehler *et al.*, 2000). The addition of saccharides in the form of LA and GA by stepwise double coupling in DMF to the PEG monolayers resulted in a slight decrease in the average water contact angle from 27.5º to 26.3º and 24.2° respectively Table 5.1. Sugars are hydrophilic in nature and they therefore act to reduce the average water contact angle on the PEG monolayers. The reduction in the average contact angle indicates the presence of saccharides on the PEG monolayers, corroborated by the ToF-SIMS analysis undertaken in Section 5.3.5. It should be noted however that a change in water contact angle does not necessarily mean that the surfaces has been homogeneously modified. However, some publications still use this technique as their main method to determine whether a surface has been modified (Lin *et al.*, 2009, Fujimoto *et al.*, 1993, Faucheux *et al.*, 2004, Alves *et al.*, 2009). Consequently it is essential that such data, whilst encouraging, should be reinforced by in depth surface characterisation techniques.

### 5.3.3 Protein Adsorption

The Quant-iT™ protein assay kit was used to determine the amount of adsorbed protein on various surfaces after 24 hours in culture media as shown in Table 5.2. The amount of protein adsorbed on glass surfaces was statistically higher than for all PEG based surfaces ($p<0.05$). The higher amount of adsorbed protein on glass than PEG is a consequence of the non-specific protein adsorption on glass. The amount of adsorbed protein is similar for all the PEG based surfaces, as determined by student t-test ($p>0.05$), confirming that the presence of step-wise conjugated sugars has no effect on the non- fouling property of the surface. This suggests that any cellular interaction with the sugar PEG surfaces would be down to specific interactions with the immobilised LA or GA sugars on the PEG monolayers rather than by interactions with an absorbed protein layer.

The steric repulsion of biomolecules by PEG is partly due to solvation of the polymer chains, (osmotic repulsion) but also due to the conformational entropy of the PEG chains, (elastic repulsion) (Harder *et al.*, 1998, Jeon *et al.*, 1991). Protein adsorption is based on a balance between this steric repulsion of the surface, Van der Waals attractions and hydrophobic interactions between the protein and the surface. The overall force, attractive or repulsive has been determined to be dependent on the thickness and surface coverage, with long chain lengths and high surface densities being the most effective at resisting protein adsorption, see Section 2.3.7 for further details (Jeon *et al.*, 1991, Harder *et al.*, 1998, Kingshott *et al.*, 2002). The presence of LA or GA on the surfaces does not effect the interactions between the PEG chains, hence the non-fouling properties of the material are maintained.

Based on previous work undertaken by Todd *et al.*, the degree of protein adsorption on the PEG based surfaces does not match previous reported work where similar non-fouling PEG surfaces recorded serum protein adsorption values of, ~8 ng/mm$^2$ and 12.6 ± 1.0 ng/mm$^2$ (Benesch *et al.*, 2001, Todd *et al.*, 2009). The amount of protein adsorbed on piranha cleaned glass 225.7 ± 9.5 ng/mm$^2$ is similar to that reported by Todd *et al.* (~ 240 ng/mm$^2$) (Todd *et al.*, 2009).

| Sample | Protein Adsorption ng/mm$^2$± (S.D.) |
|---|---|
| Piranha cleaned Glass | 225.7 (9.5) |
| PEG | 150.9 (3.6) |
| PEG+LA single coupling (DMF) | 152.6 (2.2) |
| PEG+LA double coupling (DMF) | 151.7 (2.5) |
| PEG+LA triple coupling (DMF) | 155.9 (6.3) |
| PEG+GA single coupling (DMF) | 155.0 (4.9) |
| PEG+GA double coupling (DMF) | 151.7 (2.5) |
| PEG+GA triple coupling (DMF) | 161.8 (4.1) |
| PEG+LA single coupling (DMSO) | 161.5 (5.2) |
| PEG+LA double coupling (DMSO) | 151.5 (5.0) |
| PEG+LA triple coupling (DMSO) | 158.5 (6.5) |
| PEG+GA single coupling (DMSO) | 151.7 (3.6) |
| PEG+GA double coupling (DMSO) | 156.5 (6.1) |
| PEG+GA triple coupling (DMSO) | 151.5 (14.6) |

**Table 5.2:** Amount of protein adsorbed from serum containing cell media over 24 hours at physiological conditions, using a fluorescence assay kit. Data is expressed as the mean value ± standard deviation, (n=9).

### 5.3.4. XPS analysis

Quantitative surface analysis was undertaken by using XPS. All chemical fragments expected to be present on the unmodified PEG monolayers were identified on all samples. Due to time and excess constraints only double coupled sugars (LA and GA) in DMF were analysed. Piranha cleaned glass, GOPTS coated glass and PEG monolayers were used as reference samples.

The percentage of each element present on the sample surface was determined from XPS wide scans as seen in Figure 5.3. XPS analysis of piranha cleaned glass surfaces showed ~ 28.3 % carbon, ~6.7 % nitrogen, ~ 46.2 % oxygen and 6.7 % silicon, respectively as shown in Figure 5.3. Additionally contaminants of sodium and sulphur were present at ~2.1 %, and 9.9 % respectively arising from the piranha treatment of the glass. Sodium is a common contaminant in solvents and the sulphur was most likely left behind due to insufficient washing steps before the glass was dried. The carbon concentration of the glass is much higher than previous published literature; Todd *et al.* reported piranha glass surfaces with ~11 % carbon, ~1 % nitrogen and ~ 32 % silicon (Todd *et al.*, 2009). It is likely that the low silicon content on the samples in this study is due to a sodium, sulphur, nitrogen and excess carbon contamination overlayer attenuating the signal acquired from the silicon peak, resulting in a lower than expected result.

The silanation process increased the amount of surface silicon and carbon from 6.7 % to 18.6 % and 28.3 % to 33.0 % respectively due to the silicon and carbon in the epoxy silane molecule. The oxygen and nitrogen concentrations decreased slightly as the glass substrate signal was attenuated by the GOPTS. After PEG coupling, the concentration of carbon and nitrogen species increased due to the high proportion of these elements associated with PEG molecules. The nitrogen peak was seen to be broader and split into two distinctive peaks, indicative of a change in the number of chemical bonds contributing to the peak shape. The position of the nitrogen peak also indicated a certain degree of nitrate contamination, probably introduced when the PEG monolayers were washed in distilled water. Additionally, it is likely that the PEG sample suffered from differential charging during its analysis. Differential charging occurs when there are localised differences in the charge state of the surface. An increase in percentage carbon was observed for all samples after sugar coupling, which was expected due to the presence of carbon in the sugar molecules. It would be expected that the concentration of nitrogen would increase relative to the PEG surface, confirming the introduction of nitrogen in the amide bonds of the sugars, hence authenticating the successful coupling of LA and GA. However, due to the unusual split N1s peak observed on the PEG sample, this is not the case and the percentage nitrogen content decreases on the modified samples. Previous literature by Todd *et al.* put the concentration of the PEG N1s peak at ~1

%, suggesting that the sample analysed in this study may have been contaminated (Todd *et al.*, 2009). The percentage of oxygen decreased slightly relative to the PEG surface after modification with saccharides, this was attributed to the masking of free oxygen groups from the PEG surface with the saccharides LA or GA.
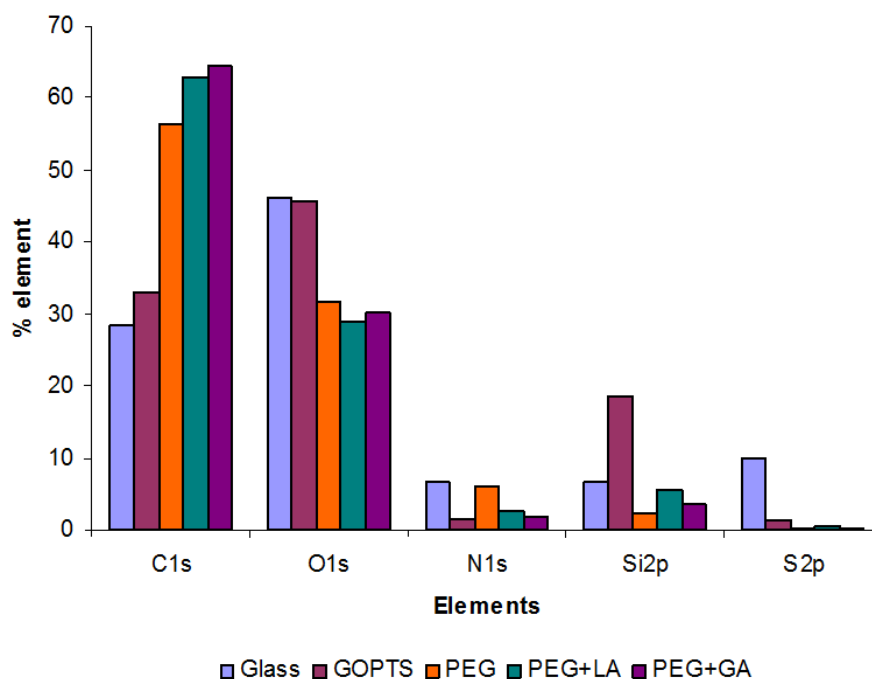


**Figure 5.3:** Percentage of elements present on each sample, as determined from XPS wide scans.

Curve fitting of XPS high resolution spectra revealed the functional nature of carbon species for each surface, as shown in Figure 5.4. and Appendix 1. The presence of hydrocarbons (C-C or C-H), C-O, C=O, NC=O and C-O-C indicate a contribution from the PEG structure. Glass had a high proportion of C-C or C-H environments, 53.7 %, with a low proportions of C-O and C=O or NC=O at 11.2 % and 3.7 % respectively, Figure 5.4. After epoxy silane (GOPTS) and PEG coupling the amount of hydrocarbon containing species decreased compared to the glass, Figure 5.4. An increase in C-O groups was observed in the presence of LA and GA from 42.6 % to 71.6 % and 76.6 % respectively, Figure 5.4. The variation in C-C or C-H was believed to be associated with the size and concentration of the attached sugar. The component at 288.2 eV, attributed to the formation of an amide bond, R-(C=O)-NHR, was observed on PEG surfaces at 9.18 %. In the LA and GA modified surfaces the amide bond concentration decreased to 2.2 % and 3.4 % respectively. It

is expected from this observation that some sugar coupling will have occurred to the PEG monolayers. However, the low amide concentrations on the sugar modified surfaces compared to the PEG monolayer (9.2 %) suggests that the sugars did not completely cover the surface. The low N/C ratio, Table 5.3, and the analysis of the C1s spectrum after sugar immobilisation further support this expectation. The XPS analysis, successfully tracked the reaction steps, however, it was also revealed that large amounts of adventitious contamination from solvents used in sample preparation of the glass and PEG samples, were present highlighting the need for careful sample preparation.

| Substrates | % C | % O | % N | N/C |
|------------|------|------|-----|------|
| Glass | 28.3 | 46.2 | 6.7 | 0.2 |
| GOPTS | 33.0 | 45.6 | 1.4 | 0.04 |
| PEG | 56.4 | 31.7 | 6.0 | 0.1 |
| PEG+LA | 62.8 | 28.8 | 2.4 | 0.03 |
| PEG+GA | 64.5 | 30.0 | 1.7 | 0.02 |

**Table 5.3:** Chemical surface composition from XPS data of chemically modified substrates.
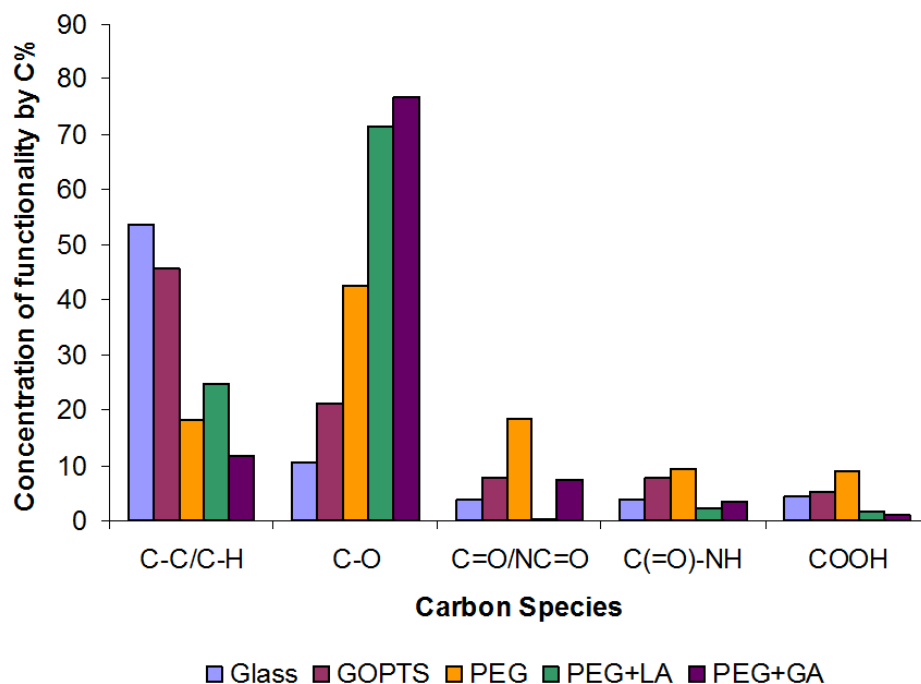
**Figure 5.4:** Concentration of functionality by carbon percentage determined by curve-fitting C1s spectra from XPS data.

### 5.3.5 ToF-SIMS analysis

ToF-SIMS analysis was used to study the qualitative distribution and the extent of coverage of both LA and GA sugars on PEG monolayers. The peak at m/z = 28 represents silicon and is the most intense on glass as expected, m/z = 45 represents $C_2H_5O$ and is indicative of PEG groups ($C_2H_5O^+$). The peaks at m/z = 338 and 675 are indicative of sugar ion fragments and have been nominally identified as $C_{12}H_{18}O_{11}$ and $C_{24}H_{35}O_{22}$ respectively.

The intensities of the 338 peaks were found to vary on different samples, as shown in Figures 5.5 and 5.6. The intensity of the 338 D peak for the PEG +LA (single coupling in DMF) was comparatively lower than the other couplings investigated, Figure 5.5. This suggests a low resultant coupling of LA on PEG monolayers using single coupling in DMF. In contrast the intensity of the 338 D peak was at its most intense for the single coupling method of LA to PEG monolayers using DMSO as the solvent, Figure 5.5 D.

The intensity of the 338 D peak for the PEG+GA (single and double coupling in DMF) as shown in Figure 5.6 A & B was comparatively lower than the PEG+GA

119

(single coupling in DMSO), Figure 5.6 D and the PEG+GA (triple coupling in both DMF and DMSO) sample, Figure 5.6 C & F . This suggests a low resultant coupling of GA on PEG monolayers using single or double coupling in DMF. In contrast, the intensity of the 338 D peak was at its most intense for the double coupling method of GA to PEG monolayers using DMSO as the solvent, Figure 5.6 E.
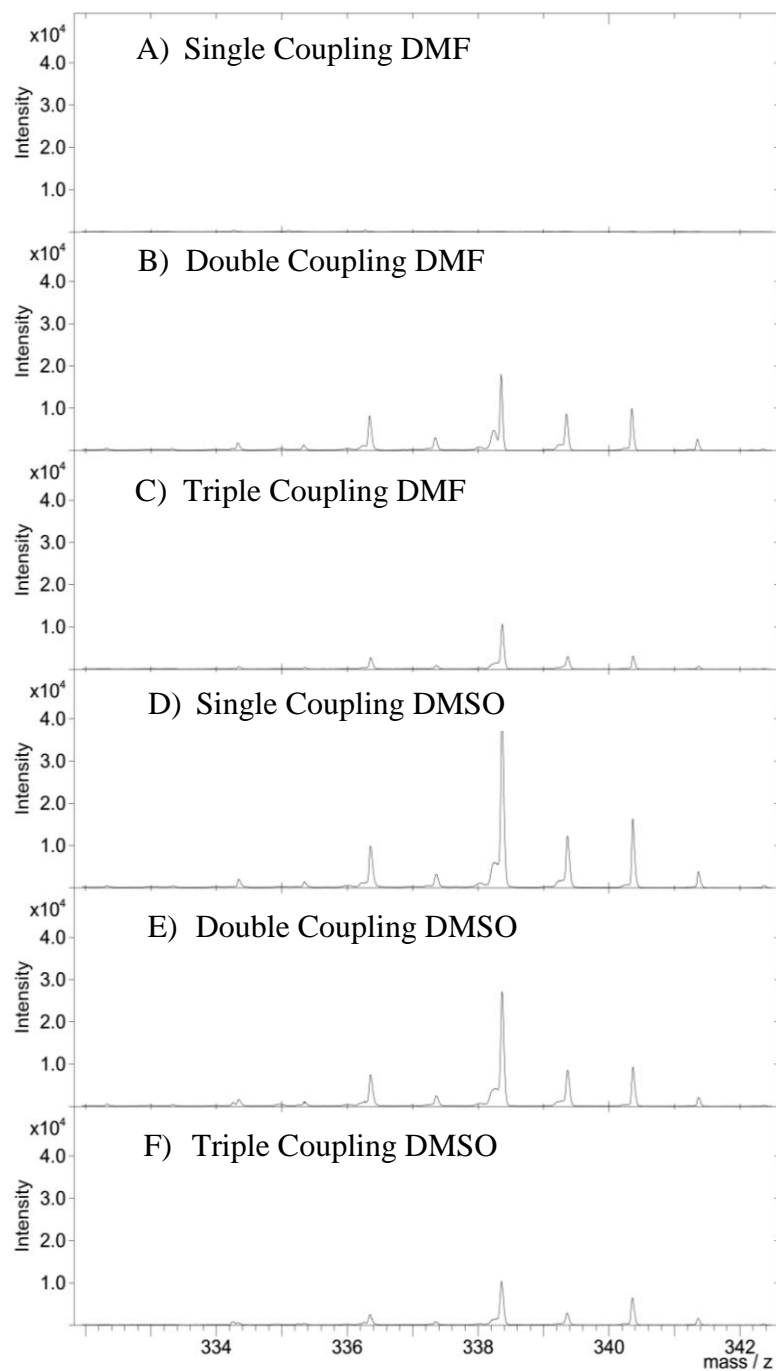
**Figure 5.5:** ToF-SIMS positive spectra for LA sugar coupled to PEG monolayers, monitored for the presence of peak at m/z 338 D for presence of sugar on **A)** Single coupling in DMF, **B)** Double coupling in DMF, **C)** Triple coupling in DMF, **D)** Single coupling in DMSO , **E)** Double coupling in DMSO, **F)** Triple coupling in DMSO.
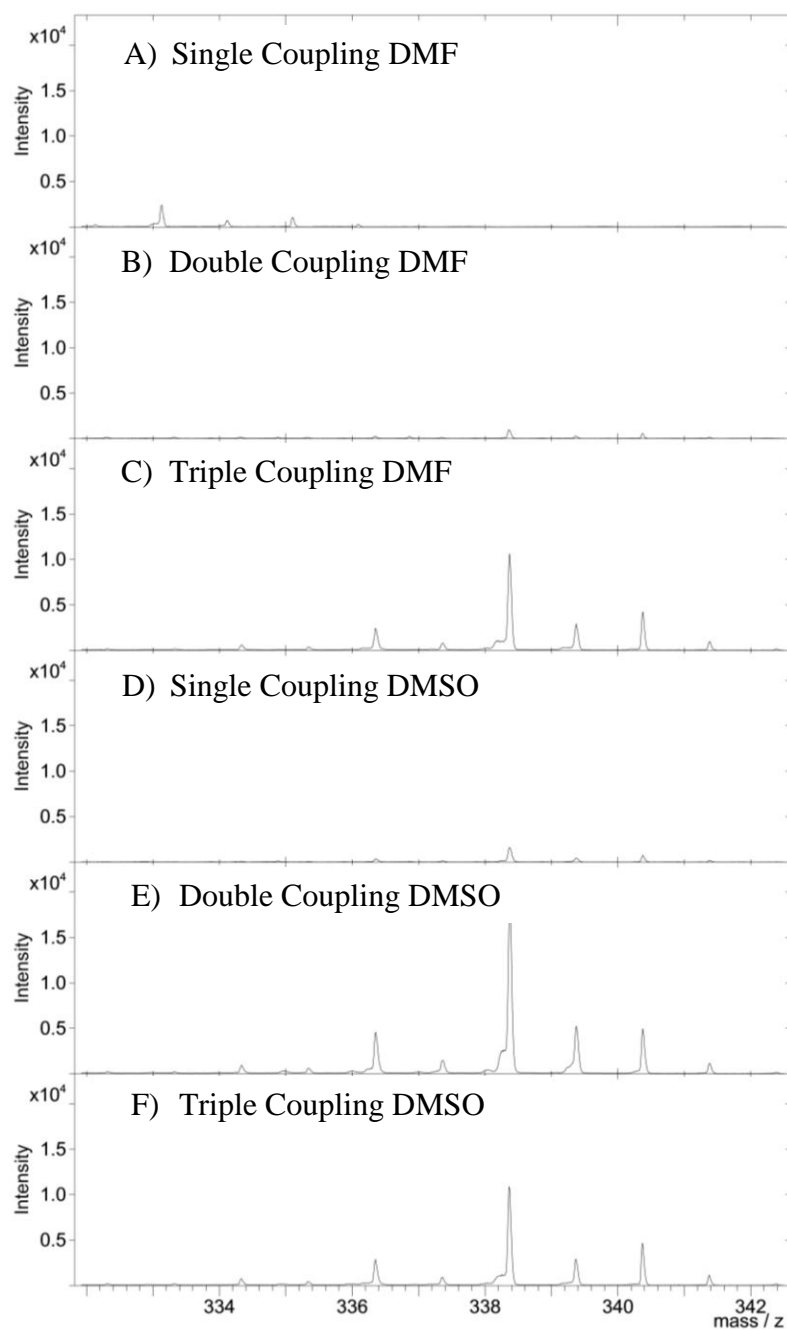
**Figure 5.6:** ToF-SIMS positive spectra for GA sugar coupled to PEG monolayers, monitored for the presence of peak at m/z 338 D for presence of sugar on **A)** Single coupling in DMF, **B)** Double coupling in DMF, **C)** Triple coupling in DMF, **D)** Single coupling in DMSO , **E)** Double coupling in DMSO, **F)** Triple coupling in DMSO.

The intensity data suggests that whilst coupling of sugars can take place using the DMF solvent system, the best coverage seemed to come from using DMSO as the solvent of choice. There was a discrepancy between the two sugars as to how many coupling steps are required to obtain the best surface coverage. The disaccharide LA ($M_w$ =358.3) required only one coupling step whereas the monosaccharide GA ($M_w$=194) required two. It is likely that DMSO solvates the sugars better than DMF by forming more hydrogen bonds with the sugars, resulting in better reaction yields.

The LA and GA sugars and their associated surface coverage resulting from varying coupling conditions are best represented by ToF-SIMS intensity maps as shown in Figures 5.7, 5.8 & 5.9. In these studies, Piranha cleaned glass, silanated glass (GOPTS) and PEG monolayers were used as reference samples. Figure 5.7 illustrates the generalised production of the surface from glass to functionalised sugar surface. Figures 5.8 & 5.9 illustrate the effects of single, double and triple coupling using two different solvents; DMF and DMSO for LA and GA respectively.

Figure 5.7 illustrates the presence of silicon at the 28 D peak which was present in significant amounts on both the piranha cleaned glass coverslips and coverslips which have been functionalised with GOPTS. There was a low level intensity signal from the 45 D peak on these surfaces, however, there was nothing to be seen at the 338 D and 675 D peaks, Figure 5.7 A & B respectively. PEG monolayers showed a decrease in the silicon intensity, and a high intensity uniform distribution from the 45 D peak associated with the repeating unit of the PEG chain, Figure 5.7 C. The coupling of LA, in this case double coupling in DMF, resulted in no discernable silicon signal, the PEG intensity was split between high and low, depending on the degree of LA sugar coverage, Figure 5.7 D. The bottom half of the image had a high PEG intensity peak and no sugar fragments were seen in the bottom half of the 338 D peak, Figure 5.7 D. The double coupling of GA in DMF resulted in a similar image, however the resulting sugar coverage was limited as shown by the intensity maps, Figure 5.7 E.
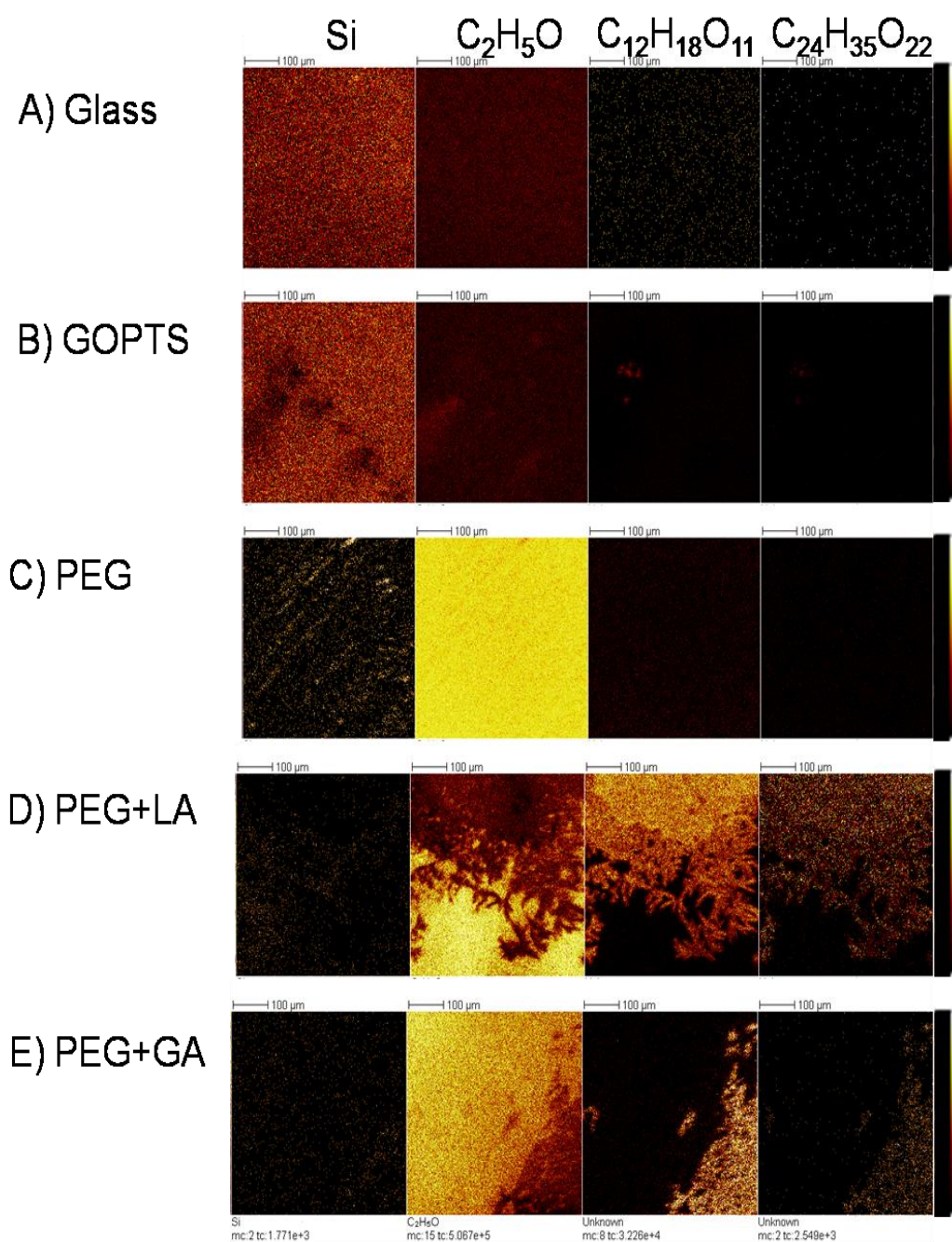
**Figure 5.7:** ToF-SIMS images (field of view 500 $\mu m^2$) for characteristic positive ions of silicon (m/z = 28), $C_2H_5O$ (m/z = 45), and sugar fragments $C_{12}H_{18}O_{11}$ (m/z = 338) and $C_{24}H_{35}O_{22}$ (m/z = 675). **A)** Glass, **B)** GOPTS, **C)** PEG monolayer **D)** PEG+LA (double coupled in DMF) **E)** PEG+GA (double coupled in DMF). The scale to the right of the image is from dark (low-intensity counts) to bright (high-intensity counts).

There was however a variation in secondary ion intensity for the 338 D peak between sugars on all samples which also suggests variable coupling of sugars on PEG monolayers. From Figures 5.8 and 5.9 the number of coupling steps and the choice of solvent had a profound effect on the attachment and distribution of LA and GA respectively. The degree of coverage mirrored that of the intensity data. Single coupling of LA in DMF did not result in any sugar fragments being detected; however the PEG intensity was homogenous across the entire sample area suggesting uniform coverage of the monolayer, Figure 5.8 A. Double coupling of LA in DMF resulted in non uniform coverage by large, high intensity, random patches of sugar attached to the PEG monolayer, Figure 5.8 B. Todd *et al.* observed that double coupling amino acids in DMF resulted in homogeneous peptide coverage on PEG monolayers which was confirmed by ToF-SIMS (Todd *et al.*, 2009). It is likely that the solubility of the sugars in DMF affected the degree of coverage seen when compared to the work of Todd *et al.* (Todd *et al.*, 2009). It would be hypothesized that triple coupling of LA in DMF would result in improved coverage; however this was not the case given that small patches of sugar were seen at the 338 D peak but the degree of coverage was negligible, Figure 5.8 C. The use of DMSO as the solvent appeared to improve the efficacy of coupling LA. Single coupling of LA using DMSO resulted in the best degree of coverage of all the coupling methods used. A small high intensity region of PEG was seen, though the remaining area was covered by the 338 D peak, Figure 5.8 D. Double coupling of LA using DMSO yielded similar results but the coverage of the single coupling method was deemed to be more complete due to the location of the PEG monolayer fragments, Figure 5.8 D & E. Triple coupling in DMSO again resulted in negligible coverage, suggesting that triple coupling in either solvent is not effective, Figure 5.8 C & F. It is possible that the numerous washing steps between each coupling may have resulted in damage to the surfaces and some to the covalently bound material being removed.
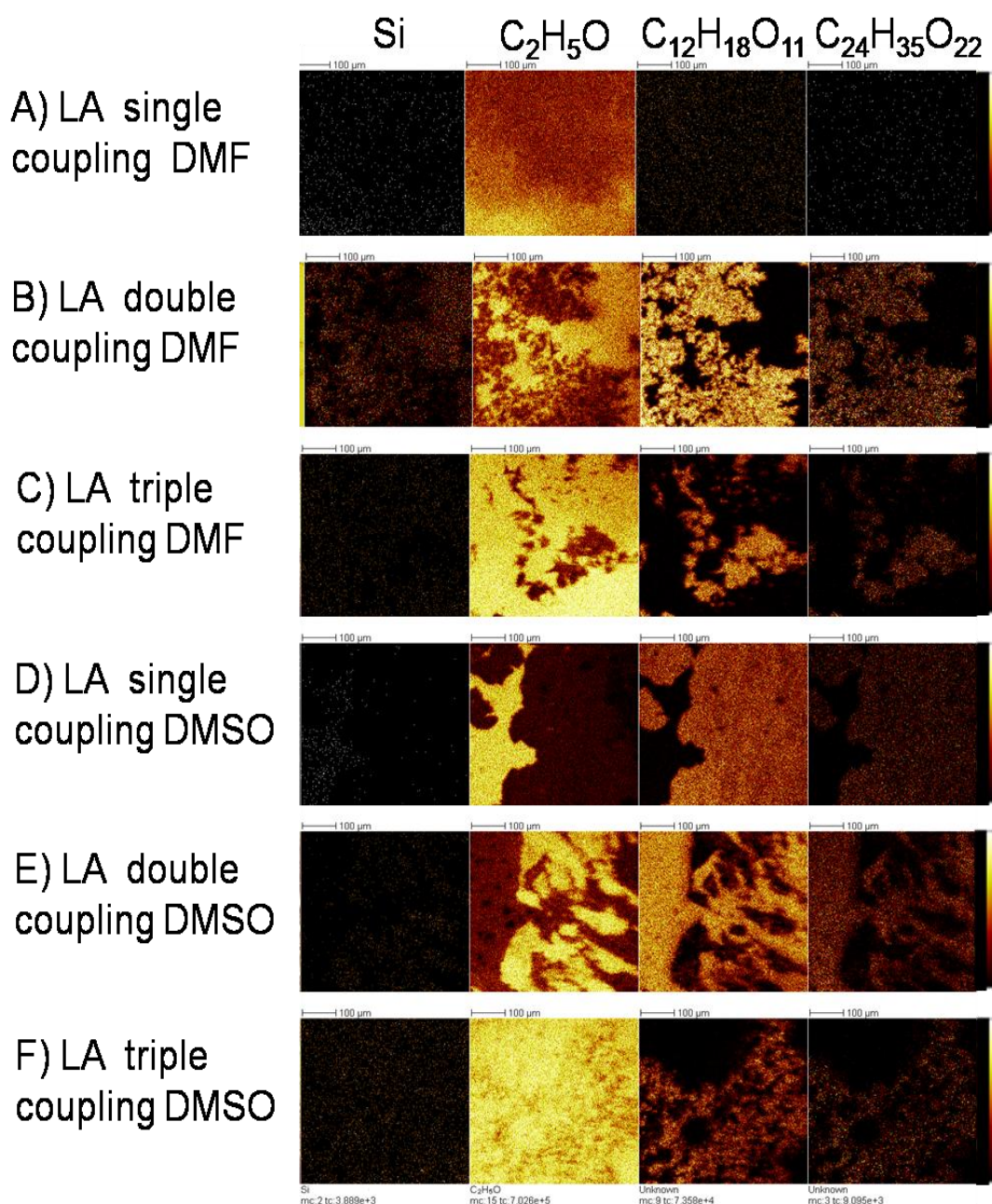
**Figure 5.8:** ToF-SIMS images (field of view 500 μm$^2$) for characteristic positive ions of silicon (m/z = 28), $C_2H_5O$ (m/z = 45), and sugar fragments $C_{12}H_{18}O_{11}$ (m/z = 338) and $C_{24}H_{35}O_{22}$ (m/z = 675), when LA is coupled to PEG monolayers **A)** LA single coupled in DMF, **B)** LA double coupled in DMF, **C)** LA triple coupled in DMF **D)** LA single coupled in DMSO, **E)** LA double coupled in DMSO, and **F)** LA triple coupled in DMSO. The scale to the right of the image is from dark (low-intensity counts) to bright (high-intensity counts).

Single coupling of GA in DMF resulted in small sugar fragments being detected at 338 D peak; however the PEG intensity was almost homogenous across the entire sample area suggesting uniform coverage of the monolayer, Figure 5.9 A. Double coupling of GA in DMF resulted in non-uniform coverage by small high intensity random patches of sugar attached to the PEG monolayer, Figure 5.9 B. Triple coupling of GA in DMF resulted in improved coverage; a band of sugar was seen across the sample at the 338 D peak but the degree of intensity was partial compared to other sugar distributions seen, Figure 5.9 C. The use of DMSO as the solvent appeared to improve the efficacy of coupling GA. Single coupling of GA using DMSO resulted in negligible coverage of sugar at the 338 D peak at low intensities. A high intensity region of PEG was seen covering the sample area at the 45 D peak, Figure 5.9 D. Double coupling of GA using DMSO yielded the best result but the coverage was deemed to be non-uniform due gaps and the PEG monolayer showing through, Figure 5.9 E. Triple coupling in DMSO again resulted in negligible coverage with poor intensity seen at the 338 D peak, Figure 5.9 F. It is believed that this variable coupling will have an effect on cell morphology.

ToF-SIMS analysis determined that using DMSO as the coupling solvent resulted in a better reaction yield than DMF, and that the number of coupling steps also affected the efficacy of the reaction. However, ToF-SIMS is a semi-quantitative technique, and so a detailed quantitative analysis was carried out using XPS, which is reported in Section 5.3.4.
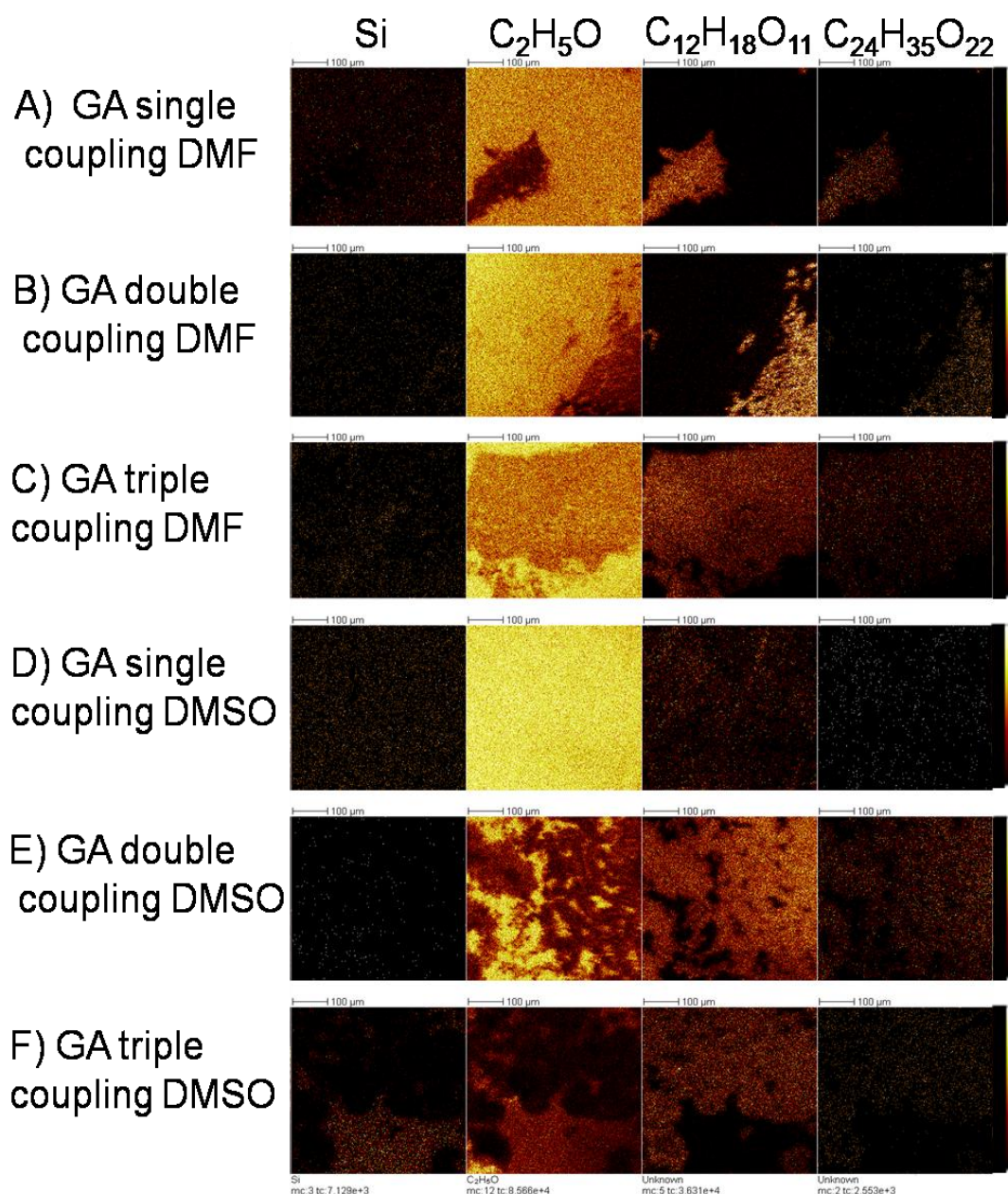
**Figure 5.9:** ToF-SIMS images (field of view 500 $\mu m^2$) for characteristic positive ions of silicon (m/z = 28), $C_2H_5O$ (m/z = 45), and sugar fragments $C_{12}H_{18}O_{11}$ (m/z = 338) and $C_{24}H_{35}O_{22}$ (m/z = 675), when GA is coupled to PEG monolayers **A)** GA single coupled in DMF, **B)** GA double coupled in DMF, **C)** GA triple coupled in DMF **D)** GA single coupled in DMSO, **E)** GA double coupled in DMSO, and **F)** GA triple coupled in DMSO. The scale to the right of the image is from dark (low-intensity counts) to bright (high-intensity counts).

**5.4 Conclusions**

Glass coverslips were modified using silane chemistry to present epoxy groups at the surface. A homogeneous layer of PEG diamine molecules were subsequently coupled to the surface via the epoxy groups to produce non-fouling surfaces. The amine-rich PEG monolayers were functionalized with saccharides using stepwise coupling of sugars, in varying solvents and coupling steps as confirmed by XPS and ToF-SIMS analysis. It was determined that using DMSO as the coupling solvent resulted in a better reaction yield than DMF, based on observations made from XPS and ToF-SIMS analysis. The number of coupling steps also affected the efficacy of the reaction.

Water contact angle measurements are a simple way to determine if surface modification has occurred. However, this method does not provide any data about the homogeneity of the surface given the macroscopic nature of the droplet. Consequently, it is essential that such data, whilst encouraging, should be reinforced by in-depth surface characterisation techniques. The XPS analysis, successfully tracked the reaction steps, however, it was also revealed that large amounts of adventitious contamination from solvents used in sample preparation of the glass and PEG samples, were present. Whilst a degree of saccharide coverage was achieved, none of the reaction conditions used produced a homogeneous coating. Consequently, further optimisation of the reaction conditions is required if a compositionally homogenous coating is to be achieved.

**Chapter 6.0 Discussion**

On a commercial level, there is need for an *in-vitro* liver model that could improve the information obtained at early points in drug design and delivery. To achieve this accurately such systems will have to mimic zonal liver functions, potentially at a small scale to allow for high-throughput drug screening. However, the system will have to maintain all the functions of hepatocytes, not just basic ones such as albumin secretion and synthesis of urea, in order to create an effective mimic of the liver tissue and its functionality.

Bioactive surfaces have been proposed to control cell or biomolecular interactions at the solid-liquid interface. Typically, these have been engineered to alter surface properties such as wettability, presentation of functional groups, topology or stiffness. It has been shown that the chemical composition of surfaces influences the properties of cultured cells, in particular cellular adhesion. However, other micro-environmental stimuli including hydrogel polymer chain length are likely to influence cellular function and fate (Underhill *et al.*, 2007, Semler *et al.*, 2005). The interaction between chemical functionality, stiffness and topography is a dynamic one and all three categories should be considered in the design of biomaterial interfaces in order to obtain the desired cellular response.

Recent tissue engineering applications have focused on regulating cell attachment to scaffolds through the immobilisation of short peptide derivatives, in particular the RGD cell-binding motif found within fibronectin and other ECM proteins (Underhill *et al.*, 2007, DeLong *et al.*, 2005, Benoit and Anseth, 2005, Kloxin *et al.*, 2009). In part, the popularity of this peptide is due to the ubiquity of the fibronectin (RGD) – integrin adhesion complex, common to almost all cell types. Therefore, if a surface is to be designed to specifically target a single cell type e.g. hepatocytes, a distinct cell binding mechanism must be utilised.

Carbohydrates, in biological systems, are often associated with specific cellular recognition events. This study focused on engineering surfaces to contain well defined carbohydrate ligands to enable good hepatocyte attachment and to support the retention of hepatocyte specific cell behaviour. The ASGP-R is a hepatocyte cell surface receptor with a unique affinity for galactose. It has previously been shown that galactose carrying polymers can be used to bind hepatocytes

through the cell specific ASGP-R mediated mechanism (Du *et al.*, 2008, Hong *et al.*, 2003, Kim *et al.*, 2003b).  The use of PEGA hydrogels containing covalently bound galactose was developed in this study to optimise the presentation of galactose moieties to hepatocytes on a non-fouling background using a fully defined synthetic system.

PEGA has a high density of functional groups which allow for its modification with biomolecules such as peptides and saccharides. Additionally, this material provides a passive background, preventing non specific protein adsorption; hence any specific cellular interaction on the PEGA surfaces would be a result of specific interactions with immobilised biomolecules rather than by interactions with an adsorbed protein layer (Zourob *et al.*, 2006, Meldal, 1992).  PEGA is an optically transparent highly hydrated semi-wet or gel like material, thus mimics the natural environment of cells and proteins whilst allowing for optical assessment of results (Meldal, 1992, Todd *et al.*, 2007, Zourob *et al.*, 2006, McDonald *et al.*, 2009).  It has previously been demonstrated that thin layers (~7µm) of cross linked PEGA hydrogels, immobilised on glass supports were modified with an inactivated precursor of the cell binding peptide RGD that could be activated by enzymatic cleavage (Todd *et al.*, 2007).

Coupling the saccharides to the PEGA was performed using EDC and NHS as coupling agents. The reaction was performed overnight at room temperature. The resulting product was spin coated onto epoxy coated glass substrates and UV crosslinked. The FTIR spectra of the reactants and products were evaluated. The carbonyl stretching seen in the FTIR spectra of LA disappeared in PEGA+LA spectra due to the amide bond formation between carboxylic acid groups of LA and amine groups of PEGA. A similar effect was observed with PEGA+GA and its respective sugar, GA. Additionally the Amine I peaks of PEGA+LA and PEGA+GA shifted slightly from 1670cm$^{-1}$ to a split peak between 1670 and 1620 cm$^{-1}$, which when compared to PEGA indicates a conformational change in PEGA after reaction with LA. These effects have previously been observed when Park *et al.* immobilised LA into chitosan (Park *et al.*, 2003).

Although no toxic effects were observed during the cellular evaluation, it should be noted that photoinitiators in general have an adverse effect on cell

viability, therefore must be kept to a minimum (Liu and Bhatia, 2002). The presence of the polymer, PEGA acts as an additional sink for free radicals during photo-crosslinking under UV. Due to oxygen quenching during the photo-crosslinking free radical reaction it was necessary to contain the pre-polymer solution within a closed chamber whilst exposing to UV light. This effect was further reduced by the use of transparent polyethylene film which prevented the pre-polymer solution from drying out and eliminated air bubbles(Todd *et al.*, 2007, Zourob *et al.*, 2006).

The distribution of chemically reactive primary amines was determined qualitatively using dansyl chloride staining and quantitatively using Fmoc-Phe loading experiments. When labelled with dansyl chloride, unmodified PEGA surfaces showed a homogeneous distribution of chemically active primary amines at the micron scale. As the concentration of the sugars incorporated into PEGA increased, fewer free amine groups were available within the material; this was also confirmed by the Fmoc-Phe labelling. The data was indicative of each of the surfaces being chemically homogeneous at the micron level as the pixel intensity i.e. fluorescence, from dansyl chloride staining was similar across each surface. The density of the coupled saccharide can be precisely controlled at any level; therefore the number of free primary amines within the hydrogel system can be adjusted. This flexibility enables free primary amines to be available for further chemical modification. These free amines may then be used to bind biological factors, such as RGD. Consequently, there is potential to create a construct with multiple biological cues.

There was no significant difference, as determined by student t-test, in the amount of protein adsorbed between unmodified PEGA, PEGA+LA (0.1 mmol) and PEGA+GA (0.1 mmol) surfaces after 24 hours in standard physiological conditions ($p>0.05$). The experiment used the same conditions i.e. 37°C, 5 % $CO_2$, and cell media supplemented with 10 % FBS, that was used for all cell culture evaluations. This observation suggests that any cell interaction with the sugar PEGA surfaces would likely be due to specific interactions with the incorporated LA or GA sugar PEGA surfaces rather than by interactions with an adsorbed protein layer. The total amount of protein on the PEGA surfaces was higher than the non-fouling PEG surfaces, prepared by Benesch *et al.* and Todd *et al.*, (~8 ng/mm$^2$ and 12.6 ± 1.0 ng/mm$^2$ respectively) for serum protein adsorption (Benesch *et al.*, 2001, Todd *et*

*al.*, 2009). It is likely that the hydrated nature of the PEGA structure entrapped small proteins within its structure, resulting in an increased amount of adsorbed protein compared to traditional two dimensional monolayer systems. It was determined by Kress *et al.* that only the smallest enzymes; matrix metalloproteinase-12, (MMP-12) (22 kDa) and thermolysin (35 kDa) were capable of entering PEGA 1900 beads and cleaving the attached peptide sequence (Kress *et al.*, 2002). This lends strength to the theory that only small proteins would be able to enter the PEGA polymer matrix and become entrapped.

In this study, a range of cellular and molecular biology techniques were utilised to examine the behaviour of hepatocytes on PEGA hydrogel platforms. The cellular morphology, functionality and attachment mechanism of a hepatocyte cell line on the PEGA hydrogels was investigated. Few cells were seen to attach to the PEGA surface, confirming the non-fouling nature of the material, (Todd *et al.*, 2007). This was additionally confirmed by the live/dead assay which showed the majority of the cells fluorescing red, indicating that the cell membranes had been compromised and the cells were non-viable. The incorporation of saccharides into PEGA resulted in the gel turning from bioinert and non-fouling to bioactive. Hepatocytes attached to PEGA+LA and PEGA+GA materials and proliferated over a 7 day period in culture. The cells generally took on a cuboidal epithelial morphology in culture forming tight cell-cell contacts which is consistent with previously observed morphologies by Breslow *et al.* (Breslow *et al.*, 1973). The presence of 0.1mmol LA within the PEGA resulted in a viable monolayer forming after 7 days of culture. It was determined that the overall cell number on the sugar containing PEGA materials were significantly higher compared to PEGA and the glass control at the day 7 time-point ($p<0.05$). The PEGA+LA material was not significantly different from TCP in terms of cell numbers, ($p>0.05$), meaning that the material performs as well as the control material. Although proliferation is an indication of metabolic activity it was essential to determine that the hepatocytes present on the sugar PEGA hydrogels were maintaining a hepatocyte specific phenotype.

A functional assay to determine if the cells could transform ammonium chloride into urea was undertaken. This is one of the first pathways found to down regulated when primary hepatocytes are exposed to *in-vitro* culture conditions. However, it had been shown that synthesis of urea by *in-vitro* cultured hepatocytes

on galactosylated surfaces is better than on non-galactosylated substrates (Yang *et al.*, 2002, Hong *et al.*, 2003). Furthermore, urea synthesis in culture systems has been shown to be enhanced by the presence of galactose moieties. However, despite this enhancement, the cells still lose functionality over time (Du *et al.*, 2006, Fan *et al.*, 2009). The generalised trend of the data obtained in Chapter 4, showed that urea synthesis decreased over time. All samples showed a decrease in mean urea synthesis from Day 1 to Day 3 of culture with the exception of TCP. TCP, glass and PEGA showed a decrease in urea synthesis on day 7 of culture. Interestingly, the sugar PEGA samples showed an increase in urea synthesis on day 7, with the PEGA+LA surface being significantly different to all the other materials, ($p<0.05$) suggesting that the cells may have conditioned their local environment and may be forming a functional architecture in which liver specific functions may be maintained.

Other markers of liver specific function were evaluated by RT-PCR namely; α-feta protein, albumin, and CK18. The cell suspension was shown to be positive for all these markers prior to cell seeding. Cells were harvested from the candidate materials after 6 days in culture and evaluated again. All the markers remained positive; however, the albumin marker appears to be down regulated in all the samples with the exception of TCP. This observation suggests there may be some fluctuations between the samples in terms of maintenance of functionality.

It has been shown, as previously mentioned in Part A of the literature review (Section 2.2.4), that ASGP-Rs bind exclusively to galactose bearing polymers. Immunocytochemical staining of the hepatocytes on the candidate materials showed internalisation of certain critical cytoskeletal components and kinases namely vinculin and pFAK on the galactose carrying PEGA+LA material (Kim *et al.*, 2003b, Cho *et al.*, 2007). A similar degree of internalisation of cytoskeletal components was observed by Kim *et al.* when hepatocytes were grown on the galactose bearing polymer PVLA. The down regulation of pFAK in hepatocytes cultured on PVLA, was likely to be the result of differences in cellular adhesion. It has also been noted that hepatocytes attached to PVLA surfaces did not exhibit localised vinculin, actin and pFAK at the point of focal attachment. In contrast, hepatocytes grown on collagen exhibited localisation of these cytoskeletal components. This is indicative that hepatocytes grown on PVLA with ASGP-R mediated adhesion do not initiate

integrin mediated signalling (Kim *et al.*, 2003b). It is possible that the internalisation of cytoskeletal components may be indicative of ASGP-R binding.

In order to evaluate the attachment mechanism, live (non-fixed, non permeabilised) hepatocytes were labelled to detect for the presence of ASGP-R on the surface of the cells by flow cytometry. In addition, RT-PCR was used to detect message for ASGP-R and compared against primary cells and an extract from liver tissue. The flow cytometry analysis confirmed that around 29 % of cells were positive for the presence of ASGP-R. Hence, it appears the ASGP-R is displayed at the plasma membrane of a sub-set of hepatocytes within the population and that these receptors would likely be available for binding galactose residues immobilised on a surface. However, no message RNA was detected for ASGP-R in the hepatocyte cell line in contrast to liver tissue and freshly isolated primary. The degree of expression of ASGP-R in primary cells was not as strong as that of liver tissue. These results suggest that this particular receptor is rapidly down-regulated in primary cells when placed *in-vitro* culture. Consequently it was necessary to determine whether that the ASGP-R receptors switched on whilst the hepatocytes were grown on the sample materials, in particular on the PEGA+LA monolayers. Cells were seeded onto the sample surfaces, grown in culture for six days then harvested for RT-PCR. On evaluation, it was clear that the surfaces did not switch on ASGP-R at the genetic level, despite verifying that the cells were still expressing other liver specific genetic markers.

It is therefore unlikely that the entirety of hepatocyte adhesion to the galactose-modified surfaces is mediated via ASGP-R. The lack of message RNA for the ASGP-R within the cell population indicates that any residual cell-membrane protein, observed in a small proportion of the population by flow cytometry, is unlikely to be replaced once internalised or shed. If the ASGP-R receptor does play a role within cellular adhesion to these sugar surfaces, it is likely to be in conjunction with integrin attachment. The probable attachment mechanism to the PEGA+LA and PEGA+GA surfaces remains unclear, but it is likely to involve ASGP-R and the recruitment of ECM proteins secreted by the hepatocytes during *in-vitro* culture. Proteins secreted during culture may attach to the surface of the material, allowing cells to attach by integrins. At high galactose coating densities the ASGP-R receptors on the hepatocyte membranes cluster within focal adhesion sites as a large patch, this

clustering prevents integrin receptors from participating in cell adhesion (Kim *et al.*, 2003b, Kim *et al.*, 2004). At low galactose coating densities, hepatocytes allow integrin receptors to take part in the adhesion process where ECM proteins have been secreted during culture alongside ASGP-R guided adhesion (Kim *et al.*, 2003b). The presence of LA and GA saccharides within the PEGA material clearly had a prevalent effect on hepatocytes in terms of attachment and functionality which merits further investigation and development with primary cells.

Our results show that it is important to characterise new scaffolds fully both chemically and biologically. ASGP-R mediated hepatocyte attachment has been widely utilised, however, the degree of ASGP-R expression either at the protein or message RNA level is rarely evaluated. Given the lack of message RNA for the ASGP-R gene shown in this study, it is likely that in primary cell studies, this gene would be rapidly down regulated in *in-vitro* conditions. Whilst a scaffold may be designed the attach cells using a particular biological mechanism, only in-depth biological evaluation can confirm the cellular attachment method.

The next strategy in this study was to use two dimensional PEG monolayer surfaces, which provide a well-defined platform for surface reactions, with a high density of surface functional groups. Unlike the PEGA hydrogel system, PEG monolayers can be fully characterised by surface chemical analysis techniques i.e. ToF-SIMS and XPS. The saccharides used in this study were synthesized directly onto the PEG surface using standard amide coupling techniques, and varying the reaction conditions; namely by altering the solvent and number of coupling steps used. ASGP-R on the cell surface of the hepatocytes would be expected to selectively bind to the surface presenting galactose moieties. The modification of PEG monolayers with saccharides allows the surface to be transformed from a bio-inert and non-fouling material to a bioactive material theoretically allowing cell specific binding to the surface.

Glass coverslips were modified with epoxy silane groups. The epoxy groups present at the surface were reacted with one of the primary amine groups on the PEG diamine (n=18), leaving the second amine available for further modification, as previously demonstrated by Piehlar *et al.* (Piehler *et al.*, 2000). There is a possibility that both amine groups could react with the surface forming PEG loops. However

the number of PEG molecules attached to the surface was close to a uniform monolayer, as shown by ToF-SIMS analysis, so if such reactions did occur they were not in large numbers and did not affect the overall aims of the study.

It is clear that the use of two dimensional PEG monolayer surfaces provides a well-defined platform for surface reactions with a high density of surface functional groups which can be chemically functionalised in a stepwise manner. The amine-rich PEG monolayers were functionalized with saccharides using stepwise coupling of sugars, in varying solvents and coupling steps as confirmed by XPS and ToF-SIMS analysis. It was determined that using DMSO as the coupling solvent resulted in a better reaction yield than DMF, based on observations made from XPS and ToF-SIMS analysis. The number of coupling steps also affected the efficacy of the reaction. Characterisation of such potentially bioactive surfaces needs careful consideration, whereas simple techniques such as water contact angle measurements may suggest chemical modification, this method does not provide any data about the homogeneity of the surface given the macroscopic nature of the droplet. The data from this study supports the need for in-depth analysis in order to accurately determine surface chemistries prior to cellular analysis. The XPS analysis, successfully tracked the reaction steps, however, it was also revealed that large amounts of adventitious contamination from solvents used in sample preparation of the glass and PEG samples, was present. Whilst a degree of saccharide coverage was achieved, none of the reaction conditions used produced a homogeneous coating. Consequently, further optimisation of the reaction conditions is required if a compositionally homogenous coating is to be achieved.

At present a bioactive surface has been developed and fully characterised; chemically and biologically. PEGA has a high density of functional groups which allowed for its modification with biomolecules, in this case saccharides. It was hoped that the incorporation of galactose bearing moieties would interact with the unique ASGP-R on hepatocyte cell surface membranes, in order to direct liver cell behaviour. It was determined that this system maintained hepatocyte viability and function over the duration of 7 days in culture conditions. Whilst the attachment mechanism of the cells to the material remains unclear, what is certain is that the presence of LA and GA saccharides within the PEGA material clearly had a prevalent effect on hepatocytes and merits further investigation.

**Chapter 7.0 Conclusions and Future Work**

**7.1 Conclusions**

The overall conclusion of this work is that saccharides within non-fouling surfaces composed of thin layers of PEG-acrylamide hydrogels are able to support hepatocyte attachment and the retention of cell type specific functions in culture. However, this preliminary work has shown that much further research is necessary to elucidate the role that the surface chemistry plays in the attachment of hepatocytes. Consequently, the principle findings of this study to characterise the surfaces of unmodified and modified materials will be enumerated before summarising the resulting cellular response.

PEG and PEGA are non-fouling materials with pendent primary amine groups available for chemical modifications. PEGA was effectively functionalised with saccharides in order to create a hydrogel surface which was suitable substrate for the adhesion, growth and maintenance of hepatocytes. The LA disaccharide used, carries a galactose moiety which should be available to exploit the unique galactose-ASGP-R recognition system on the hepatocyte plasma membrane. Analysis by FTIR and dansyl chloride labelling confirmed that both LA and a control (non-ASGP-R binding) sugar GA had been successfully immobilised throughout the PEGA structure. Increasing the concentration of sugar within the PEGA led to a detectable decrease in the number of free amines available within the hydrogel, indicating that the LA and GA were linking covalently via the amine groups.

It was observed that unmodified PEGA retained its non-fouling properties and did not support cellular adhesion and growth. The addition of LA and GA had no effect on non-specific serum protein adsorption by material. However, their inclusion did result in good hepatocyte adhesion, proliferation and the retention of some hepatocyte-specific functions e.g. urea synthesis.

It was hypothesised that galactose within LA would result in the adhesion of hepatocytes via the ASGP-R. Immunofluorescent labelling of cell-matrix adhesion complex components within the cells attached to the LA surfaces as opposed to GA surfaces appeared to provide some support for this theory. Flow cytometric detection indicated that a small proportion of hepatocytes did express a low level of this

receptor; however, no message for ASGP-R was detected by RT-PCR. This suggests that the receptor has been down regulated. Consequently the likely attachment mechanism to the surface remains unclear, but is likely to involve both some residual ASGP-R mediated attachment and additional cell binding to ECM components probably secreted by the hepatocytes during *in-vitro* culture. The presence of saccharides within the PEGA material clearly has a positive effect on hepatocyte culture, i.e. cell morphology and proliferation rate and thus merits further investigation.

Two dimensional PEG monolayer surfaces provided a well-defined platform for surface reactions which can be chemically functionalised in a stepwise manner. However, the technology for coupling saccharides (LA and GA) to this surface remains in the developmental stage. Analysis by water contact angle measurements, assays for protein adsorption, XPS and ToF-SIMS analyses highlighted the need for in depth surface characterisation techniques to confirm the homogeneity of a surface once functionalised. It was determined that using DMSO as the coupling solvent resulted in a better reaction yield than DMF, based on observations made from XPS and ToF-SIMS analysis. The number of coupling steps also affected the efficacy of the reaction. There is a discrepancy between the two sugars as to how many coupling steps in DMSO are required to obtain the best surface coverage. The disaccharide LA ($M_w$ =358.3) requires only one coupling step whereas the monosaccharide GA ($M_w$=194) requires two. The XPS analysis, successfully tracked the reaction steps, however, it also revealed that large amounts of adventitious contamination from solvents used in sample preparation, most notably the glass and PEG monolayers. This reinforces the need for care in the preparation of samples and the use of complementary analysis techniques in order to accurately determine surface chemistries prior to cellular analysis. Whilst a degree of saccharide coverage was achieved on PEG monolayers, none of the reaction conditions used produced a homogeneous coating. Consequently, further optimisation of the reaction conditions is required if a compositionally homogenous coating is to be achieved.

**7.2 Suggestions for future work**

Following the investigation and discussion in this thesis, a number of further questions have been generated. Based on this work, various possible extension studies can be postulated to investigate the potential of using saccharides to modify biomaterial surfaces for hepatocyte cell culture.

Currently, the PEGA system is has only been functionalised and characterised with saccharides. Many recent studies have focused on regulating cell adhesion through RGD, a cell binding epitope found within fibronectin. Integrin-fibronectin interactions can be found in most cell types not just hepatocytes. Given the ubiquity of RGD as an adhesion ligand, it would be interesting to evaluate and characterise PEGA hydrogel surfaces with graded saccharide and peptide ligands present within them.

Presently the likely cellular attachment mechanism to the LA functionalised PEGA surface remains unclear. Where-by residual ASGP-R mediated attachment and additional cell binding to ECM components is probable. The use of a competition reaction between free and bound galactose would result in a decrease in cell attachment if the ASGP-R-galactose binding mechanism is dominant. Additionally, testing the PEGA surfaces with a cell type which does not carry the ASGP-R on the cell surface membrane would test the unique hepatocyte specificity of the surfaces.

Co-culturing hepatocytes with another cell type such as endothelial or hepatic stellate cells may result in improved maintenance of hepatic specific functions such as albumin and urea synthesis on the PEGA surfaces.

Given the positive effect that saccharides within PEGA have on cell line hepatocyte culture, the next natural step would be to evaluate the surfaces with primary hepatocytes. Some initial primary cell work has been conducted in Helen Grant's laboratory at the University of Strathclyde, but due to the preliminary nature of the work, the data has not been incorporated into this thesis. In general, primary hepatocytes require specific micro-environmental cues to maintain the hepatic phenotype *in-vitro*. Some functions such as albumin secretion may be stable, whilst

others such as Cytochrome P450 decline under standard culture conditions. Consequently the maintenance of cell-specific phenotype would be the main goal.

Whilst a degree of saccharide coverage was achieved on PEG monolayers, none of the reaction conditions used produced a homogeneous coating. Consequently, further optimisation of the reaction conditions needs to be undertaken including dansyl chloride and Fmoc-Phe labelling of PEG monolayers, before and after LA and GA coupling to determine free amine concentration. XPS analysis of the remaining surfaces needs to be conducted to correlate the data with information generated from the ToF-SIMS spectra obtained within this study.

The following data appears in the figure:

| Name | Pos. | %Area |
|------|------|-------|
| C 1 | 285 | 53.69 |
| C 2 | 285.824 | 11.21 |
| C 3 | 286.742 | 10.50 |
| C 4 | 287.833 | 3.73 |
| C 5 | 289.232 | 4.41 |
| K 2p3/2 | 293.076 | 10.34 |
| K 2p1/2 | 295.876 | 5.17 |
| C 6 | 290.359 | 0.96 |
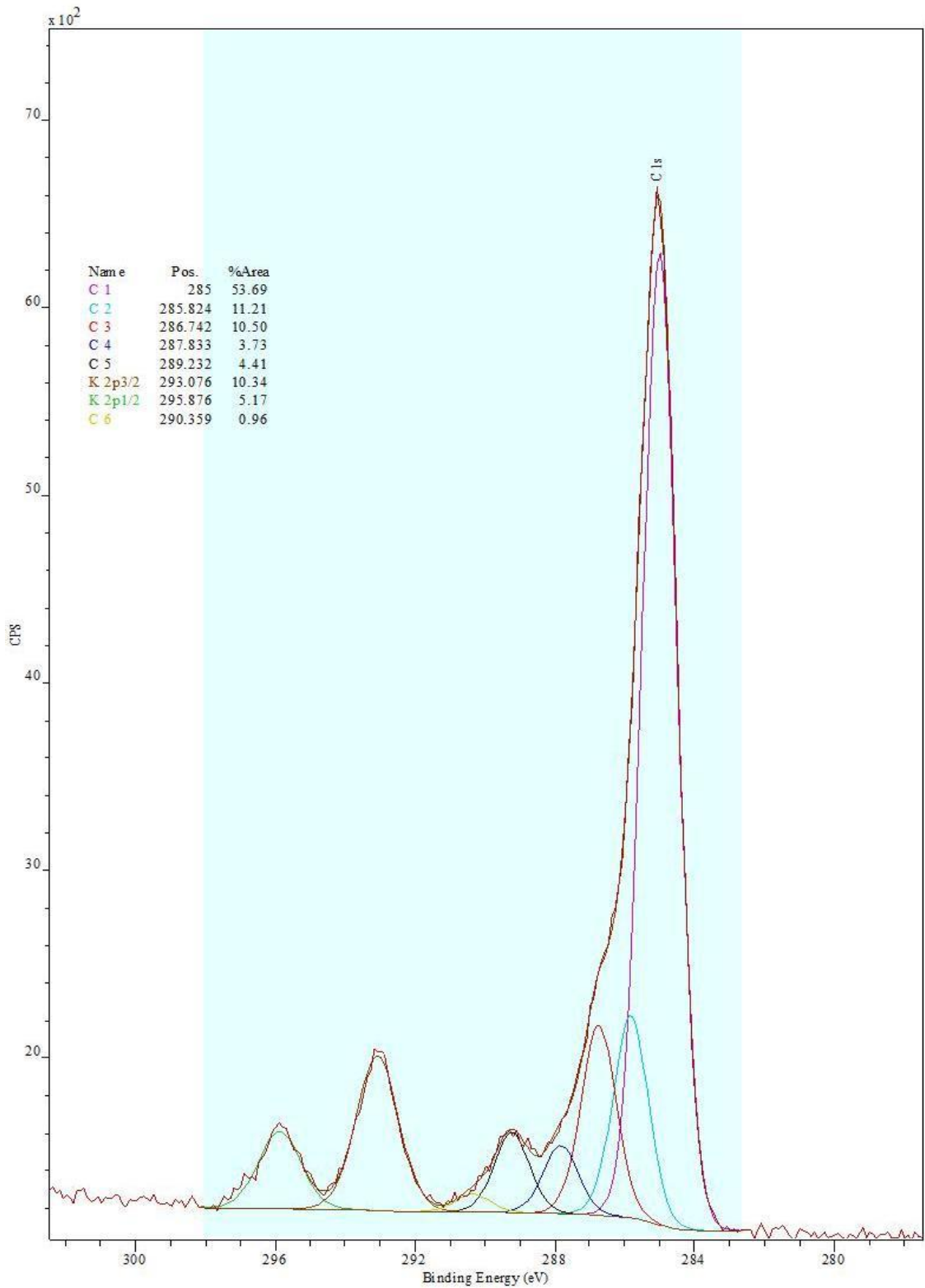
**Figure 8.1:** Curve fitting of XPS high resolution spectra for the C1S peak of glass.

| Name | Pos. | %Area |
|------|------|-------|
| C 1 | 285.007 | 45.65 |
| C 2 | 286.249 | 21.23 |
| C 3 | 286.85 | 18.99 |
| C 4 | 287.931 | 7.79 |
| C 5 | 289.105 | 5.23 |
| C 6 | 290.251 | 1.12 |
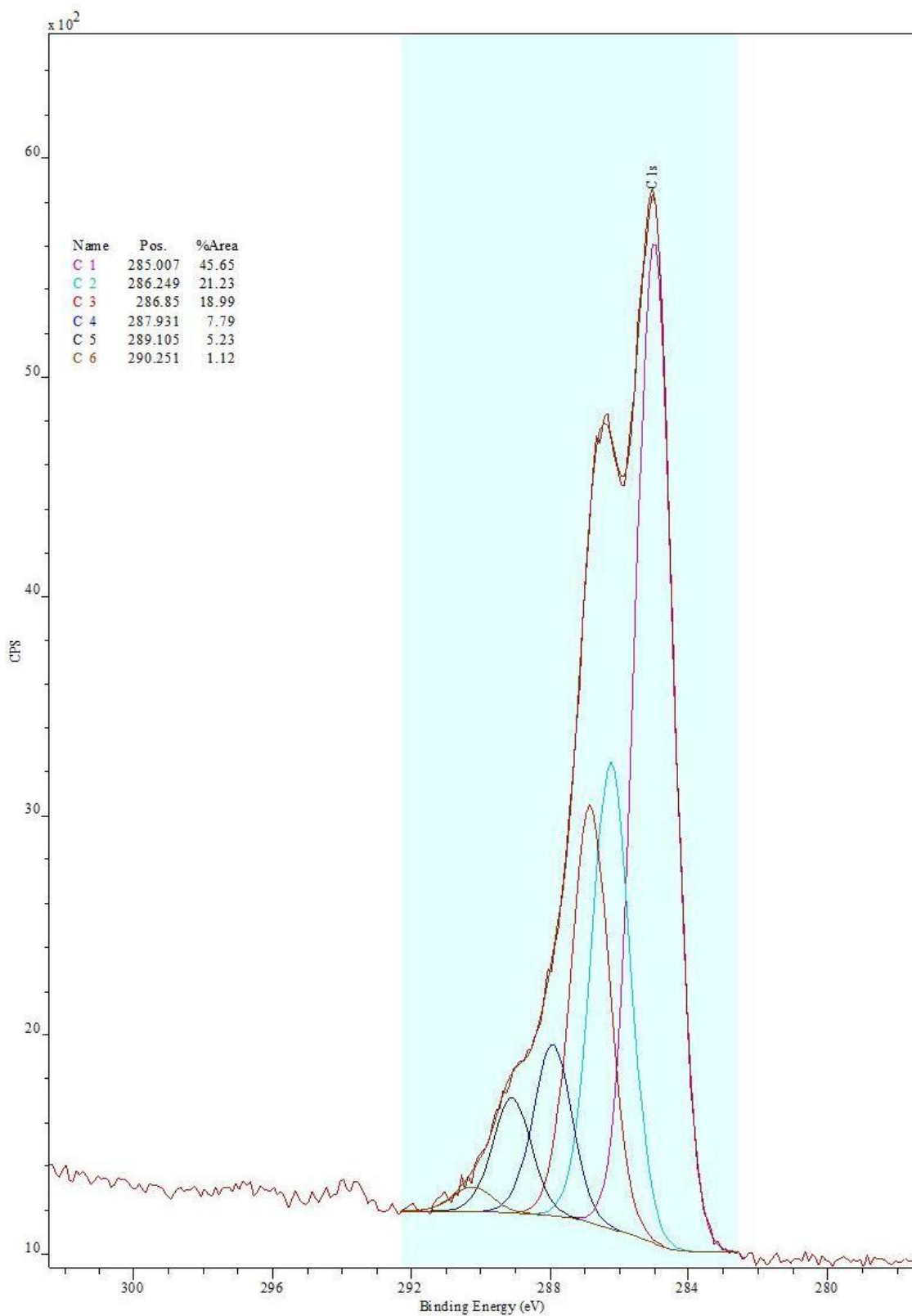
**Figure 8.2:** Curve fitting of XPS high resolution spectra for the C1S peak of GOPTS.
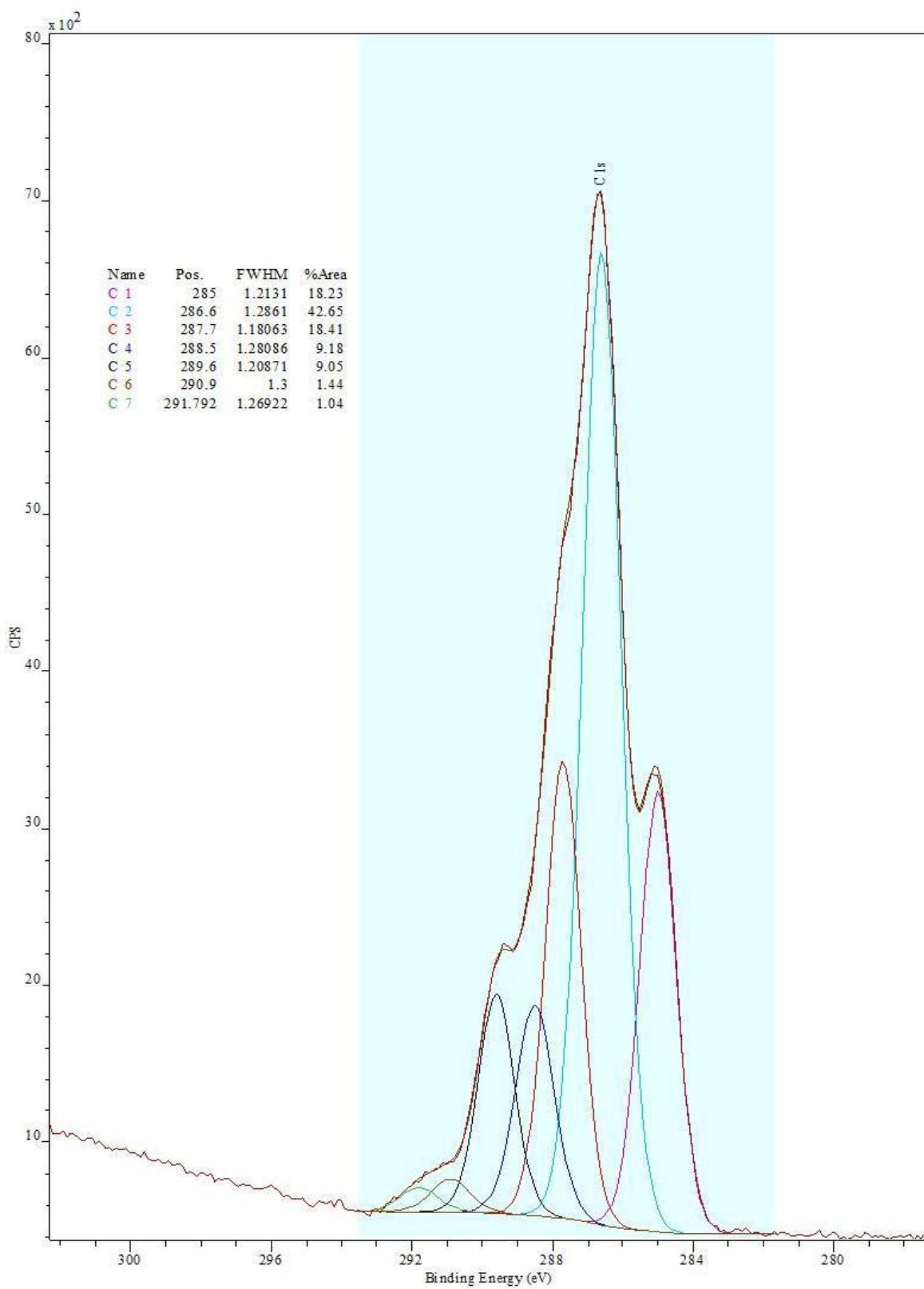
**Figure 8.3:** Curve fitting of XPS high resolution spectra for the C1S peak of PEG.

| Name | Pos. | FWHM | %Area |
|------|------|------|-------|
| C 1 | 285.001 | 1.34899 | 24.51 |
| C 2 | 286.496 | 1.3646 | 71.39 |
| C 3 | 287.34 | 1.4 | 0.41 |
| C 4 | 288.342 | 1.1 | 2.23 |
| C 5 | 289.34 | 1.12169 | 1.44 |
| C 6 | 290.447 | 1.1 | 0.01 |
| C 7 | 291.94 | 1.1 | 0.00 |
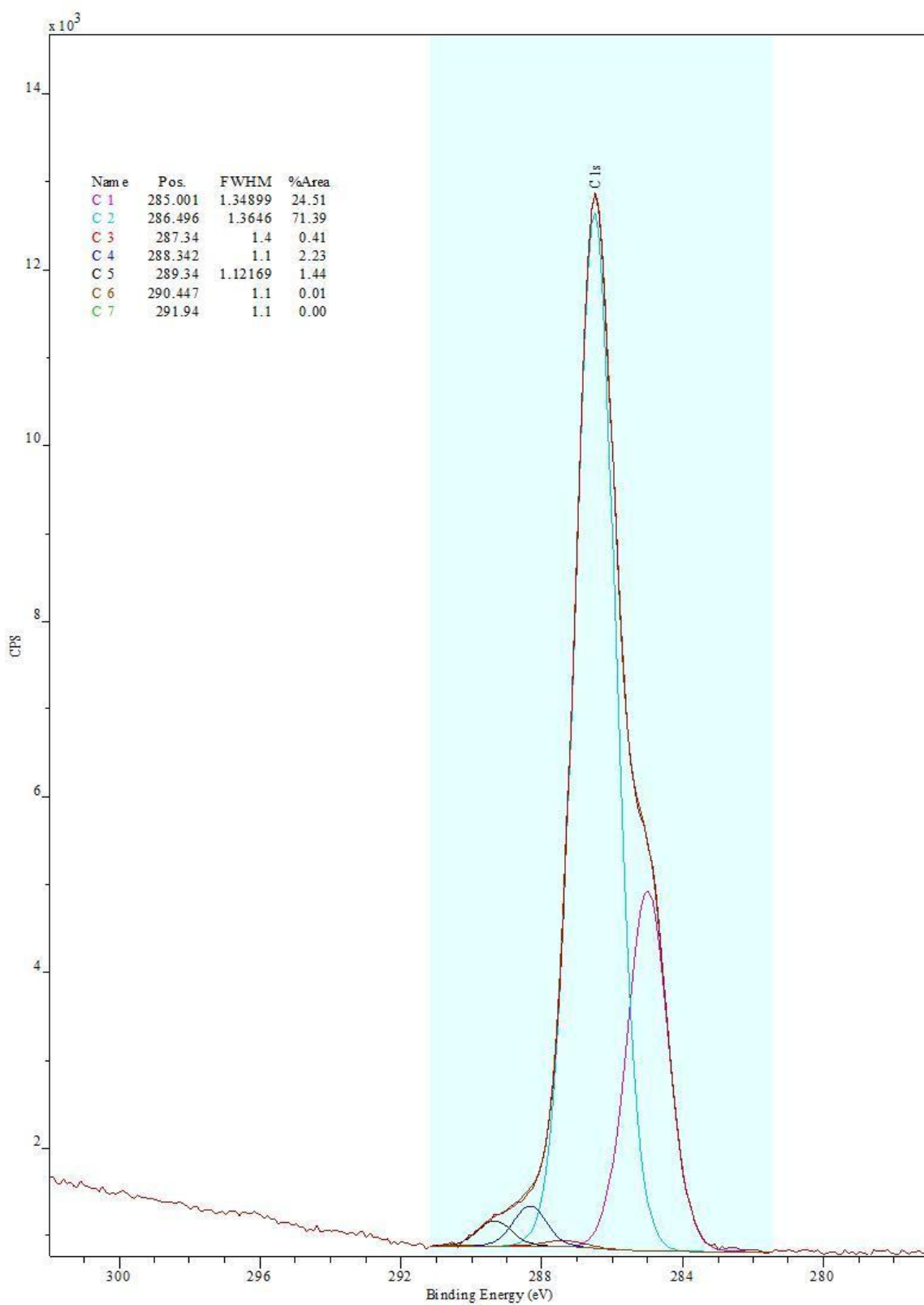
**Figure 8.4:** Curve fitting of XPS high resolution spectra for the C1S peak of PEG+LA (DMF double coupled).

| Name | Pos. | FWHM | %Area |
|------|------|------|-------|
| C 1 | 285 | 1.27213 | 11.70 |
| C 2 | 286.478 | 1.04224 | 76.66 |
| C 3 | 287.159 | 0.9 | 7.48 |
| C 4 | 288.056 | 1 | 3.39 |
| C 5 | 289.004 | 0.98332 | 0.78 |
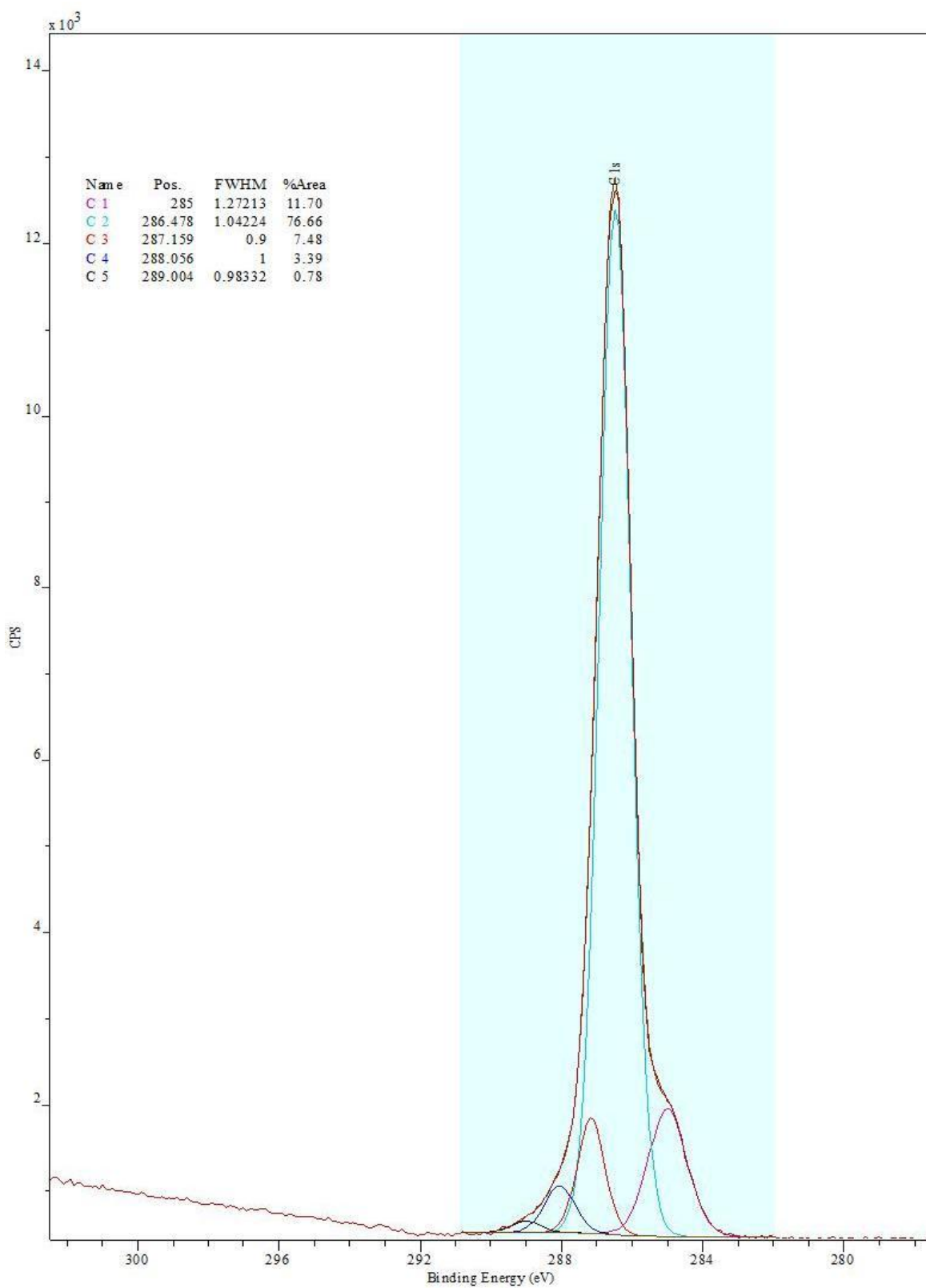
**Figure 8.5:** Curve fitting of XPS high resolution spectra for the C1S peak of PEG+GA (DMF double coupled).

## Chapter 9.0 References

Alberts, B., Bray, D., Lewis, J., Raff, M., Roberts, K. & Watson, J. D. 1994a. Cytoskeleton. *In:* Alberts, B., Bray, D., Lewis, J., Raff, M., Roberts, K. & Watson, J. D. (eds.) *Molecular Biology of the Cell.* New York: Garland Publishing. 787-861.

Alberts, B., Bray, D., Lewis, J., Raff, M., Roberts, K. & Watson, J. D. 1994b. Differentiated cells and the maintenance of tissues. *In:* Alberts, B., Bray, D., Lewis, J., Raff, M., Roberts, K. & Watson, J. D. (eds.) *Molecular Biology of the Cell.* 3rd ed. New York: Garland Publishing. 1149.

Alberts, B., Bray, D., Lewis, J., Raff, M., Roberts, K. & Watson, J. D. 1994c. Internal organisation of the cell. *In:* Alberts, B., Bray, D., Lewis, J., Raff, M., Roberts, K. & Watson, J. D. (eds.) *Molecular Biology of the Cell.* 3rd ed. New York: Garland Publishing. 475-506.

Allen, J. W. & Bhatia, S. N. 2002. Engineering liver therapies for the future. *Tissue Engineering,* 8**,** 725-737.

Allen, L. T., Tosetto, M., Miller, I. S., O'Connor, D. P., Penney, S. C., Lynch, I., Keenan, A. K., Pennington, S. R., Dawson, K. A. & Gallagher, W. M. 2006. Surface-induced changes in protein adsorption and implications for cellular phenotypic responses to surface interaction. *Biomaterials,* 27**,** 3096-3108.

Alves, P., Coelho, J. F. J., Haack, J., Rota, A., Bruinink, A. & Gil, M. H. 2009. Surface modification and characterization of thermoplastic polyurethane. *European Polymer Journal,* 45**,** 1412-1419.

An, Y. H., Friedman, R. J., Draughn, R. A., Smith, E. A., Nicholson, J. H. & John, J. F. 1995. Rapid quantification of staphylococci adhered to titanium surfaces using image analyzed epifluorescence microscopy. *Journal of Microbiological Methods,* 24**,** 29-40.

Anselme, K. 2000. Osteoblast adhesion on biomaterials. *Biomaterials,* 21**,** 667-681.

Arai, T. & Norde, W. 1990a. The behavior of some model proteins at solid liquid interfaces .1. Adsorption from single protein solutions. *Colloids and Surfaces,* 51**,** 1-15.

Arai, T. & Norde, W. 1990b. The behavior of some model proteins at solid liquid interfaces .2. Sequential and competitive adsorption. *Colloids and Surfaces,* 51**,** 17-28.

Ashwell, G. & Morell, A. G. 1974. Role of surface carbohydrates in hepatic recognition and transport of circulating glycoproteins. *Advances in Enzymology and Related Areas of Molecular Biology,* 41**,** 99-128.

Belu, A. M., Graham, D. J. & Castner, D. G. 2003. Time-of-flight secondary ion mass spectrometry: techniques and applications for the characterization of biomaterial surfaces. *Biomaterials,* 24**,** 3635-3653.

Benesch, J., Svedhem, S., Svensson, S. C. T., Valiokas, R., Liedberg, B. & Tengvall, P. 2001. Protein adsorption to oligo(ethylene glycol) self-assembled monolayers: Experiments with fibrinogen, heparinized plasma, and serum. *Journal of Biomaterials Science-Polymer Edition,* 12**,** 581-597.

Benoit, D. S. W. & Anseth, K. S. 2005. The effect on osteoblast function of colocalized RGD and PHSRN epitopes on PEG surfaces. *Biomaterials,* 26**,** 5209-5220.

Berry, M., Edwards, A. M. & Barritt, G. J. 1991. *Laboratory Techniques In Biochemistry and Molecular Biology: Isolated hepatocytes preparation, properties and applications,* New York, Elsevier.

Berthiaume, F., Moghe, P. V., Toner, M. & Yarmush, M. L. 1996. Effect of extracellular matrix topology on cell structure, function, and physiological responsiveness: Hepatocytes cultured in a sandwich configuration. *Faseb Journal,* 10**,** 1471-1484.

Braet, F. & Wisse, E. 2002. Structural and functional aspects of liver sinusoidal endothelial cell fenestrae: a review. *Comparative Hepatology,* 1**,** 1.

Brash, J. L. 1983. Protein interactions at solid-surfaces. *Abstracts of Papers of the American Chemical Society,* 185**,** 190-ORPL.

Breslow, J. L., Sloan, H. R., Ferrans, V. J., Anderson, J. L. & Levy, R. I. 1973. Characterization of mouse liver-cell line FL83B. *Experimental Cell Research,* 78**,** 441-453.

Briggs, D. 1998. Surface analysis of polymers by XPS and static SIMS. *In:* Clarke, D. R., Suresh, S. & Ward, I. M. (eds.). Cambridge: Cambridge University Press.

Briggs, D. & Seah, M. P. 1990. *Practical Surface Analysis: Auger and X-ray photoelectron spectroscopy,* Chichester, Wiley.

Butcher, G. 2003. *Gastroenterology: An illustrated colour text,* Edinburgh, Churchill Livingstone.

Campbell, N. & Reece, J. B. 2007. Ch 6: A tour of the cell. *In:* Campbell, N. & Reece, J. B. (eds.) *Biology.* 8th ed. New York: Benjamin Cummings. 119-121.

Cao, X. D. & Shoichet, M. S. 1999. Delivering neuroactive molecules from biodegradable microspheres for application in central nervous system disorders. *Biomaterials,* 20**,** 329-339.

Castner, D. G. & Ratner, B. D. 2002. Biomedical surface science: Foundations to frontiers. *Surface Science,* 500**,** 28-60.

Cho, C. S., Hoshiba, T., Harada, I. & Akaike, T. 2007. Regulation of hepatocyte behaviors by galactose-carrying polymers through receptor-mediated mechanism. *Reactive & Functional Polymers,* 67**,** 1301-1310.

Cho, C. S., Seo, S. J., Park, I. K., Kim, S. H., Kim, T. H., Hoshiba, T., Harada, I. & Akaike, T. 2006. Galactose-carrying polymers as extracellular matrices for liver tissue engineering. *Biomaterials,* 27**,** 576-585.

Chu, X. H., Shi, X. L., Feng, Z. Q., Gu, J. Y., Xu, H. Y., Zhang, Y., Gu, Z. Z. & Ding, Y. T. 2009. In vitro evaluation of a multi-layer radial-flow bioreactor based on galactosylated chitosan nanofiber scaffolds. *Biomaterials,* 30**,** 4533-4538.

Cima, L. G., Ingber, D. E., Vacanti, J. P. & Langer, R. 1991. Hepatocyte culture on biodegradable polymeric substrates. *Biotechnology and Bioengineering,* 38**,** 145-158.

Clark, P. 1994. Cell behavior on micropatterned surfaces. *Biosensors & Bioelectronics,* 9**,** 657-661.

Colognato, H. & Yurchenco, P. D. 2000. Form and function: The laminin family of heterotrimers. *Developmental Dynamics,* 218**,** 213-234.

Cousins, B. G., Doherty, P. J., Williams, R. L., Fink, J. & Garvey, M. J. 2004. The effect of silica nanoparticulate coatings on cellular response. *Journal of Materials Science-Materials in Medicine,* 15**,** 355-359.

Critchley, D. R. 2000. Focal adhesions - the cytoskeletal connection. *Current Opinion in Cell Biology,* 12**,** 133-139.

Cunningham, C. C. & Van Horn, C. G. 2003. Energy availability and alcohol-related liver pathology. *Alcohol Research & Health,* 27**,** 291-299.

Davila, J. C. & Morris, D. L. 1999. Analysis of cytochrome P450 and phase II conjugating enzyme expression in adult male rat hepatocytes. *In Vitro Cellular & Developmental Biology-Animal,* 35**,** 120-130.

Dee, K. C. & Bizios, R. 1996. Mini-review: Proactive biomaterials and bone tissue engineering. *Biotechnology and Bioengineering,* 50**,** 438-442.

DeLong, S. A., Gobin, A. S. & West, J. L. 2005. Covalent immobilization of RGDS on hydrogel surfaces to direct cell alignment and migration. *Journal of Controlled Release,* 109**,** 139-148.

Desimone, V. & Cortese, R. 1992. Transcription factors and liver-specific genes. *Biochimica Et Biophysica Acta,* 1132**,** 119-126.

Devlin, T. M. 1992. *Textbook of biochemistry with clinical correlations; Third edition,* Chichester, England, Uk. Illus, Wiley-Liss, Inc.

Du, Y., Han, R. B., Wen, F., San, S. N. S., Xia, L., Wohland, T., Leo, H. L. & Yu, H. 2008. Synthetic sandwich culture of 3D hepatocyte monolayer. *Biomaterials,* 29**,** 290-301.

Du, Y. N., Chia, S. M., Han, R. B., Chang, S., Tang, H. H. & Yu, H. 2006. 3D hepatocyte monolayer on hybrid RGD/galactose substratum. *Biomaterials,* 27**,** 5669-5680.

Elbert, D. L. & Hubbell, J. A. 1996. Surface treatments of polymers for biocompatibility. *Annual Review of Materials Science,* 26**,** 365-394.

Ezzell, R. M., Toner, M., Hendricks, K., Dunn, J. C. Y., Tompkins, R. G. & Yarmush, M. L. 1993. Effect of collagen gel configuration on the cytoskeleton in cultured rat hepatocytes. *Experimental Cell Research,* 208**,** 442-452.

Fan, J., Shang, Y., Yang, J. & Yuan, Y. 2009. Preparation of galactosylated hyaluronic acid/chitosan scaffold for liver tissue engineering. *Sheng Wu Yi Xue Gong Cheng Xue Za Zhi,* 26**,** 1271-5.

Faucheux, N., Schweiss, R., Lutzow, K., Werner, C. & Groth, T. 2004. Self-assembled monolayers with different terminating groups as model substrates for cell adhesion studies. *Biomaterials,* 25**,** 2721-2730.

Feng, Z. Q., Chu, X. H., Huang, N. P., Wang, T., Wang, Y. C., Shi, X. L., Ding, Y. T. & Gu, Z. Z. 2009. The effect of nanofibrous galactosylated chitosan scaffolds on the formation of rat primary hepatocyte aggregates and the maintenance of liver function. *Biomaterials,* 30**,** 2753-2763.

Filippini, P., Rainaldi, C., Ferrante, A., Mecheri, B., Gabrielli, G., Bombace, M., Indovina, P. L. & Santini, M. T. 2001. Modulation of osteosarcoma cell growth and differentiation by silane-modified surfaces. *Journal of Biomedical Materials Research,* 55**,** 338-349.

Fujimoto, K., Tadokoro, H., Ueda, Y. & Ikada, Y. 1993. Polyurethane surface modification by graft-polymerization of acrylamide for reduced protein adsorption and platelet-adhesion. *Biomaterials,* 14**,** 442-448.

Fujita, M., Spray, D. C., Choi, H., Saez, J. C., Watanabe, T., Rosenberg, L. C., Hertzberg, E. L. & Reid, L. M. 1987. Glycosaminoglycans and proteoglycans induce gap junction expression and restore transcription of tissue-specific messenger-RNAs in primary liver cultures. *Hepatology,* 7**,** S1-S9.

Gebhardt, R. 1992. Metabolic zonation of the liver - regulation and implications for liver-function. *Pharmacology & Therapeutics,* 53**,** 275-354.

Geerts, A., Vrijsen, R., Rauterberg, J., Burt, A., Schellinck, P. & Wisse, E. 1989. Invitro differentiation of fat-storing cells parallels marked increase of collagen-synthesis and secretion. *Journal of Hepatology,* 9**,** 59-68.

Geffen, I. & Spiess, M. 1992. Asialoglycoprotein receptor. *International Review of Cytology-a Survey of Cell Biology,* 137B**,** 181-219.

Giancotti, F. G. & Ruoslahti, E. 1999. Transduction - Integrin signaling. *Science,* 285**,** 1028-1032.

Glicklis, R., Merchuk, J. C. & Cohen, S. 2004. Modeling mass transfer in hepatocyte spheroids via cell viability, spheroid size, and hepatocellular functions. *Biotechnology and Bioengineering,* 86**,** 672-680.

Glicklis, R., Shapiro, L., Agbaria, R., Merchuk, J. C. & Cohen, S. 2000. Hepatocyte behavior within three-dimensional porous alginate scaffolds. *Biotechnology and Bioengineering,* 67**,** 344-353.

Gombotz, W. R. & Hoffman, A. S. 1987. Functionalization of polymeric films by plasma polymerization of allyl alcohol and allylamine. *Abstracts of Papers of the American Chemical Society,* 193**,** 163-PMSE.

Gotoh, Y., Niimi, S., Hayakawa, T. & Miyashita, T. 2004. Preparation of lactose-silk fibroin conjugates and their application as a scaffold for hepatocyte attachment. *Biomaterials,* 25**,** 1131-1140.

Graaff, K. V. d. 1998. *Human Anatomy*, McGraw-Hill.

Grant, M. H., Morgan, C., Henderson, C., Malsch, G., Seifert, B., Albrecht, W. & Groth, T. 2005. The viability and function of primary rat hepatocytes cultured on polymeric membranes developed for hybrid artificial liver devices. *Journal of Biomedical Materials Research Part A,* 73A**,** 367-375.

Gray, J. J. 2004. The interaction of proteins with solid surfaces. *Current Opinion in Structural Biology,* 14**,** 110-115.

Greengar.O, Federman, M. & Knox, W. E. 1972. Cytomorphometry of developing rat-liver and its application to enzymic differentiation. *Journal of Cell Biology,* 52**,** 261-&.

Griffiths, M. R., Keir, S. & Burt, A. D. 1991. Basement-membrane proteins in the space of disse - a reappraisal. *Journal of Clinical Pathology,* 44**,** 646-648.

Gutsche, A. T., Parsons-Wingerter, P., Chand, D., Saltzman, W. M. & Leong, K. W. 1994a. N-acetylglucosamine and adenosine derivatized surfaces for cell culture: 3T3 fibroblast and chicken hepatocyte response. *Biotechnology and Bioengineering,* 43**,** 801-809.

Gutsche, A. T., Zurlo, J., Lo, H. & Leong, K. W. 1994b. Synthesis and characterization of polymer substrates for rat hepatocyte culture. *Biomolecular Materials by Design,* 330**,** 243-248.

Guyton, A. C. & Hall, J. E. 1996. *Textbook of Medical Physiology*, W.B. Saunders.

Hahn, E., Wick, G., Pencev, D. & Timpl, R. 1980. Distribution of basement-membrane proteins in normal and fibrotic human-liver - collagen type-IV, laminin, and fibronectin. *Gut,* 21**,** 63-71.

Halling, P. J., Ulijn, R. V. & Flitsch, S. L. 2005. Understanding enzyme action on immobilised substrates. *Current Opinion in Biotechnology,* 16**,** 385-392.

Hammond, J. S., Beckingham, I. J. & Shakesheff, K. M. 2006. Scaffolds for liver tissue engineering. *Expert Review of Medical Devices,* 3**,** 21-27.

Harder, P., Grunze, M., Dahint, R., Whitesides, G. M. & Laibinis, P. E. 1998. Molecular conformation in oligo(ethylene glycol)-terminated self-assembled

monolayers on gold and silver surfaces determines their ability to resist protein adsorption. *Journal of Physical Chemistry B,* 102**,** 426-436.

Haslam, J. & Willis, H. A. 1972. *Identification and analysis of plastics*, Butterworth&Co Ltd.

Hayashi, M., Sumi, Y., Mizuno, H., Mizutani, H., Ueda, M. & Hata, K.-i. 2004. An experimental study of novel bioartificial materials applied to glycotechnology for tissue engineering. *Materials Science and Engineering: C,* 24**,** 447-455.

Hersel, U., Dahmen, C. & Kessler, H. 2003. RGD modified polymers: biomaterials for stimulated cell adhesion and beyond. *Biomaterials,* 24**,** 4385-4415.

Hirose, S., Ise, H., Uchiyama, M., Cho, C. S. & Akaike, T. 2001. Regulation of asialoglycoprotein receptor expression in the proliferative state of hepatocytes. *Biochemical and Biophysical Research Communications,* 287**,** 675-681.

Hoffman, A. S. 1984. *In:* Dusek, K. (ed.) *Advances in Polymer Science.* Berlin: Springer-Verlag.

Hong, S. R., Lee, Y. M. & Akaike, T. 2003. Evaluation of a galactose-carrying gelatin sponge for hepatocytes culture and transplantation. *Journal of Biomedical Materials Research Part A,* 67A**,** 733-741.

Hu, S. G., Jou, C. H. & Yang, M. C. 2003. Protein adsorption, fibroblast activity and antibacterial properties of poly(3-hydroxybutyric acid-co-3-hydroxyvaleric acid) grafted with chitosan and chitooligosaccharide after immobilized with hyaluronic acid. *Biomaterials,* 24**,** 2685-2693.

Hubbell, J. A. 2003. Materials as morphogenetic guides in tissue engineering. *Current Opinion in Biotechnology,* 14**,** 551-558.

Hubbell, J. A., Massia, S. P., Desai, N. P. & Drumheller, P. D. 1991. Endothelial cell-selective materials for tissue engineering in the vascular graft via a new receptor. *Bio-Technology,* 9**,** 568-572.

Ise, H., Sugihara, N., Negishi, N., Nikaido, T. & Akaike, T. 2001. Low asialoglycoprotein receptor expression as markers for highly proliferative potential hepatocytes. *Biochemical and Biophysical Research Communications,* 285**,** 172-182.

Istone, W. K. 1995. X-ray photoelectron spectroscopy (XPS). *In:* Conners, T. E. & Banerjee, S. (eds.) *Surface analysis of paper.* New York: CRC Press. 235-368.

Jeon, S. I. & Andrade, J. D. 1991. Protein surface interactions in the presence of polyethylene oxide .2. Effect of protein size. *Journal of Colloid and Interface Science,* 142**,** 159-166.

Jeon, S. I., Lee, J. H., Andrade, J. D. & Degennes, P. G. 1991. Protein surface interactions in the presence of polyethylene oxide .1. Simplified theory. *Journal of Colloid and Interface Science,* 142**,** 149-158.

Jo, S. & Park, K. 1999. Novel poly(ethylene glycol) hydrogels from silylated PEGs. *Journal of Bioactive and Compatible Polymers,* 14**,** 457-473.

Johansson, S., Svineng, G., Wennerberg, K., Armulik, A. & Lohikangas, L. 1997. Fibronectin-integrin interactions. *Frontiers in Bioscience (online),* 2**,** D126-146.

Jones, C. 1993. Effects of electrochemical and plasma treatments on carbon-fiber surfaces. *Surface and Interface Analysis,* 20**,** 357-367.

Juliano, R. L. & Haskill, S. 1993. Signal transduction from the extracellular-matrix. *Journal of Cell Biology,* 120**,** 577-585.

Jungermann, K. & Sasse, D. 1978. Heterogeneity of liver parenchymal-cells. *Trends in Biochemical Sciences,* 3**,** 198-202.

Kanda, S., Miyata, Y. & Kanetake, H. 2004. Role of focal adhesion formation in migration and morphogenesis of endothelial cells. *Cellular Signalling,* 16**,** 1273-1281.

Kataropoulou, M., Henderson, C. & Grant, M. H. 2005. Metabolic studies of hepatocytes cultured on collagen substrata modified to contain glycosaminoglycans. *Tissue Engineering,* 11**,** 1263-1273.

Keselowsky, B. G., Collard, D. M. & Garcia, A. J. 2005. Integrin binding specificity regulates biomaterial surface chemistry effects on cell differentiation. *Proceedings of the National Academy of Sciences of the United States of America,* 102**,** 5953-5957.

Kim, S. H., Hoshiba, T. & Akaike, T. 2003a. Effect of carbohydrates attached to polystyrene on hepatocyte morphology on sugar-derivatized polystyrene matrices. *Journal of Biomedical Materials Research Part A,* 67A**,** 1351-1359.

Kim, S. H., Hoshiba, T. & Akaike, T. 2004. Hepatocyte behavior on synthetic glycopolymer matrix: inhibitory effect of receptor-ligand binding on hepatocyte spreading. *Biomaterials,* 25**,** 1813-1823.

Kim, S. H., Kim, J. H. & Akaike, T. 2003b. Regulation of cell adhesion signaling by synthetic glycopolymer matrix in primary cultured hepatocyte. *Febs Letters,* 553**,** 433-439.

Kim, Y. J., Kang, I. K., Huh, M. W. & Yoon, S. C. 2000. Surface characterization and in vitro blood compatibility of poly(ethylene terephthalate) immobilized with insulin and/or heparin using plasma glow discharge. *Biomaterials,* 21**,** 121-130.

Kingshott, P., Thissen, H. & Griesser, H. J. 2002. Effects of cloud-point grafting, chain length, and density of PEG layers on competitive adsorption of ocular proteins. *Biomaterials,* 23**,** 2043-2056.

Kloxin, A. M., Kasko, A. M., Salinas, C. N. & Anseth, K. S. 2009. Photodegradable Hydrogels for Dynamic Tuning of Physical and Chemical Properties. *Science,* 324**,** 59-63.

Kobayashi, A., Goto, M., Kobayashi, K. & Akaike, T. 1994. Receptor-mediated regulation of differentiation and proliferation of hepatocytes by synthetic-polymer model of asialoglycoprotein. *Journal of Biomaterials Science-Polymer Edition,* 6**,** 325-342.

Koo, L. Y., Irvine, D. J., Mayes, A. M., Lauffenburger, D. A. & Griffith, L. G. 2002. Co-regulation of cell adhesion by nanoscale RGD organization and mechanical stimulus. *Journal of Cell Science,* 115**,** 1423-1433.

Krasteva, N., Groth, T., Fey-Lamprecht, F. & Altankov, G. 2001. The role of surface wettability on hepatocyte adhesive interactions and function. *Journal of Biomaterials Science-Polymer Edition,* 12**,** 613-627.

Kress, J., Zanaletti, R., Amour, A., Ladlow, M., Frey, J. G. & Bradley, M. 2002. Enzyme accessibility and solid supports: Which molecular weight enzymes can be used on solid supports? an investigation using confocal Raman microscopy. *Chemistry-a European Journal,* 8**,** 3769-3772.

Lecluyse, E. L., Audus, K. L. & Hochman, J. H. 1994. Formation of extensive canalicular networks by rat hepatocytes cultured in collagen-sandwich configuration. *American Journal of Physiology,* 266**,** C1764-C1774.

Leeson, T. S. & Leeson, C. R. 1970. *Histology,* Philidelphia, USA, W.B. Saunders Company.

Lewandowska, K., Balachander, N., Sukenik, C. N. & Culp, L. A. 1989. Modulation of fibronectin adhesive functions for fibroblasts and neural cells by chemically derivatized substrata. *Journal of Cellular Physiology,* 141**,** 334-345.

Lewandowska, K., Kaetzel, C. S., Zardi, L. & Culp, L. A. 1988. Binding characteristics of complementary fibronectin fragments on artificial substrata. *Febs Letters,* 237**,** 35-39.

Lewandowska, K., Pergament, E., Sukenik, C. N. & Culp, L. A. 1992. Cell-type-specific adhesion mechanisms mediated by fibronectin adsorbed to chemically derivatized substrata. *Journal of Biomedical Materials Research,* 26**,** 1343-1363.

Li, S. H., Edgar, D., Fassler, R., Wadsworth, W. & Yurchenco, P. D. 2003. The role of laminin in embryonic cell polarization and tissue organization. *Developmental Cell,* 4**,** 613-624.

Lin, Y. C., Brayfield, C. A., Gerlach, J. C., Rubin, J. P. & Marra, K. G. 2009. Peptide modification of polyethersulfone surfaces to improve adipose-derived stem cell adhesion. *Acta Biomaterialia,* 5**,** 1416-1424.

Liu, V. A. & Bhatia, S. N. 2002. Three-dimensional photopatterning of hydrogels containing living cells. *Biomedical Microdevices,* 4**,** 257-266.

Lord, M. S., Cousins, B. G., Doherty, P. J., Whitelock, J. M., Simmons, A., Williams, R. L. & Milthorpe, B. K. 2006. The effect of silica nanoparticulate coatings on serum protein adsorption and cellular response. *Biomaterials,* 27**,** 4856-4862.

Loreal, O., Clement, B., Schuppan, D., Rescan, P. Y., Rissel, M. & Guillouzo, A. 1992. Distribution and cellular-origin of collagen-VI during development and in cirrhosis. *Gastroenterology,* 102**,** 980-987.

Lutolf, M. P. & Hubbell, J. A. 2005. Synthetic biomaterials as instructive extracellular microenvironments for morphogenesis in tissue engineering. *Nature Biotechnology,* 23**,** 47-55.

Ma, Z. W., Gao, C. Y., Gong, Y. H. & Shen, J. C. 2003. Chondrocyte behaviors on poly-L-lactic acid (PLLA) membranes containing hydroxyl, amide or carboxyl groups. *Biomaterials,* 24**,** 3725-3730.

Maher, J. 1998. The extracellular matrix in liver regeneration. *In:* Strain, A. J. & Diehl, A. M. (eds.) *Liver growth and repair.* London: Chapman & Hall. 451-464.

Marieb, E. N. 1998. *Human anatomy and physiology,* New York, Benjamin-Cummings.

Maroudas, N. G. 1975. Adhesion and spreading of cells on charged surfaces. *Journal of Theoretical Biology,* 49**,** 417-424.

Martinez-Hernandez, A. 1984. The hepatic extracellular-matrix .1. Electron immunohistochemical studies in normal rat-liver. *Laboratory Investigation,* 51**,** 57-74.

Martinez-Hernandez, A. & Amenta, P. S. 1993. The hepatic extracellular matrix: I. Components and distribution in normal liver. *Virchows Archiv A Pathological Anatomy and Histopathology,* 423**,** 1-11.

Martini, F. H. 2006. The Digestive System. *In:* Martini, F. H. (ed.) *Fundementals of Anatomy and Physiology.* Benjamin-Cummings Publishing Company.

Massia, S. P. & Hubbell, J. A. 1991. An RGD spacing of 440nm is sufficient for integrin alpha-V-beta-3-mediated fibroblast spreading and 140nm for focal contact and stress fiber formation. *Journal of Cell Biology,* 114**,** 1089-1100.

Masters, K. S. & Anseth, K. S. 2004. Cell-material interactions. *Advances in Chemical Engineering.* 7-42.

Mathiowitz, E. & Langer, R. 1987. Polyanhydride microspheres as drug carriers I. hot-melt microencapsulation. *Journal of Controlled Release,* 5**,** 13-22.

Matsushita, N., Oda, H., Kobayashi, K., Akaike, T. & Yoshida, A. 1994. Induction of cytochrome P-450s and expression of liver-specific genes in rat primary hepatocytes cultured on different extracellular matrices. *Bioscience Biotechnology and Biochemistry,* 58**,** 1514-1516.

McCourt, P. A. G. 1999. How does the hyaluronan scrap-yard operate? *Matrix Biology,* 18**,** 427-432.

McDonald, T. O., Qu, H. L., Saunders, B. R. & Ulijn, R. V. 2009. Branched peptide actuators for enzyme responsive hydrogel particles. *Soft Matter,* 5**,** 1728-1734.

McFarland, C. D., Jenkins, M., Griesser, H. J., Chatelier, R. C., Steele, J. G. & Underwood, P. A. 1998. Albumin-binding surfaces: synthesis and characterization. *Journal of Biomaterials Science-Polymer Edition,* 9**,** 1207-1225.

Meldal, M. 1992. PEGA - a flow stable polyethylene-glycol dimethyl acrylamide copolymer for solid-phase synthesis. *Tetrahedron Letters,* 33**,** 3077-3080.

Mitaka, T. 1998. The current status of primary hepatocyte culture. *International Journal of Experimental Pathology,* 79**,** 393-409.

Mitzner, W. 1974. Hepatic outflow resistance, sinusoid pressure, and vascular waterfall. *American Journal of Physiology,* 227**,** 513-519.

Moghe, P. V., Coger, R. N., Toner, M. & Yarmush, M. L. 1997. Cell-cell interactions are essential for maintenance of hepatocyte function in collagen gel but not on Matrigel. *Biotechnology and Bioengineering,* 56**,** 706-711.

Mooney, D. J., Kaufmann, P. M., Sano, K., Schwendeman, S. P., Majahod, K., Schloo, B., Vacanti, J. P. & Langer, R. 1996. Localized delivery of epidermal growth factor improves the survival of transplanted hepatocytes. *Biotechnology and Bioengineering,* 50**,** 422-429.

Mrksich, M. 2000. A surface chemistry approach to studying cell adhesion. *Chemical Society Reviews,* 29**,** 267-273.

Mrksich, M. 2002. What can surface chemistry do for cell biology? *Current Opinion in Chemical Biology,* 6**,** 794-797.

Nakata, K., Leong, G. F. & Brauer, R. W. 1960. Direct measurement of blood pressures in minute vessels of the liver. *American Journal of Physiology,* 199**,** 1181-1188.

Nath, N., Hyun, J., Ma, H. & Chilkoti, A. 2004. Surface engineering strategies for control of protein and cell interactions. *Surface Science,* 570**,** 98-110.

Neumann, A. W., Absolom, D. R., Zinng, W., Oss, C. J. V. & Francis, D. W. 1983. Surface thermodynamics of protein adsorption, cell adhesion and cell engulfment. *In:* Szycher, M. (ed.) *Biocompatible polymers, metals and composites.* Lancaster: Technomic Publishing. 53-80.

Newman, K. D. & McBurney, M. W. 2004. Poly(D,L lactic-co-glycolic acid) microspheres as biodegradable microcarriers for pluripotent stem cells. *Biomaterials,* 25**,** 5763-5771.

Oe, S., Fukunaka, Y., Hirose, T., Yamaoka, Y. & Tabata, Y. 2003. A trial on regeneration therapy of rat liver cirrhosis by controlled release of hepatocyte growth factor. *Journal of Controlled Release,* 88**,** 193-200.

Ostuni, E., Grzybowski, B. A., Mrksich, M., Roberts, C. S. & Whitesides, G. M. 2003. Adsorption of proteins to hydrophobic sites on mixed self-assembled monolayers. *Langmuir,* 19**,** 1861-1872.

Park, I. K., Yang, J., Jeong, H. J., Bom, H. S., Harada, I., Akaike, T., Kim, S. & Cho, C. S. 2003. Galactosylated chitosan as a synthetic extracellular matrix for hepatocytes attachment. *Biomaterials,* 24**,** 2331-2337.

Peppas, N. A., Huang, Y., Torres-Lugo, M., Ward, J. H. & Zhang, J. 2000. Physicochemical, foundations and structural design of hydrogels in medicine and biology. *Annual Review of Biomedical Engineering,* 2**,** 9-29.

Piehler, J., Brecht, A., Valiokas, R., Liedberg, B. & Gauglitz, G. 2000. A high-density poly(ethylene glycol) polymer brush for immobilization on glass-type surfaces. *Biosensors & Bioelectronics,* 15**,** 473-481.

Popper, H. & Schaffner, S. 1957. *Liver: Structure and Function,* London, McGraw-Hill.

Prime, K. L. & Whitesides, G. M. 1991. Self-assembled organic monolayers - model systems for studying adsorption of proteins at surfaces. *Science,* 252**,** 1164-1167.

Quirk, R. A., Kellam, B., Bhandari, R. N., Davies, M. C., Tendler, S. J. B. & Shakesheff, K. M. 2003. Cell-type-specific adhesion onto polymer surfaces from mixed cell populations. *Biotechnology and Bioengineering,* 81**,** 625-628.

Rabek, J. 1980. *Experimental methods in polymer chemistry: physical principles and applications,* Chichester, Wiley.

Raeber, G. P., Lutolf, M. P. & Hubbell, J. A. 2005. Molecularly engineered PEG hydrogels: A novel model system for proteolytically mediated cell migration. *Biophysical Journal,* 89**,** 1374-1388.

Ramirez, F. & Rifkin, D. B. 2003. Cell signaling events: a view from the matrix. *Matrix Biology,* 22**,** 101-107.

Rang, H. P. & Dale, M. M. 1991. *Pharmacology; second edition,* New York, USA, Churchill Livingstone Inc.

Ranieri, J. P., Bellamkonda, R., Jacob, J., Vargo, T. G., Gardella, J. A. & Aebischer, P. 1993. Selective neuronal cell attachment to a covalently patterned monoamine on fluorinated ethylene-propylene films. *Journal of Biomedical Materials Research,* 27**,** 917-925.

Ranucci, C. S., Kumar, A., Batra, S. P. & Moghe, P. V. 2000. Control of hepatocyte function on collagen foams: sizing matrix pores toward selective induction of 2-D and 3-D cellular morphogenesis. *Biomaterials,* 21**,** 783-793.

Rappaport, A. M., Borowy, Z. J., Lougheed, W. M. & Lotto, W. N. 1954. Subdivision of hexagonal liver lobules into a structural and functional unit - role in hepatic physiology and pathology. *Anatomical Record,* 119**,** 11-33.

Ratner, B. D. 1996. Surface Properties of Materials. *In:* Ratner, B. D., Hoffman, A. S., Schoen, F. J. & Lemons, J. E. (eds.) *Biomaterials Science: An introduction to materials in medicine.* San Diego: Academic Press. 21-35.

Ratner, B. D. & Bryant, S. J. 2004. Biomaterials: Where we have been and where we are going. *Annual Review of Biomedical Engineering,* 6**,** 41-75.

Ratner, B. D. & Hoffman, A. S. 1996. Thin films,grafts and coatings. *In:* Ratner, B. D., Hoffman, A. S., Schoen, F. J. & Lemons, J. E. (eds.) *Biomaterials Science:An introduction to materials in medicine.* San Diego: Academic Press. 105-118.

Reid, L. M., Fiorino, A. S., Sigal, S. H., Brill, S. & Holst, P. A. 1992. Extracellular-matrix gradients in the space of disse - relevance to liver biology. *Hepatology,* 15**,** 1198-1203.

Roach, P., Farrar, D. & Perry, C. C. 2005. Interpretation of protein adsorption: Surface-induced conformational changes. *Journal of the American Chemical Society,* 127**,** 8168-8173.

Romanic, A. M., Adachi, E., Kadler, K. E., Hojima, Y. & Prockop, D. J. 1991. Copolymerization of PNcollagen-III and collagen-I - PNcollagen-III decreases the rate of incorporation of collagen-I into fibrils, the amount of collagen-I incorporated, and the diameter of the fibrils formed. *Journal of Biological Chemistry,* 266**,** 12703-12709.

Roskams, T., Moshage, H., Devos, R., Guido, D., Yap, P. & Desmet, V. 1995. Heparan-sulfate proteoglycan expression in normal human liver. *Hepatology,* 21**,** 950-958.

Ross, M. H., Reith, E. J. & Romrell, L. J. 1989. *Histology: A text and atlas*, Williams & Wilkins.

Ruoslahti, E. 1991. Integrins as receptors for extracellular matrix. *In:* Hay, E. D. (ed.) *Cell Biology of Extracellular Matrix.* 2 ed. New York: Plennum Press. 343-363.

Ruoslahti, E. & Obrink, B. 1996. Common principles in cell adhesion. *Experimental Cell Research,* 227**,** 1-11.

Sakiyama-Elbert, S. E. & Hubbell, J. A. 2001. Functional biomaterials: Design of novel biomaterials. *Annual Review of Materials Research,* 31**,** 183-201.

Saltzman, M. 2004. *Tissue Engineering: Engineering principles for the design of replacement organs and tissues,* Oxford, Oxford University Press.

Schaller, M. D., Hildebrand, J. D., Shannon, J. D., Fox, J. W., Vines, R. R. & Parsons, J. T. 1994. Autophosphorylation of the focal adhesion kinase, PP125(FAK), directs SH2 dependent binding of PP60(SRC). *Molecular and Cellular Biology,* 14**,** 1680-1688.

Schiff, L. 1975. *Diseases of the liver,* Philadelphia, J.B. Lippincott.

Schueler, B., Sander, P. & Reed, D. A. 1990. A time-of-flight secondary ion-microscope. *Vacuum,* 41**,** 1661-1664.

Schuppan, D. 1990. Structure of the extracellular-matrix in normal and fibrotic liver - collagens and glycoproteins. *Seminars in Liver Disease,* 10**,** 1-10.

Schuppan, D., Ruehl, M., Somasundaram, R. & Hahn, E. G. 2001. Matrix as a modulator of hepatic fibrogenesis. *Seminars in Liver Disease,* 21**,** 351-372.

Seeley, R. R. & Tate, P. 1995. *Anatomy and Physiology*, Mosby.

Selden, C., Khalil, M. & Hodgson, H. 2000. Three dimensional culture upregulates extracellular matrix protein expression in human liver cell lines - a step towards mimicking the liver in vivo? *International Journal of Artificial Organs,* 23**,** 774-781.

Semler, E. J., Lancin, P. A., Dasgupta, A. & Moghe, P. V. 2005. Engineering hepatocellular morphogenesis and function via ligand-presenting hydrogels with graded mechanical compliance. *Biotechnology and Bioengineering,* 89**,** 296-307.

Sendil, D., Gursel, I., Wise, D. L. & Hasirci, V. 1999. Antibiotic release from biodegradable PHBV microparticles. *Journal of Controlled Release,* 59**,** 207-217.

Sigal, G. B., Mrksich, M. & Whitesides, G. M. 1998. Effect of surface wettability on the adsorption of proteins and detergents. *Journal of the American Chemical Society,* 120**,** 3464-3473.

Sofia, S. J., Premnath, V. & Merrill, E. W. 1998. Poly(ethylene oxide) grafted to silicon surfaces: Grafting density and protein adsorption. *Macromolecules,* 31**,** 5059-5070.

Steffen, H. J., Schmidt, J. & Gonzalez-Elipe, A. 2000. Biocompatible surfaces by immobilization of heparin on diamond-like carbon films deposited on various substrates. *Surface and Interface Analysis,* 29**,** 386-391.

Stevens, M. M., Mayer, M., Anderson, D. G., Weibel, D. B., Whitesides, G. M. & Langer, R. 2005. Direct patterning of mammalian cells onto porous tissue engineering substrates using agarose stamps. *Biomaterials,* 26**,** 7636-7641.

Sugimoto, Y. 1981. Effect on the adhesion and locomotion of mouse fibroblasts by their interacting with differently charged substrates - a quantitative study by ultrastructural method. *Experimental Cell Research,* 135**,** 39-45.

Taborelli, M., Eng, L., Descouts, P., Ranieri, J. P., Bellamkonda, R. & Aebischer, P. 1995. Bovine serum-albumin conformation on methyl and amine functionalized surfaces compared by scanning force microscopy. *Journal of Biomedical Materials Research,* 29**,** 707-714.

Takagi, J. & Springer, T. A. 2002. Integrin activation and structural rearrangement. *Immunological Reviews,* 186**,** 141-163.

Tkachenko, E., Rhodes, J. M. & Simons, M. 2005. Syndecans - New kids on the signaling block. *Circulation Research,* 96**,** 488-500.

Todd, S. J., Farrar, D., Gough, J. E. & Ulijn, R. V. 2007. Enzyme-triggered cell attachment to hydrogel surfaces. *Soft Matter,* 3**,** 547-550.

Todd, S. J., Scurr, D. J., Gough, J. E., Alexander, M. R. & Ulijn, R. V. 2009. Enzyme-Activated RGD Ligands on Functionalized Poly(ethylene glycol) Monolayers: Surface Analysis and Cellular Response. *Langmuir,* 25**,** 7533-7539.

Tsang, V. L., Chen, A. A., Cho, L. M., Jadin, K. D., Sah, R. L., DeLong, S., West, J. L. & Bhatia, S. N. 2007. Fabrication of 3D hepatic tissues by additive photopatterning of cellular hydrogels. *Faseb Journal,* 21**,** 790-801.

Underhill, G. H., Chen, A. A., Albrecht, D. R. & Bhatia, S. N. 2007. Assessment of hepatocellular function within PEG hydrogels. *Biomaterials,* 28**,** 256-270.

Van Kooten, T. G., Schakenraad, J. M., Vandermei, H. C. & Busscher, H. J. 1992. Influence of substratum wettability on the strength of adhesion of human fibroblasts. *Biomaterials,* 13**,** 897-904.

Vickerman, J. C. & Briggs, D. 2001. *ToF-SIMS Surface Analysis by Mass Spectrometry,* Chichester, IM Publications.

Vitte, J., Benoliel, A. M., Pierres, A. & Bongrand, P. 2004. Is there a predictable relationship between surface physical-chemical properties and cell behaviour at the interface? *Eur Cell Mater,* 7**,** 52-63; discussion 63.

Vroman, L. 1962. Effect of adsorbed proteins on wettability of hydrophilic and hydrophobic solids. *Nature,* 196**,** 476-&.

Vu, T. H. & Werb, Z. 2000. Matrix metalloproteinases: effectors of development and normal physiology. *Genes & Development,* 14**,** 2123-2133.

Wang, Y. X., Robertson, J. L., Spillman, W. B. & Claus, R. O. 2004. Effects of the chemical structure and the surface properties of polymeric biomaterials on their biocompatibility. *Pharmaceutical Research,* 21**,** 1362-1373.

Webb, K., Hlady, V. & Tresco, P. A. 1998. Relative importance of surface wettability and charged functional groups on NIH 3T3 fibroblast attachment, spreading, and cytoskeletal organization. *Journal of Biomedical Materials Research,* 41**,** 422-430.

Webb, K., Hlady, V. & Tresco, P. A. 2000. Relationships among cell attachment, spreading, cytoskeletal organization, and migration rate for anchorage-dependent cells on model surfaces. *Journal of Biomedical Materials Research,* 49**,** 362-368.

Weigel, P. H. 1980. Rat hepatocytes bind to synthetic galactoside surfaces via a patch of asialoglycoprotein receptors. *Journal of Cell Biology,* 87**,** 855-861.

Weisz, O. A. & Schnaar, R. L. 1991. Hepatocyte adhesion to carbohydrate-derivatized surfaces .1. Surface-topography of the rat hepatic lectin. *Journal of Cell Biology,* 115**,** 485-493.

Wells, R. G. 2007. Function and metabolism of collagen and other extracellular matrix proteins. *In:* Rodes, J., Benhamou, J. P., Blei, A., Reichen, J. & Rizzetto, M. (eds.) *The textbook of hepatology: From basic science to clinical practise.* 3rd ed. Oxford: Blackwell Publishing.

Wells, R. G. 2008. The role of matrix stiffness in regulating cell behavior. *Hepatology,* 47**,** 1394-1400.

Williams, D. H. & Flemming, I. 1996. *Spectroscopic methods in organic chemistry,* London, McGraw-Hill Book Company.

Wisse, E., Braet, F., Luo, D. Z., DeZanger, R., Jans, D., Crabbe, E. & Vermoesen, A. 1996. Structure and function of sinusoidal lining cells in the liver. *Toxicologic Pathology,* 24**,** 100-111.

Wright, M. C. & Paine, A. J. 1992. Evidence that the loss of rat-liver cytochrome-P450 invitro is not solely associated with the use of collagenase, the loss of cell-cell contacts and or the absence of an extracellular-matrix. *Biochemical Pharmacology,* 43**,** 237-243.

Yang, J., Chung, T. W., Nagaoka, M., Goto, M., Cho, C. S. & Akaike, T. 2001. Hepatocyte-specific porous polymer-scaffolds of alginate/galactosylated chitosan sponge for liver-tissue engineering. *Biotechnology Letters,* 23**,** 1385-1389.

Yang, J., Goto, M., Ise, H., Cho, C. S. & Akaike, T. 2002. Galactosylated alginate as a scaffold for hepatocytes entrapment. *Biomaterials,* 23**,** 471-479.

Yoon, J. J., Nam, Y. S., Kim, J. H. & Park, T. G. 2002. Surface immobilization of galactose onto aliphatic biodegradable polymers for hepatocyte culture. *Biotechnology and Bioengineering,* 78**,** 1-10.

Zhu, X. H., Wang, C. H. & Tong, Y. W. 2007. Growing tissue-like constructs with Hep3B/HepG2 liver cells on PHBV microspheres of different sizes. *Journal of Biomedical Materials Research Part B-Applied Biomaterials,* 82B**,** 7-16.

Zourob, M., Gough, J. E. & Ulijn, R. V. 2006. A micropatterned hydrogel platform for chemical synthesis and biological analysis. *Advanced Materials,* 18**,** 655-+.